

Development of Raman spectroscopy-integrated calcium oxalate crystallization index (rCOCI) test and its clinical validation for diagnosing calcium oxalate urolithiasis



A Thesis Submitted in Partial Fulfillment of the Requirements
for the Degree of Master of Science in Medical Biochemistry
Department of Biochemistry
Faculty Of Medicine
Chulalongkorn University
Academic Year 2023

การพัฒนาวิธี Raman spectroscopy-integrated calcium oxalate crystallization index (อาร์โคซี่) และการทดสอบทางคลินิกสำหรับวินิจฉัยโรคนิ่วปัสสาวะชนิดแคลเซียมออกซาเลต



วิทยานิพนธ์นี้เป็นส่วนหนึ่งของการศึกษาตามหลักสูตรปริญญาวิทยาศาสตรมหาบัณฑิต
สาขาวิชาชีวเคมีทางการแพทย์ ภาควิชาชีวเคมี
คณะแพทยศาสตร์ จุฬาลงกรณ์มหาวิทยาลัย
ปีการศึกษา 2566

Thesis Title Development of Raman spectroscopy-integrated calcium oxalate crystallization index (rCOCI) test and its clinical validation for diagnosing calcium oxalate urolithiasis

By Miss Kamonchat Boonkam

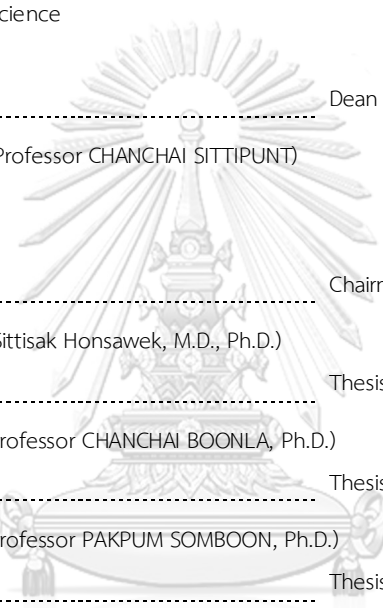
Field of Study Medical Biochemistry

Thesis Advisor Assistant Professor CHANCHAI BOONLA, Ph.D.

Thesis Co Advisor Assistant Professor PAKPUM SOMBOON, Ph.D.
Associate Professor ALONGKORN PIMPIN, Ph.D.

Accepted by the FACULTY OF MEDICINE, Chulalongkorn University in Partial Fulfillment of the Requirement for the Master of Science

THESIS COMMITTEE



..... Dean of the FACULTY OF MEDICINE
(Associate Professor CHANCHAI SITTIPUNT)

..... Chairman
(Professor Sittisak Honsawek, M.D., Ph.D.)

..... Thesis Advisor
(Assistant Professor CHANCHAI BOONLA, Ph.D.)

..... Thesis Co-Advisor
(Assistant Professor PAKPUM SOMBOON, Ph.D.)

..... Thesis Co-Advisor
(Associate Professor ALONGKORN PIMPIN, Ph.D.)

..... Examiner
(PORNCHAI KAEWSAPSAK, Ph.D.)

..... External Examiner
(Assistant Professor Supranee Kongkham, Ph.D.)

กมลฉัตร บุญคำ : การพัฒนาวิธี Raman spectroscopy-integrated calcium oxalate crystallization index (อาร์โคซี) และการทดสอบทางคลินิกสำหรับวินิจฉัยโรคนิ่วปัสสาวะชนิดแคลเซียมออกซาเลต . (Development of Raman spectroscopy-integrated calcium oxalate crystallization index (rCOCI) test and its clinical validation for diagnosing calcium oxalate urolithiasis) อ.ที่ปรึกษาหลัก : ผศ. ดร.ชาญชัย บุญหล้า, อ.ที่ปรึกษาร่วม : ผศ. ดร.ภาคภูมิ สมบูรณ์, รศ. ดร.อลงกรณ์ พิมพ์พิณ

โรคนิ่วปัสสาวะส่วนใหญ่เกิดในไตและเกิดซ้ำได้บ่อย ชนิดของนิ่วที่พบได้บ่อย คือ นิ่วแคลเซียมออกซาเลต ปัจจุบันการพัฒนาวิธีการตรวจปัสสาวะเพื่อประเมินความเสี่ยงของการเกิดนิ่วแคลเซียมออกซาเลต ยังเป็นเรื่องท้าทาย เมื่อเร็วๆ นี้คณะผู้วิจัยได้พัฒนาการทดสอบปัสสาวะที่เรียกว่า indole-reacted calcium oxalate crystallization index (iCOCI) test ที่มีความแม่นยำสูงในการวินิจฉัยโรคนิ่วปัสสาวะชนิดแคลเซียมออกซาเลต อย่างไรก็ตาม การทดสอบต้องใช้เวลาและต้องใช้สารเคมีที่มีกรดสูงในการวัดปริมาณผลึกแคลเซียมออกซาเลต ในการศึกษาครั้งนี้ คณะผู้วิจัยมีวัตถุประสงค์เพื่อพัฒนาวิธีการตรวจวัดใหม่ เรียกว่า Raman spectroscopy-integrated calcium oxalate crystallization index (rCOCI) test ซึ่งใช้รามานสเปกโตรสโกปีวัดปริมาณผลึกแคลเซียมออกซาเลตแทนการใช้ปฏิกิริยาเคมีอินโดล ค่า rCOCI ในปัสสาวะที่คำนวณจาก Raman intensity เป็นค่าที่ดีที่สุดสำหรับการหาปริมาณผลึกแคลเซียมออกซาเลต ตรวจสอบความถูกต้องของ rCOCI test และรายงานค่า specificity, linearity, limit of detection (LOD), limit of quantitation (LOQ), repeatability และ reproducibility ผลการตรวจสอบพบว่าวิธี rCOCI ให้ค่าความเป็นเส้นตรงอยู่ในช่วง 50-100 mM ค่า LOD เท่ากับ 24 mM และค่า LOQ เท่ากับ 72 mM ความแม่นยำของ rCOCI test ทั้ง repeatability และ reproducibility อยู่ในช่วงที่ยอมรับได้ การศึกษานี้ยังได้ตรวจสอบความถูกต้องทางคลินิกของ rCOCI test โดยตรวจวัดค่า rCOCI ในตัวอย่างปัสสาวะ 24 ชั่วโมง เพื่อประเมินประสิทธิภาพในการจำแนกผู้ป่วยนิ่วแคลเซียมออกซาเลตออกจากผู้ที่ไม่เป็นนิ่ว ผลการศึกษาพบว่า ระดับ rCOCI ในผู้ป่วยโรคนิ่วแคลเซียมออกซาเลต ($n = 44$) สูงกว่าคนที่ไม่เป็นนิ่ว ($n = 98$) อย่างมีนัยสำคัญ ผลการวิเคราะห์ receiver operating characteristic (ROC) ของ rCOCI test สำหรับจำแนกผู้ป่วยแคลเซียมออกซาเลตออกจากคนที่ไม่เป็นนิ่ว พบว่ามีค่า area under ROC curve เท่ากับ 0.8244 (95% CI: 0.7438 - 0.9051) เมื่อใช้ค่า cutoff ของ urinary rCOCI test ที่ 1.40 จะคำนวณการวินิจฉัยนิ่วแคลเซียมออกซาเลต sensitivity, specificity, positive predictive value, negative predictive value, positive likelihood ratio, negative likelihood ratio และ accuracy ได้เท่ากับ 80.00%, 57.00%, 45.45%, 86.15%, 1.86, 0.36 และ 64.00% ตามลำดับ การศึกษานี้สรุปได้ว่า การทดสอบ urinary rCOCI test สามารถพัฒนาขึ้นได้สำเร็จ ผลการตรวจสอบความถูกต้องของวิธี urinary rCOCI test ยืนยันว่าเหมาะสมสำหรับการหาปริมาณแคลเซียมออกซาเลตเหนี่ยวนำให้เกิดขึ้นในปัสสาวะได้ การตรวจสอบความแม่นยำทางคลินิกแสดงให้เห็นว่า urinary rCOCI test มีประสิทธิภาพดีในการจำแนกผู้ป่วยนิ่วแคลเซียมออกซาเลตออกจากผู้ที่ไม่เป็นนิ่ว คณะผู้วิจัยมีความเชื่อมั่นว่านวัตกรรมวิธี urinary rCOCI test นี้สามารถใช้เป็นวิธีตรวจกรองโรคนิ่วปัสสาวะแคลเซียมออกซาเลต และมีศักยภาพสูงที่จะสร้างผลกระทบทางพาณิชย์ได้

สาขาวิชา ชีวเคมีทางการแพทย์
ปีการศึกษา 2566

ลายมือชื่อนิสิต
ลายมือชื่อ อ.ที่ปรึกษาหลัก
ลายมือชื่อ อ.ที่ปรึกษาร่วม
ลายมือชื่อ อ.ที่ปรึกษาร่วม

6270003130 : MAJOR MEDICAL BIOCHEMISTRY

KEYWORD: Urinary stone disease, calcium oxalate, rCOCI method, Raman spectroscopy, diagnosis

Kamonchat Boonkam : Development of Raman spectroscopy-integrated calcium oxalate crystallization index (rCOCI) test and its clinical validation for diagnosing calcium oxalate urolithiasis.

Advisor: Asst. Prof. CHANCHAI BOONLA, Ph.D. Co-advisor: Asst. Prof. PAKPUM SOMBOON, Ph.D., Assoc. Prof. ALONGKORN PIMPIN, Ph.D.

Urinary stone disease is mostly formed in the kidney and is highly recurrent. The most common type of urinary stones is calcium oxalate (CaOx). The development of urinary screening tests for estimating risk of CaOx stone formation is still challenging. Recently, we developed a urinary test, called indole-reacted calcium oxalate crystallization index (iCOCI) test, that provided a high diagnostic accuracy for CaOx urolithiasis. However, the iCOCI test is time-consuming and highly acidic chemicals are required for quantifying amount of CaOx. In this study, we proposed to develop a new method, called Raman spectroscopy-integrated calcium oxalate crystallization index (rCOCI) test, that used Raman spectroscopy to quantify amount of CaOx produced in the supersaturated urine instead of the indole reaction. Urinary rCOCI value calculated from the Raman peak intensity was the best value for CaOx quantitation. Method validation of the rCOCI test was conducted, and analytical validation parameters including specificity, linearity, limit of detection (LOD), limit of quantitation (LOQ), repeatability, and reproducibility were reported. The rCOCI method was validated within the linear range of 50-100 mM. The LOD and LOQ of the test were 24 mM and 72 mM, respectively. The repeatability and reproducibility of the test were acceptable. For clinical validation, the rCOCI levels were determined in 24-h urine samples to evaluate the performance for distinguishing CaOx stone patients from non-stone forming (NSF) subjects. Urinary rCOCI levels in CaOx stone patients (n = 44) were significantly higher than NSF subjects (n = 98). Receiver operating characteristic (ROC) analysis of urinary rCOCI test for separating CaOx stone patients from NSF subjects revealed an area under the ROC curve of 0.8244 (95%CI: 0.7438-0.9051). At the cutoff of 1.40, the sensitivity, specificity, positive predictive value, negative predictive value, positive likelihood ratio, negative likelihood ratio and accuracy of urinary rCOCI test for diagnosing CaOx urolithiasis were 80.00%, 57.00%, 45.45%, 86.15%, 1.86, 0.36 and 64.00%, respectively. In conclusion, the urinary rCOCI test was successfully developed. Method validation parameters suggested that urinary rCOCI test was suitable for quantifying CaOx produced in supersaturated urine. Clinical accuracy testing demonstrated that urinary rCOCI test had a good performance for separating CaOx urolithiasis from NSF individuals. We believed that this innovative urinary rCOCI test could be used for screening CaOx urolithiasis, and it could provide a significant commercial impact in the future.

Field of Study: Medical Biochemistry

Student's Signature

Academic Year: 2023

Advisor's Signature

Co-advisor's Signature

Co-advisor's Signature

ACKNOWLEDGEMENTS

First of all, I would like to express my gratitude to my advisor, Asst. Prof. Chanchai Boonla, Ph.D., for helping and suggesting my master's degree study. I appreciate his kindness, high endurance, and always caring for me. The successful completion of this study is attributed to the guidance of my professors who have provided both knowledge and critical thinking skills. Furthermore, I would like to thank you for supporting me in giving me a good experience for student exchange in Germany.

Second, I would like to special thank my thesis co-advisor, Asst. Prof. Pakpum Somboon, Ph.D. and Assoc. Prof. Alongkorn Pimpin, Ph.D. for equipment and guidelines that help improve me. I am grateful for your kindness. Especially, getting new knowledge and new experiments in the engineering field. In addition, I would like to express thank you to the professors from the engineering department, who have provided idea guidance and offered new ideas, especially Assistant Professor Nitiphan Sribunruangrit, Ph.D.

I am grateful and thank you for the opportunity to research exchange scholarship at Charité – Universitätsmedizin Berlin. I would like to express gratitude to Professor Hans Bäumlér for giving me a wonderful chance to experience research, life, culture, and society. All of my skills were improved with confidence, including my English skills.

I am grateful and thank you to my thesis committee, Prof. Sittisak Honsawek, M.D., Ph.D., Asst. Prof. Supranee Kongkham, Ph.D., and Ponchai Kaewsapsak, Ph.D for their valuable advice, which contributed to the successful completion of my thesis Thank you for “the rCOCI scholarship” from Program Management. Unit Competitiveness (PMUC), Ratchadapisek type I research Fund, Chulalongkorn University” that support research fee and "60/40 study scholarship in academic year 2019 faculty of graduate school, Chulalongkorn University" for the one-year semester fee.

Finally, my special thanks to the members 806 lab for always supporting and encouraging me. One thing that is indispensable and important for me is my family for supporting and encouraging me with love.

จุฬาลงกรณ์มหาวิทยาลัย
CHULALONGKORN UNIVERSITY

Kamonchat Boonkam

TABLE OF CONTENTS

	Page
.....	iii
ABSTRACT (THAI).....	iii
.....	iv
ABSTRACT (ENGLISH).....	iv
ACKNOWLEDGEMENTS.....	v
TABLE OF CONTENTS.....	vi
LIST OF TABLES.....	xi
LIST OF FIGURES.....	xii
Chapter1 Introduction.....	1
1. Background and rationales.....	1
Chapter2 Literature review.....	5
2.1 Urinary stone disease.....	5
2.2 Types of urinary stones.....	7
2.3 Risk factors of urinary stones disease.....	7
2.4 Mechanism of stone formation.....	8
2.5 Diagnosis of urinary stones disease.....	9
2.6 Estimating the risk of urinary calcium oxalate formation.....	10
2.7 Urinary COCI test.....	11
2.8 Test accuracy study according to the STARD guideline.....	12
2.9 Urinary indole-reacted calcium crystallization index (iCOCI) test.....	14
2.10 Raman spectroscopy.....	16

2.11 Method validation.....	18
2.12 Clinical validation.....	22
Conceptual framework.....	23
Chapter 3 Material and methods.....	25
3.1 Study design.....	25
3.2 Equipment and Chemicals.....	26
3.3 24-h urine specimen collection.....	28
3.4 Procedure of urinary rCOCI test.....	28
3.5 Method validation of urinary rCOCI test.....	31
3.6 Urinary iCOCI test and correlation between urinary rCOCI and iCOCI values.....	32
3.7 Calcium measurement in urine by Arsenazo III method.....	33
3.8 The creatinine assay.....	34
3.9 Protein concentration measurement in urine.....	35
3.10 2 x 2 Table for calculation of diagnostic values of rCOCI test.....	36
3.11 Statistical analysis.....	36
Chapter 4 Results.....	37
Part I: Development and optimization of the urinary rCOCI test.....	37
4.1 Establishment of rCOCI method for detecting and quantitating CaOx crystallization in 24-h urine.....	37
4.1.1 CaOx in liquid form could not be measured properly by Raman spectroscopy.....	37
4.1.2 Light and coverslip were interfered with the Raman signal.....	38
4.1.3 To increase the Raman signal, CaOx crystal sample must be placed on slide as a small disc (0.3 cm diameter).....	39

4.1.4 The precision of CaOx Raman spectra measurement in one sample with different microscopic areas.....	40
4.1.5 Optimization of spiked oxalic acid concentration to be able to clearly detect the Raman signal.....	41
4.1.6 Removal of calcium phosphate interference by acetic acid.	42
4.1.7 Not only COM, COD could also co-precipitated in urine sample after adding oxalic acid and CaCl ₂	43
4.1.8 COD crystals were confirmed by FTIR analysis.....	44
4.1.9 The quantification of calcium oxalate crystals in the rCOCI test.	45
4.1.10 The size of CaOx crystals produced by COCI procedure.....	46
Part II. Method validation.....	47
4.2 Method validation of the rCOCI procedure.....	47
4.2.1 The specificity.....	48
4.2.2 The linearity.....	56
4.2.3 Sensitivity.....	59
Limit of detection (LOD) and limit of quantitation (LOQ).....	59
4.2.4 Precision (repeatability and reproducibility).....	61
Repeatability.....	61
Reproducibility.....	64
Stability of CaOx crystals produced by COCI procedure.....	66
Correlation of urinary rCOCI values calculated from spectrum of FTIR and Raman spectroscopy.....	67
Part III: Clinical validation.....	68
4.3.1. 24-h urine samples.....	68
4.3.2. Determination of rCOCI levels in 24-h urine samples.....	69

4.3.3. rCOCI measurement in 24-hour urine samples.....	70
1. rCOCI measurement in 98 NS subjects and 127 stone patients (n= 225)	70
2. Urinary rCOCI levels compared between the NS (n=98) subjects and stone patients with known stone type (n=58).....	71
3. The urinary rCOCI levels compared among the NS subjects (n=98) and stone patients (n=58) with different stone types.	72
4. The urinary rCOCI levels compared between the NS subjects (n=98) and CaOx stone patients (n=44).....	73
5. ROC analysis of the urinary rCOCI test.....	74
5.1 The result of ROC analysis to classify NS (n=98) and ST (n=127) subjects.....	74
5.2 The result of the ROC analysis of the urinary rCOCI test for classifying NS subjects (n=98) and ST patients with known type of stones (n=58).....	75
5.3 The result of the ROC analysis of the urinary rCOCI test for classifying NS subjects (n = 98) and CaOx stone patients (n=44).....	75
6. Selection of urinary rCOCI cutoff values.....	76
7. Diagnostic values of urinary rCOCI test for CaOx urolithiasis.....	76
8. The correlation among urinary rCOCI values calculated from peak intensity, AUP and FWHM.....	78
9. The diagnostic performance of all three calculations of urinary rCOCI test assessed by multiple logistic regression.....	79
Chapter 5 Discussion and Conclusion.....	81
APPENDIX.....	89

REFERENCES..... 95

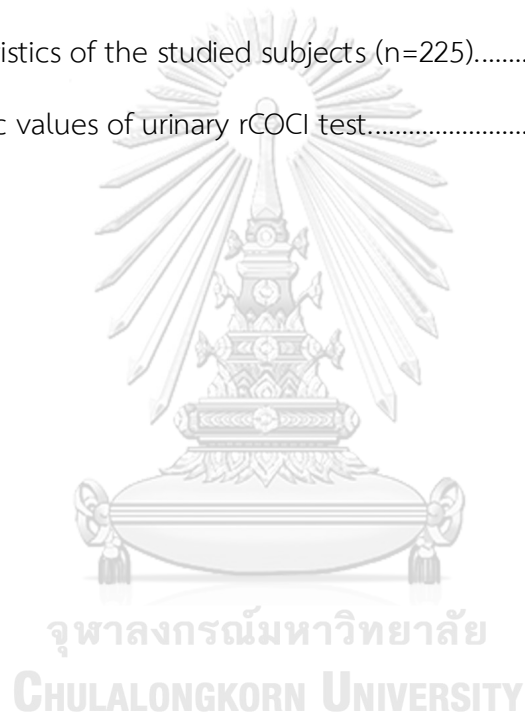
REFERENCES..... 104

VITA..... 106



LIST OF TABLES

	Page
Table 1 Sensitivity and specificity of common imaging modality.....	10
Table 2 The STARD 2015 checklist for diagnostic accuracy study.....	13
Table 3 List of equipment used in this study.....	26
Table 4 List of chemicals used in this study.....	27
Table 5 Characteristics of the studied subjects (n=225).....	68
Table 6 Diagnostic values of urinary rCOCl test.....	77



LIST OF FIGURES

	Page
Figure 1 Urinary stone location in the urinary tract.....	5
Figure 2 World map of the magnitude of nephrolithiasis prevalence modeled based on the three risk factors.....	6
Figure 3 Schematic step of stone formation	9
Figure 4 Level of urinary COCI compared between nephrolithiasis patients and healthy controls.....	11
Figure 5 ROC analysis of COCI test for distinguishing between nephrolithiasis and healthy.....	11
Figure 6 STARD flow diagram 2015.....	12
Figure 7 STRAD flow diagram for accuracy testing of the urinary iCOCI test	15
Figure 8 urinary iCOCI compare between stone and non-stone formers.....	15
Figure 9 Generation of the three types of Raman scattering lights.....	16
Figure 10 The Raman spectrum of COM.....	17
Figure 11 Type of analytical process and ICH characteristic.....	19
Figure 12 Process diagram for validation of the analytical method.....	19
Figure 13 Summary of planning experiment for validation of a new analytical method.....	21
Figure 14 Precision of reproducibility of measurement voriconazole in human plasma	22
Figure 15 The 2 x 2 Table for calculating sensitivity, specificity, and accuracy	22
Figure 16 Flow chart of the analytical and clinical validation	23
Figure 17 The simplified cartoon depicting the procedure of urinary rCOCI test.....	24

Figure 18 Workflow of the study.....	26
Figure 19 The Raman spectroscopy from HORIBA Instruments with laser module 785 nm.....	30
Figure 20 The characteristic Raman peaks of standard COM&COD reference.....	30
Figure 21 Calculation of urinary rCOCl value. Quantitative parameters (peak intensity (I) or AUP or FWHM) of CaOx crystals.....	31
Figure 22 The standard curve of COM used in the urinary iCOCl test.....	33
Figure 23 The standard curve of calcium chloride used in the Arsenazo III for urinary calcium determination.....	34
Figure 24 The standard curve of creatinine.....	35
Figure 25 2 x 2 Table for calculation of diagnostic values.....	36
Figure 26 Raman spectra of solid CaOx samples.....	37
Figure 27 Raman spectra of liquid CaOx samples.....	38
Figure 28 Effect of light and coverslip on Raman signal.....	39
Figure 29 The optimized diameter of CaOx crystal samples for Raman spectroscopy analysis.....	40
Figure 30 Precision of the quantitative measurement of the CaOx Raman signal in control (water) and test (real urine).	41
Figure 31 The CaOx crystals are produced from different concentrations of spiked oxalic acid in control (A) and test (B) conditions.....	42
Figure 32 Removing calcium phosphate interference by acetic acid.	43
Figure 33 Raman spectroscopy of COM and COD.....	44
Figure 34 Comparison of FTIR spectrum of COM and COD.....	45
Figure 35 The standard curve of the Raman intensity against spiked oxalic acid concentrations.....	46
Figure 36 The COCl crystals imaged by EVOS FL Ato2 Imaging System.	47

Figure 37 Electron micrographs of COCl crystals.....	47
Figure 38 Removal of calcium phosphate by acetic acid treatment.....	48
Figure 39 The normal ranges of urine components in healthy urine.	49
Figure 40 The Raman characteristics of creatinine, urea, CaP, and uric acid.....	50
Figure 41 Comparison of Raman spectrum of CaOx crystals produced in artificial urine and water (control).	50
Figure 42 Interfering effect of creatinine in quantifying CaOx.....	52
Figure 43 Interfering effect of phosphate in quantifying CaOx.....	53
Figure 44 Interfering effect of urea in quantifying CaOx.....	54
Figure 45 Interfering effect of uric acid (UA) in quantifying CaOx.....	55
Figure 46 Characteristics of CaOx generated in water (control).	57
Figure 47 Characteristics of CaOx generated by COCl procedure in pooled non-stone urine.....	58
Figure 48 Characteristics of CaOx generated by COCl procedure in pooled stone urine.....	59
Figure 49 LOD and LOQ of rCOCl measurement performed in water sample.....	60
Figure 50 LOD and LOQ of rCOCl measurement performed in pooled non-stone (NS) and pooled stone (ST) urine samples.....	61
Figure 51 10 different batches of rCOCl measurement in control (water).	62
Figure 52 10 different batches of rCOCl measurement in urine samples.....	63
Figure 53 10 different batches of rCOCl measurement in pooled urine samples.	64
Figure 54 Reproducibility of rCOCl measurement (between day measurement).....	65
Figure 55 Stability of CaOx crystals produced from COCl procedure in a month.....	66
Figure 56 Correlation of CaOx quantitative measurement by Raman spectroscopy and FTIR technique.....	67

Figure 57 Raman spectra of urine samples with high background noise and no signal of CaOx.....	70
Figure 58 The level of urinary rCOCI calculated from peak intensity (left), FWHM (middle), and AUP (right).....	71
Figure 59 The levels of urinary rCOCI compared between 58 stone patients and 98 NS subjects.....	71
Figure 60 Comparison of urinary rCOCI levels calculated from intensity of peak, FWHM, and AUP between NS subjects and ST patients with different type of stones.	73
Figure 61 The comparison of urinary rCOCI levels between 98 NS subjects and 44 CaOx stone patients.	74
Figure 62 ROC analysis of urinary rCOCI calculated from peak intensity, FWHM, and AUP for distinguishing NS subjects (n=98) from ST patients (n=127).....	74
Figure 63 ROC analysis of urinary rCOCI calculated from the intensity of peak, and FWHM for separating NS subjects from stone patients with known stone type (n=58)	75
Figure 64 ROC analysis of urinary rCOCI calculated from the intensity of peak, FWHM and AUP to distinguish NS subjects (N=98) from CaOx stone patients (n=44).	76
Figure 65 The correlation of urinary rCOCI levels calculated from intensity, FWHM, and AUP.....	79
Figure 66 The combination of rCOCI values (Intensity, FWHM, AUP) for predicting urolithiasis.....	80
Figure 67 The characteristics of CaOx were confirmed by FTIR and XRD in the urine sample spiked with oxalic acid and CaCl ₂	89
Figure 68 The Raman characteristic of COCI crystals that were produced by varying sodium citrate and calcium chloride concentrations.....	90

Figure 69 The level of urinary rCOCl calculated for COM compared between stone and non-stone groups.....	91
Figure 70 The level of urinary rCOCl calculated for COD compared between stone and non-stone groups.....	91
Figure 71 ROC analysis of urinary rCOCl value of COM for distinguishing NS subjects (n=62) from ST patients (n=78).	92
Figure 72 ROC analysis of urinary rCOCl of COD for distinguishing NS subjects (n=36) from ST patients (n=49).....	92



Chapter1 Introduction

The title

(ภาษาไทย): การพัฒนาวิธี Raman spectroscopy-integrated calcium oxalate crystallization index(อาร์โคซี)และการทดสอบทางคลินิกสำหรับวินิจฉัยโรคนิ่วปัสสาวะชนิดแคลเซียมออกซาเลต

(English): Development of Raman spectroscopy-integrated calcium oxalate crystallization index (rCOCI) test and its clinical validation for diagnosing calcium oxalate urolithiasis.

1. Background and rationales

Urinary stone disease or urolithiasis is a common urologic condition with calcified masses in urinary tract. Globally, prevalence of urolithiasis is ranging from 1% to 20% depending on regions[1]. In Asia, prevalence of urolithiasis is generally higher than in western countries, reported up to 20%[2]. Stone disease is highly recurrent. The recurrence rate in Asia is reported about 50% within five years after stone removal[3]. In Thailand, the highest stone prevalence (17%) is reported in the northeastern region with a recurrence rate of 53% within 3 to 5 years[2]. In fact, urinary stone disease is an ancient condition inflicted on humankind since antiquity. The oldest urinary stone was found in a 7,000-year-old Egyptian mummy. However, stone disease is still a common disease in humans nowadays. To reduce the burden of urinary stone disease, the mechanism of urinary stone formation must be fully elucidated. Furthermore, accurate diagnostic tools and effective therapeutic regimens must be developed.

Etiology of urolithiasis is multifactorial. Several stone risk factors including extrinsic factors such as dietary, lifestyle and climate, and intrinsic factors such as age, sex and genetic susceptibility have been identified[4]. Most stones form in the kidneys, known as kidney stone disease or nephrolithiasis. Kidney stone recurrence progressively impairs kidney function and reduces glomerular filtration rate (GFR), hence increasing risks of chronic kidney disease (CKD) and end-stage renal disease (ESRD)[5]. Moreover, kidney stone disease is closely linked to developments of many

chronic diseases such as diabetes, obesity, hypertension, and cardiovascular disease[6].

Urinary stones are basically classified into two main classes according to calcium composition, calcium, and non-calcium stones. Calcium stones are more prevalent than non-calcium stones, accounting for up to 80% of all stones. The most common type of calcium stone is calcium oxalate (CaOx), and the CaOx stone is frequently mixed with calcium phosphate (CaP)[7]. Hyperoxaluria, hypercalciuria, and hypocitraturia are the main causes of CaOx stone formation. Together with low fluid intake, urine becomes supersaturated and CaOx crystal formation is initiated. The predominant CaOx crystals formed in the supersaturated urine is calcium oxalate monohydrate (COM) that directly drives CaOx lithogenic process[7],[1, 8].

Diagnosis of urinary stones requires radioimaging tools such as kidney-ureter-bladder (KUB) x-ray, ultrasonography, and computed tomography (CT). CT scan is a gold standard method for stone diagnosis because it has the highest diagnostic sensitivity and accuracy[9],[10],[11, 12]. However, CT scan has some disadvantages. The cost is relatively high. It is usually available only in well-equipped hospitals. It is not available in the hospitals in rural communities. Therefore, development of an innovative diagnostic tool with high diagnostic accuracy, easy to use, and relatively low cost, is needed.

In CaOx lithogenesis, CaOx crystallization is a key prerequisite step for stone formation. Therefore, measurement of CaOx crystal formation capacity in urine can be used to predict or estimate the risk of CaOx formation. The Bonn-Risk Index (BRI) has been developed to quantify the potentiality of CaOx crystallization in urine, and it shows high sensitivity and specificity for diagnosing urinary stone disease[13, 14][15]. However, this method is relatively complicated because it needs to measure calcium ion concentration and monitor the first crystals formed (crystal nucleation) in the sample. We recently developed an alternative method that measured the total capacity of CaOx crystallization in supersaturated urine, called calcium oxalate crystallization index (COCI) test. This urinary COCI test provided the high diagnostic power for separating non-stone individuals from stone patients[16]. Later, we modified the COCI method to be more specific to CaOx stone using an indole-

oxalate chemical reaction, and we called it the indole-reacted calcium oxalate crystallization index (iCOCI) test[17]. Our urinary iCOCI test has a high accuracy for diagnosing CaOx urolithiasis, and it is promising to be used as a screening test for CaOx urolithiasis. 24-h urine sample is required for the iCOCI measurement, and the cutoff value for a positive iCOCI result is of more than 0.8 COM equivalence, g/day[17]. Although iCOCI test has high sensitivity, specificity, and accuracy for diagnosing CaOx stone disease, it is relatively time-consuming (approximately 2-3 h for the whole procedure) and it has a relatively low throughput. Therefore, the new method for measuring CaOx crystallization capacity is required to minimize the measurement time and increase the throughput.

Raman spectroscopy has been successfully and widely used for identification and quantitation of molecules and compounds. In this study, we purpose to use the Raman spectroscopy for detection and quantitation of CaOx crystals produced by the COCI procedure instead of using the indole-oxalate reaction. This proposed method is called the Raman spectroscopy-integrated calcium oxalate crystallization index (rCOCI) test. We hypothesized that the urinary rCOCI method would be less time-consuming (about 30-60 min for the whole procedure) than urinary iCOCI test with a comparable diagnostic accuracy for CaOx urolithiasis to the urinary iCOCI test.

Fundamentally, after establishing the new analytical method, the method validation is required to demonstrate that the new method is suitable for the intended use or purpose. The method validation parameters for the quantitative method include selectivity, linearity (calibration model), accuracy (bias), precision, and limit of quantification (LOQ). Other parameters, such as the limit of detection (LOD), recovery, repeatability, and robustness, are also related and needed to be reported[18-20]. After method validation, clinical validation in real clinical specimens must be carried out to obtain the diagnostic performance of the new method, and diagnostic values including sensitivity, specificity, and accuracy must be reported.

In this study, we aimed to develop the urinary rCOCI test employing Raman spectroscopy for detecting and quantitating CaOx crystals that were produced by the COCI procedure. Method validation of the urinary rCOCI test was carried out. Finally, clinical validation was conducted to evaluate the diagnostic accuracy of the urinary

rCOCI test. The urinary rCOCI values were determined in 24-h urine samples obtained from urolithiasis patients and non-stone forming subjects. Correlation between urinary rCOCI and urinary iCOCI test results was also assessed.

Keywords: Urinary stone disease, Urolithiasis, Calcium oxalate, Raman spectroscopy, rCOCI, iCOCI, Screening test

Research questions

1. Was the rCOCI test successfully established for detecting and quantitating CaOx crystals produced in supersaturated urine?
2. What were method validation parameters (selectivity, linearity, accuracy, precision, limit of detection and repeatability) of the established urinary rCOCI test?
3. What was the diagnostic performance of urinary rCOCI test for CaOx urolithiasis using CT scan as a gold standard method?

Research hypotheses

1. The urinary rCOCI test could be successfully established for detecting and quantitating CaOx crystals produced in supersaturated urine.
2. Based on the method validation parameters, the established urinary rCOCI test was suitable for the intended use.
3. The diagnostic performance of urinary rCOCI test was good for separating CaOx urolithiasis patients from non-stone forming (NSF) individuals.

Research objectives

1. To develop a new method, urinary rCOCI test, for quantitative detection of CaOx crystals produced in the supersaturated urine samples (challenged with oxalate and excessive calcium).
2. To perform method validation of the urinary rCOCI test.
3. To conduct clinical validation of the urinary rCOCI test to assess the diagnostic performance of the test for CaOx urolithiasis.

Chapter2 Literature review

2.1 Urinary stone disease

Urinary stone disease or urolithiasis is a common urological condition found in all countries across the world[21]. The stone is formed by accumulation of mineral masses in the urinary tract either in kidney (nephrolithiasis), ureter (ureterolithiasis), or bladder (cystolithiasis) (Figure 1). Urolithiasis is a true ancient condition[22]. The first stone in human is found in the bladder of Egyptian mummy, and it consists of uric acid (UA), calcium oxalate (CaOx), and calcium phosphate (CaP)[23]. Most urinary stones form in the kidney, and they progressively cause the decline of kidney function, decreases the estimated glomerulus filtration (eGFR) and increase the risk of chronic kidney disease (CKD) that finally lead to end-stage renal disease (ESRD)[6]. Importantly, the stone disease has a high recurrence rate. Stone surgery removes only the symptoms of stone, but not the cause. Therefore, investigating the cause of stone formation and implementing the preventive measure are key factors to prevent the stone recurrence. Furthermore, the stone disease is associated with the development of other chronic diseases such as cardiovascular disease, hypertension, diabetes, and obesity, suggesting that urinary stone disease can be considered as a systemic metabolic disorder[5-7, 24].

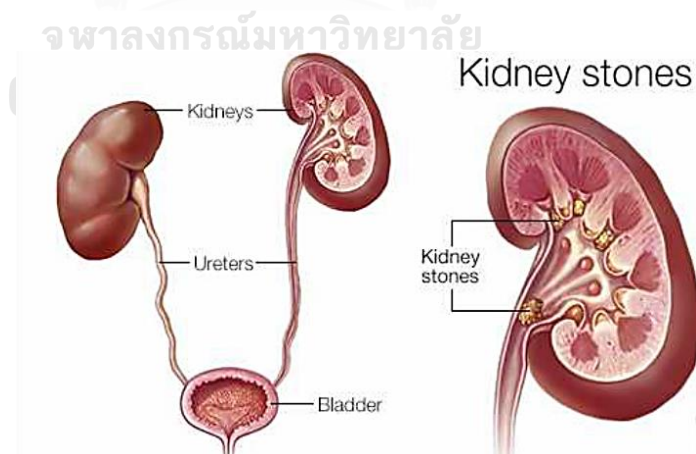


Figure 1 Urinary stone location in the urinary tract. (kidney, ureter, and bladder)[7, 25].

Globally, the prevalence of urolithiasis is varied among regions, for instances, about 7-13% in North America, 5-9% in Europe, and 1-5% in Asia[26][27],[28]. Because stone disease is a multifactorial disease, there are several factors associated with stone formation such as climate, occupation, socioeconomic status, race, lifestyle, and dietary habit[2, 26]. In Asia, the highest prevalence of stone is reported in the Middle East (Saudi Arabia) because of climate, lifestyle, and dietary habit[2]. In Thailand, the highest prevalence is reported at 17% in the northeast region[2, 29]. The stone recurrence rate is documented approximately at 6-17% within 1 year, and at 21-53% within 3-5 years, and the risk of recurrence is approximately 60-80%[2]. Therefore, urolithiasis is a significant public health problem worldwide that requires an accurate diagnosis and effective and affordable treatment[30]. Dietary intake, lifestyle, genetic, and environmental factors are the four significant risk factors of urinary stone formation[31]. Lifestyle and diet are highly causative for kidney stone formation in the US, and the projected prevalence of nephrolithiasis based on the three influential factors (dietary intake, obesity, and climate) compared among countries is shown in Figure 2[31].

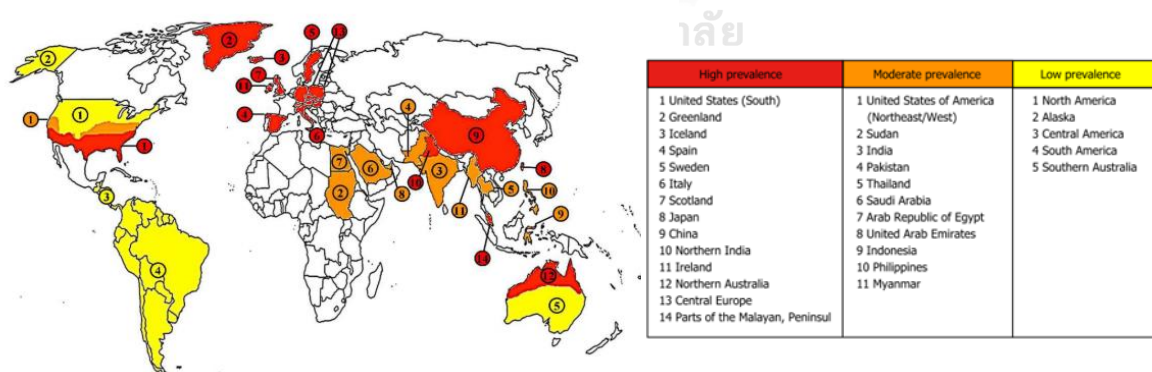


Figure 2 World map of the magnitude of nephrolithiasis prevalence modeled based on the three risk factors including dietary intake, obesity, and climate. Degree of prevalence (high: red), (moderate orange), (low: yellow)[31].

2.2 Types of urinary stones

The types of urinary calculi are classified by the mineral composition of stones divided into two main types, calcium stones and non-calcium stones. The calcium stone can be composed of pure calcium oxalate (CaOx), calcium phosphate (CaP), or mixture of CaOx and CaP[32]. Non-calcium stones include uric acid (UA), struvite or magnesium ammonium phosphate (MAP), and cystine. The most common type of stones is CaOx stone, and it can be found up to 80%. In the western countries, the patients are mostly characterized by hypercalciuria urinary calcium > 250 mg/day (for female), > 300 mg/day (for male) and hyperoxaluria (urinary oxalate levels > 40 mg/day)[33-35]. CaP stone frequently consists of apatite or brushite, which is associated with urinary pH > 7, and this stone type is found at approximately 5%[7]. In non-calcium stones, UA is the most prevalent one, and it is associated with acidic urine (urinary pH < 5.5)[7, 33, 36]. MAP stone is associated with urinary infection and alkali urine (pH > 7.2), and it is found at approximately 10-15%[33]. Cysteine is a form of genetic stone that is found less than 2%[7].

In Thailand, CaOx, CaP, UA, and struvite stones were found at 70%, 5%, 16%, and 5%, respectively[36]. Therefore, CaOx is the most common in urinary stone disease in Thailand. The CaOx crystals are found in three different hydrated forms, including CaOx monohydrate (COM; $\text{CaC}_2\text{O}_4 \cdot \text{H}_2\text{O}$) that COM most common form found in CaOx stone[24, 37], dihydrate (COD; $\text{CaC}_2\text{O}_4 \cdot 2\text{H}_2\text{O}$), and trihydrate (COT; $\text{CaC}_2\text{O}_4 \cdot 3\text{H}_2\text{O}$).

2.3 Risk factors of urinary stones disease

The risk factors of stone formation are divided into two groups, the intrinsic factors, and the extrinsic factors. Intrinsic factors include age, gender, ethics, family history, and body mass index (BMI). Extrinsic factors include dietary intake, lifestyle, climate, occupation, drugs, and stress[38].

For intrinsic factors, previous studies showed that men are still more affected than women, and one possible explanation is that women have higher urinary pH than men due to the greater absorption of dietary organic anion that further

increases the urinary citrate excretion[39]. In the current literature, the ratio of males-to-females for stone disease is less than 2:1[2, 29, 39]. The incidence of urolithiasis begins to increase after the age of 20 years old in males, and the peak is between 40 and 70 years old[40, 41]. In addition, the data from the National Health and Nutrition Examination Survey (NHANES) in 2007-2012 demonstrate that there is no difference in stone prevalence between males and females in adults younger than 50 years old[39]. In Thailand, the northeastern region has the highest rate of family history of kidney stone disease than the other regions, and the risk of stone formation is increased with a relative risk of 3.18 among affected family member[42].

The main extrinsic factors for stone disease are lifestyle and dietary habits that include high calcium, high oxalate, low fluid, and low citrate intake. Climate and occupation also contribute to stone formation. Climate and geography related to high temperatures can hasten the evaporation of body water from the skin, and occupation exposed to heat can cause dehydration and decrease urine volume[26, 43].

2.4 Mechanism of stone formation

The main concept of urinary stone formation is the imbalance between stone promoters and stone inhibitors such as hypercalciuria (urinary calcium excretion > 250 mg/d (F), > 300 mg/d (M)), hypocitraturia (urinary citrate excretion < 320 mg/d), and hyperoxaluria (urinary oxalate excretion > 40 mg/d) that directly causes urine supersaturation and crystallization[44]. The building block of stone is lithogenic crystals formed in supersaturated urine such as CaOx, CaP, and UA crystals. CaOx is the most common lithogenic crystals, and it mostly exists in the form of COM. The mechanism of stone formation is divided into 2 phases, nucleation, and crystal growth phases. Nucleation occurs in the urine saturated with free calcium and oxalate ions. The newly formed crystals will further aggregate, grow, and finally become stone. The crystals can also directly interact and injure the renal tubular cell resulting in cell injury and crystal adhesion. After crystals are retained and adhered, the nidus (stone origin) is formed, grown, and eventually becomes stone[7, 45]. In

addition, the lithogenic crystals induce tubular injury, stimulate an inflammatory response and oxidative stress that in turn increases renal tubular injury and enhance stone formation (Figure 3)[7, 45].

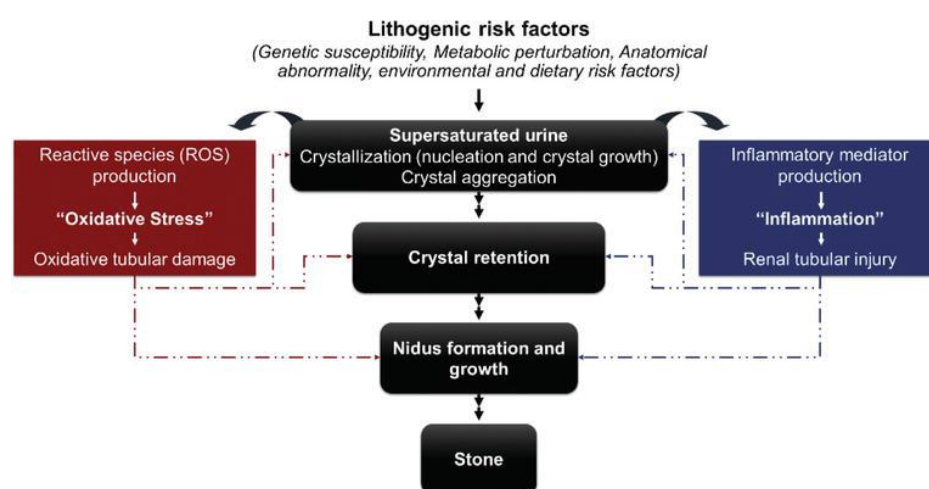


Figure 3 Schematic step of stone formation [45].

2.5 Diagnosis of urinary stones disease

Current technology used to diagnose urinary stone disease includes plain film KUB (located in the kidney, ureter, and bladder), ultrasonography, non-contrast computed tomography (CT), and magnetic resonance imaging (MRT). Each imaging technique has different sensitivity and specificity for stone diagnosis as shown table 1.

The gold standard for urolithiasis diagnosis is a non-contrast computed tomography (CT). It can detect all stone types. The disadvantages of CT scan are that patients expose to radiation, small stones (<5 mm) can be missed, it has high cost, and it is not available in all hospitals, particularly those in rural areas[40]. Ultrasonography is often more common than CT because it has a lower cost, and it

can evaluate kidney edema. The advantages of ultrasonography are non-invasive, easy to use, and safe for pregnant women; however, the small stone can be undetected[12, 46, 47]. MRI is useful in the case of pregnancy and children (3D imaging). The disadvantage of MRI are time-consuming and expensive[48]. Therefore, development of the new diagnostic tools is still needed for screening the risk of urolithiasis, and for detecting the small stone that cannot be detected by the imaging modalities.

Table 1 Sensitivity and specificity of common imaging modality [40]

Imaging modality	Sensitivity, %	Specificity, %
KUB	45-58	60-77
Ultrasonography	54-64	91-100
CT	91-100	95-100
MRI	Not reported	~ 93

2.6 Estimating the risk of urinary calcium oxalate formation

As mentioned above, CaOx crystallization leads to urinary CaOx stone formation. Thus, measuring the CaOx crystallization potential in urine is helpful for diagnosis or estimating the risk of CaOx calculi development. Sriboonlue et al. established an indirect method for estimating urinary oxalate from calcium oxalate precipitate (COP) induced by excess calcium ion and ethanol[14]. This method eliminates phosphate by acetic acid[14]. The calcium level in COP is measured by absorption spectrophotometer that was correlated with urinary oxalate measured by enzymatic method[14]. Later, Laube et al. developed a new method called Bonn Risk Index (BRI) for calculating the risk of CaOx crystallization in the urine by using a ratio of calcium ion to oxalate ions[13, 15, 49, 50]. The BRI is effective in distinguishing CaOx stone from healthy subjects (sensitivity 69.7%, specificity 100%)[16].

2.7 Urinary COCI test

In 2014, we developed an alternative method, called Calcium Oxalate Crystallization Index (COCI), for distinguishing nephrolithiasis patients from healthy (Figure 4)[16]. The oxalate detection of COCI method is based on the measurement of absorbance at 215 nm (for oxalate detection). The COCI cutoff value is set at 165 mg oxalate equivalence/day. The COCI test provides high diagnostic power with sensibility at 83.33%, specificity at 97.18%, accuracy at 90.21%. The area under ROC curve of the urinary COCI test is 0.95 (95%CI: 0.9131-0.9868) (Figure 5) indicating that it is promising to be useful in the real clinical setting. However, the downside of COCI test is that measurement of absorbance at 215 nm is not only specific to oxalate. Other organic acids in the sample could also absorb at this UV wavelength.

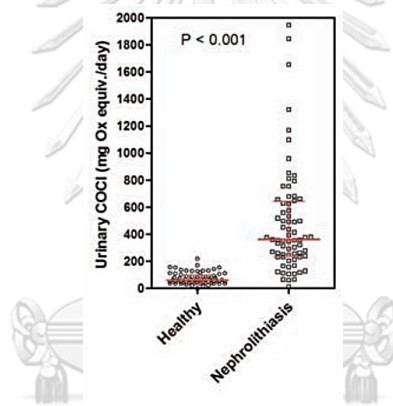


Figure 4 Level of urinary COCI compared between nephrolithiasis patients and healthy controls [16].

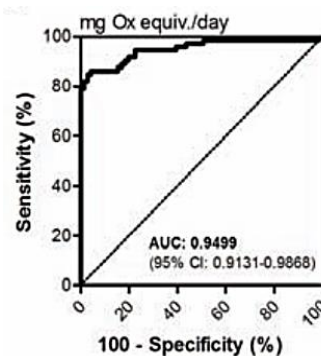


Figure 5 ROC analysis of COCI test for distinguishing between nephrolithiasis and healthy [16].

2.8 Test accuracy study according to the STARD guideline

In general, after the development of the prototype of the new diagnostic test (called index test), the index test must be validated before the implementation in clinics to avoid the risk of bias, and the validation protocol is recommended to follow the Standard for Reported of Diagnostic Accuracy Studies (STARD) statement[51, 52]. According to the STARD guideline, the major source of bias is from the methodology, participant recruitment, data collection, and data analysis.

The diagnostic accuracy of the new index test must be assessed and compared against the gold standard method. The STARD flow diagram and checklist derived from the STARD guideline 2015 are displayed in Figure 6 and Table 2.

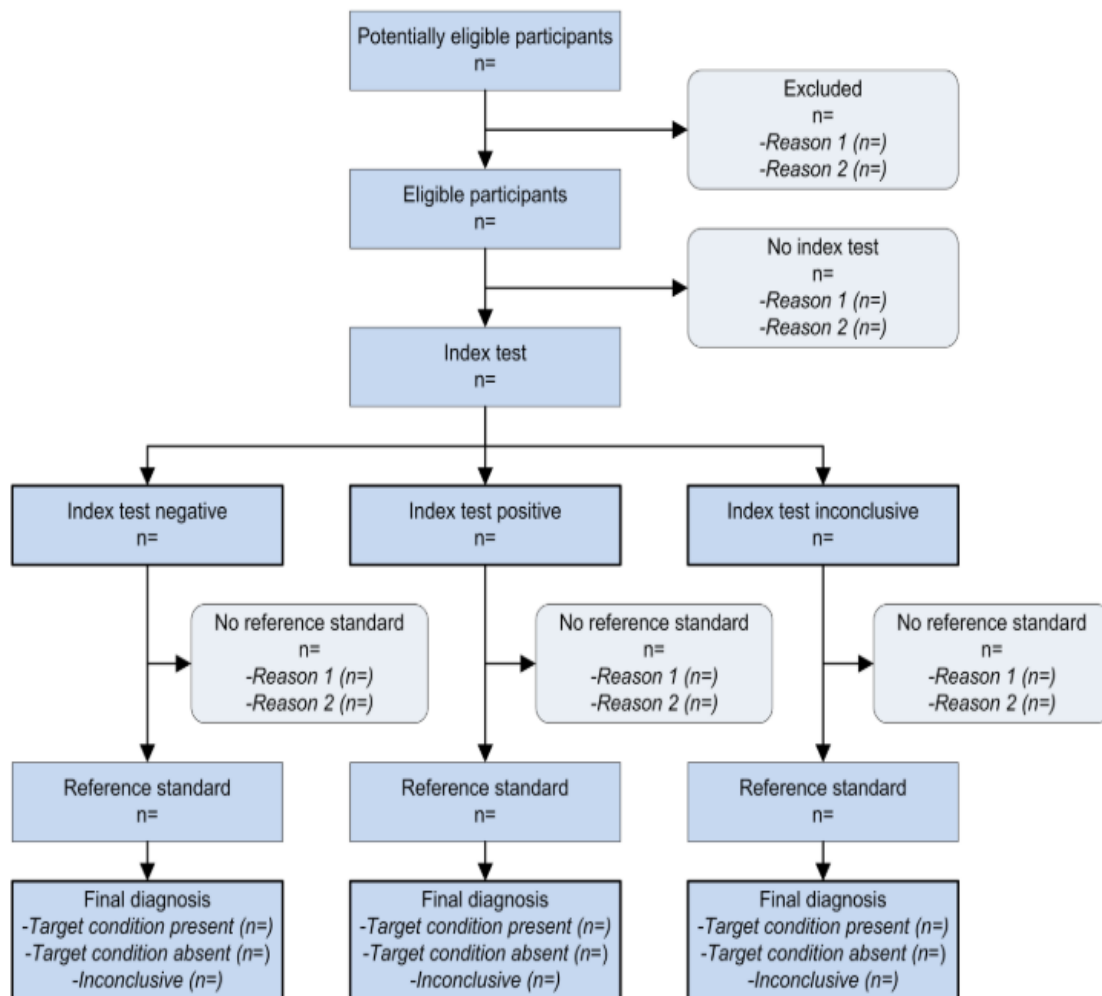


Figure 6 STARD flow diagram 2015 [51].

Table 2 The STARD 2015 checklist for diagnostic accuracy study [52].

Section and topic	No	Item
Title or abstract		
	1	Identification as a study of diagnostic accuracy using at least one measure of accuracy (such as sensitivity, specificity, predictive values, or AUC)
Abstract		
	2	Structured summary of study design, methods, results, and conclusions (for specific guidance, see STARD for Abstracts)
Introduction		
	3	Scientific and clinical background, including the intended use and clinical role of the index test
	4	Study objectives and hypotheses
Methods		
Study design	5	Whether data collection was planned before the index test and reference standard were performed (prospective study) or after (retrospective study)
Participants	6	Eligibility criteria
	7	On what basis potentially eligible participants were identified (such as symptoms, results from previous tests, inclusion in registry)
	8	Where and when potentially eligible participants were identified (setting, location, and dates)
	9	Whether participants formed a consecutive, random, or convenience series
Test methods	10a	Index test, in sufficient detail to allow replication
	10b	Reference standard, in sufficient detail to allow replication
	11	Rationale for choosing the reference standard (if alternatives exist)
	12a	Definition of and rationale for test positivity cut-offs or result categories of the index test, distinguishing pre-specified from exploratory
	12b	Definition of and rationale for test positivity cut-offs or result categories of the reference standard, distinguishing pre-specified from exploratory
	13a	Whether clinical information and reference standard results were available to the performers or readers of the index test
	13b	Whether clinical information and index test results were available to the assessors of the reference standard
Analysis	14	Methods for estimating or comparing measures of diagnostic accuracy
	15	How indeterminate index test or reference standard results were handled
	16	How missing data on the index test and reference standard were handled
	17	Any analyses of variability in diagnostic accuracy, distinguishing pre-specified from exploratory
	18	Intended sample size and how it was determined
Results		
Participants	19	Flow of participants, using a diagram
	20	Baseline demographic and clinical characteristics of participants
	21a	Distribution of severity of disease in those with the target condition
	21b	Distribution of alternative diagnoses in those without the target condition
	22	Time interval and any clinical interventions between index test and reference standard
Test results	23	Cross tabulation of the index test results (or their distribution) by the results of the reference standard
	24	Estimates of diagnostic accuracy and their precision (such as 95% confidence intervals)
	25	Any adverse events from performing the index test or the reference standard
Discussion		
	26	Study limitations, including sources of potential bias, statistical uncertainty, and generalisability
	27	Implications for practice, including the intended use and clinical role of the index test
Other information		
	28	Registration number and name of registry
	29	Where the full study protocol can be accessed
	30	Sources of funding and other support; role of funders

2.9 Urinary indole-reacted calcium crystallization index (iCOCI) test

Since the urinary COCI test is not very specific to oxalate detection, we further modified the COCI procedure and changed the oxalate detection mode to be more specific to oxalate. In 2020, we reported the urinary indole-reacted calcium crystallization index (iCOCI) and validated its diagnostic performance for CaOx urolithiasis[17]. The iCOCI method is modified from the COCI method. The detection of oxalate in iCOCI test is based on the chemical reaction of oxalate with indole reagent. In 1995, Bergerman and Elliot reported that a specific direct reaction of oxalate with indole that produces the pink color product[53]. Thus, we integrated the indole-oxalate reaction into the COCI method in order to selectively detect and quantify the oxalate content in crystals precipitated from the COCI procedure (called COCI crystals). We validated the diagnostic accuracy of urinary iCOCI method according to the STARD guideline (Figure 7). The cutoff value of the urinary iCOCI test is ≥ 0.8 COM equivalence, g/day or ≥ 0.6 COM equivalence, g/L. The urinary iCOCI level in stone patients is significantly higher than that in non-stone subjects (Figure 8A). The diagnostic performance of the urinary iCOCI test evaluated by the receiver operating characteristic (ROC) analysis indicates that this test has very high diagnostic power to separate CaOx stone patients from non-stone individuals (Figure 8B). At the cutoff of ≥ 0.8 COM equivalence, g/day, the urinary iCOCI test provides the ROC analysis 0.946 (95% CI: 0.914–0.978) for separating CaOx stone patients from non-stone individuals[17]. Sensitivity, specificity, positive predictive value (PPV), negative predictive value (NPV), accuracy, positive likelihood ratio (LH^+) and negative likelihood ratio (LH^-) of urinary iCOCI test for diagnosing CaOx stone patients from non-stone individuals were 95%, 86%, 68%, 98%, 88%, 6.80 and 0.06, respectively[17].

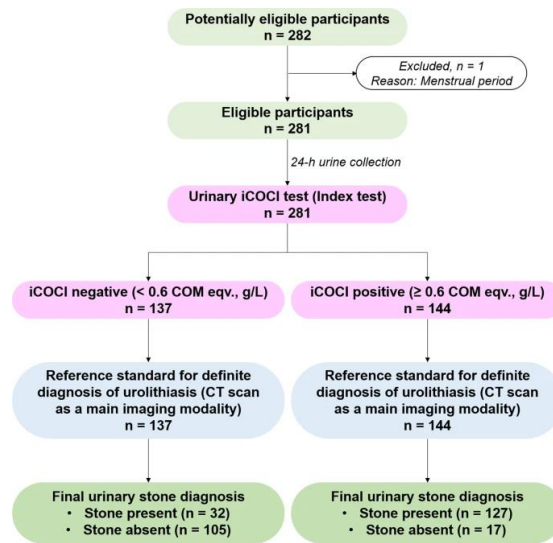


Figure 7 STRAD flow diagram for accuracy testing of the urinary iCOCI test [17].

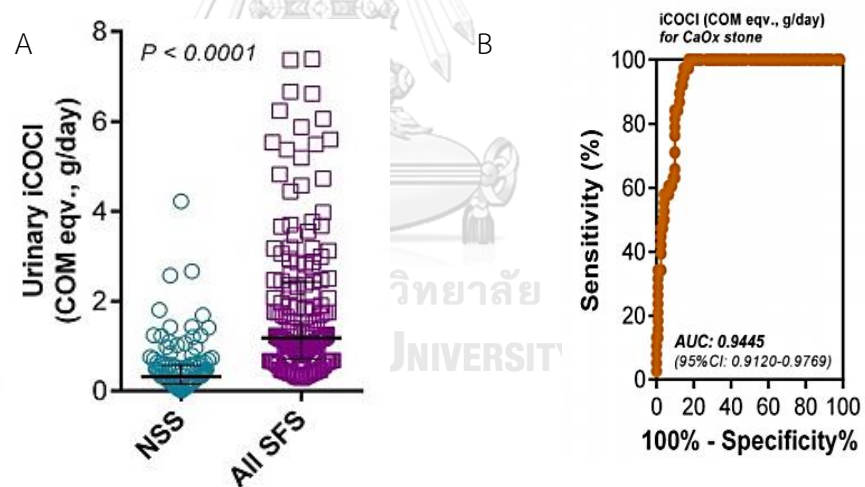


Figure 8 urinary iCOCI compare between stone and non-stone formers [17].

Although the urinary iCOCI test is sensitive and accurate for use as a screening test for CaOx urolithiasis, the problems of urinary iCOCI test are that it is time-consuming, and it is relatively low throughput. Therefore, it is necessary to develop a new method that can overcome these disadvantages. Instead of using indole

chemical reaction for detection of oxalate in iCOCl method, we are interested in using Raman spectroscopy for fingerprint detection of oxalate.

2.10 Raman spectroscopy

The principle of Raman spectroscopy is based on the inelastic light scattering after molecular vibration excited by the monochromatic light source, and the light scattering pattern provides a specific molecular fingerprint of the molecule^{[54],[55],55}. The majority of the photon scattering has the same energy as the incident photon that is called elastic scattering or Rayleigh scattering (Figure 9A) [55]. Raman spectroscopy focuses on the different frequencies after exposure from incident light, called inelastic scattering or Raman scattering, that is specific to each different chemical functional group. Raman scattering can be divided into two types, Stokes and anti-Stokes scattering. Stokes scattering light has lower energy than the incident photon (Figure 9B), whereas anti-Stokes scattering has higher energy than the incident photon (Figure 9C)^[56]. Stokes scattering is often used for generating molecular fingerprints because it has higher intensity than the anti-Stokes scattering.

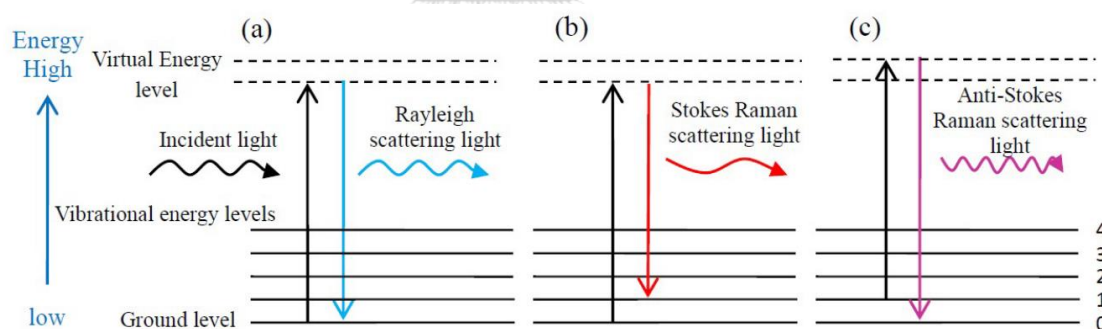


Figure 9 Generation of the three types of Raman scattering lights [56, 57].

A: Rayleigh scattering, B: Stokes Raman scattering, C: Anti-Stokes Raman scattering

Raman spectroscopy is widely used for chemical structure identification in biological samples such as cells, tissues, and biofluids^[54, 55, 58-61]. It is also used for diagnosing breast cancer and identifying the mineral composition of renal calculi^{[62][63, 64]}. Recently, Zhu et al. established the portable Raman spectroscopy

for quantitative detection of urine creatinine, and it was clinically useful with a cheaper cost and less time-consuming than the gold standard method[65]. Lo, et al. showed that automatic Raman spectroscopic with a microscope together with a fluorescent image guide could identify the urine crystals[66]. The specific Raman spectrum of CaOx is established[67, 68]. We hypothesize that the specific Raman spectrum of CaOx crystals generated from the Raman spectroscopy can be used for identifying and quantitating CaOx in the COCI crystals.

The advantages of Raman spectroscopy are that it is a non-destructive method, it can be a real-time measurement, and the Raman spectrum is well corresponded with the IR spectrum. The FTIR method is widely used and considered as a reference standard method for identifying mineral composition of stones. It is well accepted that the Raman spectroscopy and FTIR provide corresponding results regarding the mineral composition of stones [60, 69, 70]. In general, analysis of mineral composition in solid mixtures/deposits is mostly carried out by IR spectroscopy, X-ray diffraction, and Raman spectroscopy.[60, 67] For oxalate detection, Kodita et al. report that the specific Raman peaks of oxalate ion ($C_2O_4^{2-}$) are at 1,465 and 1,491 cm^{-1} , a reflective of C-O symmetric stretching[71]. Kontoyanis et al. also report that a unique Raman spectrum of COM is at 1,462 and 1,489 cm^{-1} (Figure 10)[67].

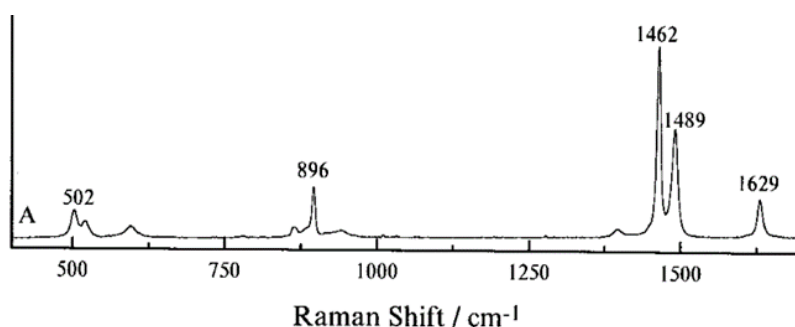


Figure 10 The Raman spectrum of COM [69].

2.11 Method validation

The validation method is important for developing or improving a new analytical method in order to understand new test principles and limitations related to reliability results. The analytical approaches can be divided into several types such as electrochemical analysis, chromatography analysis, and spectral analysis [72, 73]. In analytical method development, several factors are essential to consider such as chemical property, concentration, samples matrix, the rapid and cost of test, and type of measurement[74].

The types of methods are divided into identification test and analytical test. The analytical method can be an analysis of impurity that consists of quantitative for impurity content and limit test of control, or an analysis pharmaceutical (assay) such as drug or metabolism (Figure 11)[72, 74, 75].

The process of confirming the analytical use for specific tests, known as method validation, refers to an establishment of analytical techniques that are appropriate for the use for which they are designed[74, 76]. Developing an analytical approach helps identify the process factor and reduce the influencing parameters that affect have on the accuracy and precision of the test results[77]. The International Conference on Harmonization (ICH) describes system appropriateness as "a checking of the system" before or during the analysis of unknowns to ensure system performance [72, 77]. According to the ICH guidelines, measurement tools includes accuracy, precision, specificity, limit of detection, quantitation, linearity, range, and robustness (Figure 12) and technique validation assures that the chosen technique will produce data that are reproducible, believable, and consistent[20, 72, 74, 77].

Characteristics	Test of Identification	Kinds of Analytical Procedure		
		Impurities test		Assay
		Quantification	Limit	<ul style="list-style-type: none"> • Test of Dissolution (measurement only) • Content/Potency
Accuracy	-ve	+ve	-ve	+ve
Precision <ul style="list-style-type: none"> • Repeatability • Intermediate Precision 	-ve -ve	+ve +ve(1)	-ve -ve	+ve +ve
Specificity(2)	+ve	+ve	+ve	+ve
Limit of Detection	-ve	-ve(3)	+ve	-ve
Limit of Quantification	-ve	+ve	-ve	-ve
Linearity	-ve	+ve	-ve	+ve
Range	-ve	+ve	-ve	+ve

Figure 11 Type of analytical process and ICH characteristic [72].

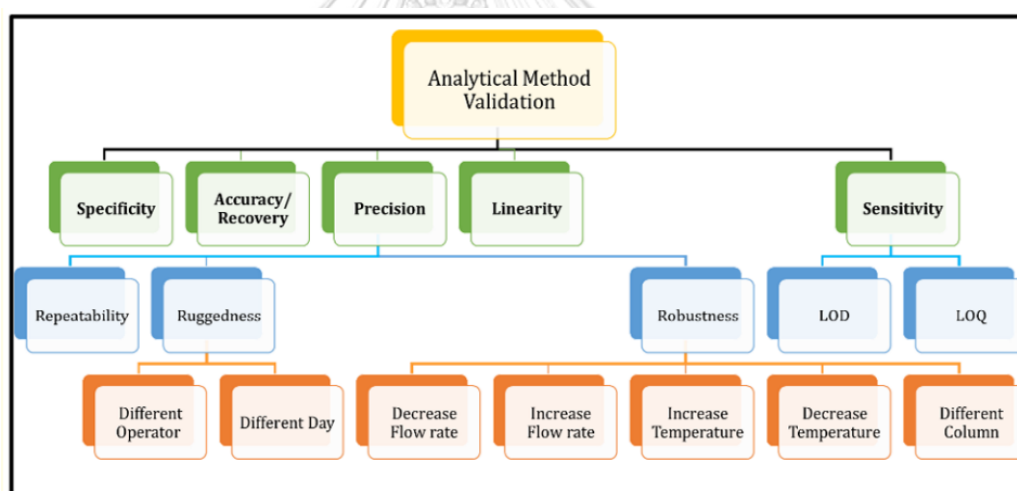


Figure 12 Process diagram for validation of the analytical method [78].

Validation parameters of the clinical tests used for disease screening, identifying drugs and metabolism (quantitative bioanalysis) include selectivity (sensitivity, specificity), linearity (calibration model), accuracy (bias), precision, and lower limit of quantification (LLOQ). Other parameters such as the limit of detection (LOD), recovery, repeatability, and robustness are also related[18-20].

Selectivity or selectivity is the detection ability that the test can identify desired analyte in biological matrix (plasma, urine, another matrix) and interference,

such as measuring of drugs in plasma, measuring of creatinine in urine, and detection of bacterial pathogens in urine. For the interference, it can be observed by checking in different matrix sources [62,77]. Selectivity must determine the target analyte in a complex biological mixture[19, 65, 72, 78, 79]. It is commonly used for estimating the proportion of actual analyte to specified chemicals[78]. High sensitivity tests can detect the minimum concentration of analyte. The limit of detection (LOD) is the lowest concentration of analyte that can be detected. The limit of quantitation is the lowest amount of analyte that can be precisely determined. The calculated LOD should not have the coefficient of variant (%CV) over 20%[20, 74].

Linearity (calibration model) can provide the range that concentrations are related to the testing results (within range). The excellent linearity has r square of 0.99.

The accuracy of the analytical method indicates how much the testing value is close to the actual value. Accuracy can be calculated from the %recovery of the assay[77]. Precision is determined based on the replicate analysis of the same samples. It can generally be measured by the relative standard deviation (RSD) or the coefficient of variant (%CV). Precision can be divided into two types: (1) repeatability (measuring the same sample at the same condition and same time) or intra-assay (within-run) precision, and (2) reproducibility (measuring in the same sample in different conditions such as different day, different equipment, different laboratory). The accepted calculated precision at each level should not exceed 15% of %CV[19, 20, 74].

Stability testing is important for determining how long and what temperature the sample can be kept prior to testing[20, 74].

The process of developing a new analytical method can follow the summary of validation parameters shown in Figure 13 that provides the guideline information of the step of measuring validation parameters, the procedure of evaluation, and the criteria [18].

Validation parameter	Experiments	Evaluation	Acceptance criteria
Selectivity	Analysis of at least six sources of blank matrix; analysis of 1–2 zero samples (blank matrix + internal standard)	Checking for interfering signals	Absence of interfering signals
Calibration model	At least 4–5 concentration levels; analysis of duplicates at each level	Evaluation of linear model; evaluation of non-linear model, if linear model not applicable	Acceptable accuracy and precision data
Accuracy (bias) and precision	QC samples at low and high concentrations relative to calibration range; analysis of 5–6 replicates per level under repeatability conditions	Calculation of bias as percent deviation of mean calculated value from nominal value; calculation of precision data as R.S.D.	Bias within $\pm 15\%$ of nominal value ($\pm 20\%$ near LLOQ); precision within 15% R.S.D. (20% near LLOQ)
LOD	Analysis of spiked samples with decreasing concentrations of analyte	Checking for compliance with identification criteria; alternatively, evaluation of S/N	Compliance with identification criteria; alternatively, $S/N \geq 3$
LLOQ	Use of accuracy and precision experiments with QC samples with analyte concentration near LLOQ; alternatively, analysis of spiked samples with decreasing concentrations of analyte	Use of accuracy and precision data of QC samples with analyte concentration near LLOQ; alternatively, evaluation of S/N in spiked samples	Compliance with accuracy and precision criteria near LLOQ, see above; alternatively, $S/N \geq 10$

Figure 13 Summary of planning experiment for validation of a new analytical method [18].

The application of method validation parameters is widely used in bio-analysis methods for biological samples[80, 81]. In 2016, Jie Cheng et al. established the highly sensitive detection of clenbuterol in animal urine by Raman spectroscopy[82]. In 2018, B. Ashwini et al. established the analytical method for determining glycopyrrocate and formoterol fumerate by RP-HPLC. Recently, Jing Liu et al. developed a rapid quantitative detection of voriconazole in plasma by Raman scattering, and they showed that the developed method has linearity of the calibration range of 0.2-10 ppm with high efficiency and excellent reproducibility, satisfactory recovery, and stability (Figure 14)[83]. Therefore, we proposed to develop the Raman spectroscopy screening method for quantifying calcium oxalate produced in supersaturated urine. The method validation was performed to calculate validation parameters to show that the newly established method is an appropriate technique and reliable.

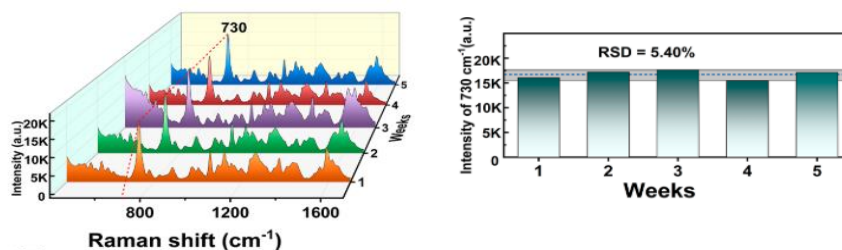


Figure 14 Precision of reproducibility of measurement voriconazole in human plasma [83].

2.12 Clinical validation

Clinical validation is carried out to confirm the accuracy and credibility of clinical results. The parameter of clinical validation includes clinical sensitivity, specificity, and accuracy.

Specificity refers to the proportion of true negative results. It is calculated by the number of true negative divided by total number of non-disease cases (true negative + false positive).

Sensitivity refers to the proportion of true positive results. It is calculated from the number of true positive divided by total number of disease cases (true positive + false negative) (Figure 15).

Accuracy refers to the proportion of the true value (both true positive and true negative). It is calculated from total number of true negative and true positive divided by total number of all cases both non-disease and disease (true negative + false negative + true positive + false positive) (Figure 15).

		Ground truth / label Gold standard / Reference test			
		Condition Positive	Condition Negative		
ML model Index test	Predicted Positive	True Positive TP	False Positive FP	Precision Positive predictive value $\frac{TP}{(TP + FP)}$	
	Predicted Negative	False Negative FN	True Negative TN	Negative predictive value $\frac{FN}{(FN + TN)}$	
		Recall Sensitivity $\frac{TP}{(TP + FN)}$	Specificity $\frac{FP}{(FP + TN)}$		
		Accuracy $\frac{TP + TN}{(TP + FP + TN + FN)}$		F1 Score $\frac{2TP}{(2TP + FP + FN)}$	

Figure 15 The 2 x 2 Table for calculating sensitivity, specificity, and accuracy [84].

Therefore, after we develop a new method for quantifying calcium oxalate crystals produced in supersaturated urine, the analytical method validation and clinical validation to evaluate its diagnostic performance must be performed as summarized in the flow chart below (Figure 16).

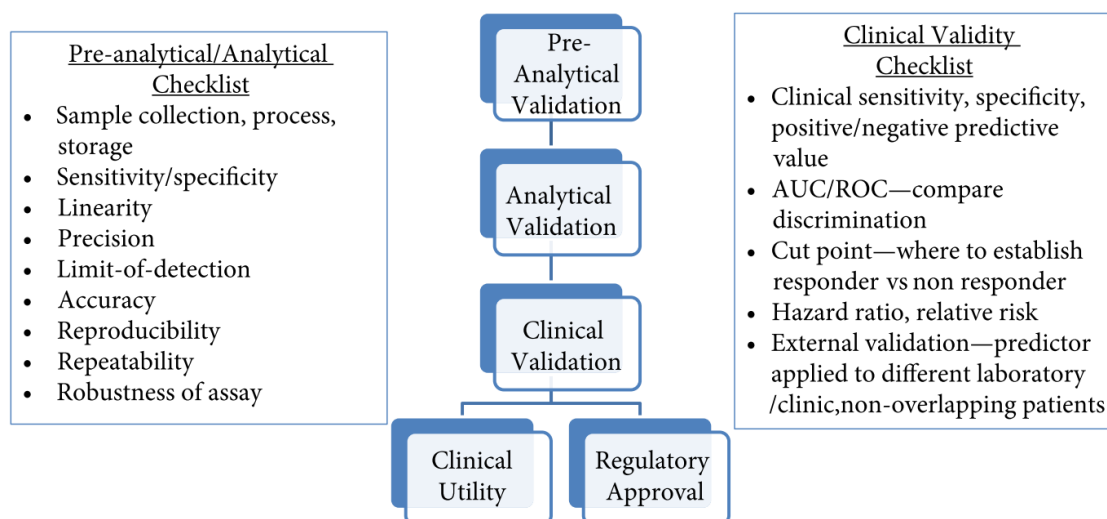


Figure 16 Flow chart of the analytical and clinical validation [85].

Conceptual framework

The conceptual framework of this study is shown in Figure 17. CaOx stone is the most common type of urinary stone. Rapid quantitative and inexpensive detection of CaOx crystallization potentiality in the supersaturated urine could be used for estimating the risk of CaOx stone formation. More-Krong et al. developed a method called indole-reacted calcium oxalate crystallization index (iCOCI) test for the diagnosis of CaOx urolithiasis. Although iCOCI test has high accuracy, it is time-consuming, and the indole-oxalate reaction requires a strong acid. Raman spectroscopy generates the molecular fingerprint of chemicals and is widely used for identifying and quantifying the chemicals of interest.

This study proposed to integrate the Raman spectroscopy into the COCI procedure to determine the amount of the CaOx crystals formed in the supersaturated urine instead of using the indole-oxalate reaction. This would shorten

the time measurement from 2-3 h to 30-60 min without the use of chemical hazards. The proposed method is called Raman spectroscopy-integrated COCI or rCOCI. Following the establishment of rCOCI procedure (Figure 17), the method validation was conducted. The diagnostic accuracy of the urinary rCOCI test for CaOx urolithiasis was finally tested.

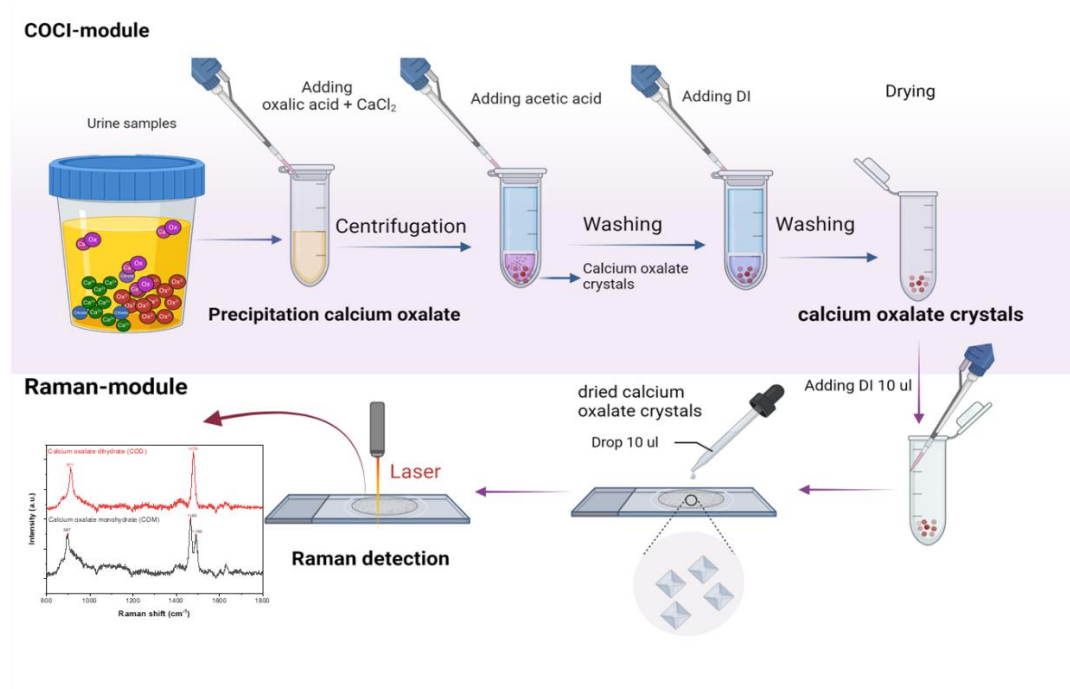


Figure 17 The simplified cartoon depicting the procedure of urinary rCOCI test.

Chapter 3 Material and methods

3.1 Study design

The study was divided into three parts (Figure 18). The first part was to develop the rCOCI method for detecting and quantifying CaOx crystals produced in the supersaturated urine (spiked with oxalate and excessive calcium). Addition of oxalate and excessive calcium chloride is a COCI procedure that we established to determine the total capacity of urine to form CaOx crystals[16, 17]. COCI procedure induces CaOx crystallization by increasing urine supersaturation of calcium and oxalate. We called the crystals produced in this supersaturated urine “COCI crystals”. The CaOx in COCI crystals was then detected and quantified by Raman spectroscopy. The specific Raman peaks for COM were 1464 cm^{-1} and 1490 cm^{-1} , and for COD was 1477 cm^{-1} .

After the rCOCI was developed, we performed the method validation to evaluate the suitability of rCOCI method for the intended use of detecting and quantifying CaOx crystals. The method validation parameters including linearity, sensitivity (limit of detection; LOD and limit of quantitative; LOQ), precision (repeatability and reproducibility), and stability were reported. After the method was validated, we conducted the clinical validation study to investigate the performance of rCOCI method for diagnosing CaOx urolithiasis. rCOCI values were determined in 24-h urine samples from urolithiasis patients (n=145) and non-stone forming subjects (n=117). Receiver operating characteristic curve (ROC) analysis was performed to evaluate the diagnostic performance of rCOCI test. The cutoff value of rCOCI test was selected, and diagnostic values including specificity, sensitivity, positive predictive value (PPV), negative predictive value (NPV), and accuracy were calculated and reported (Figure 18).

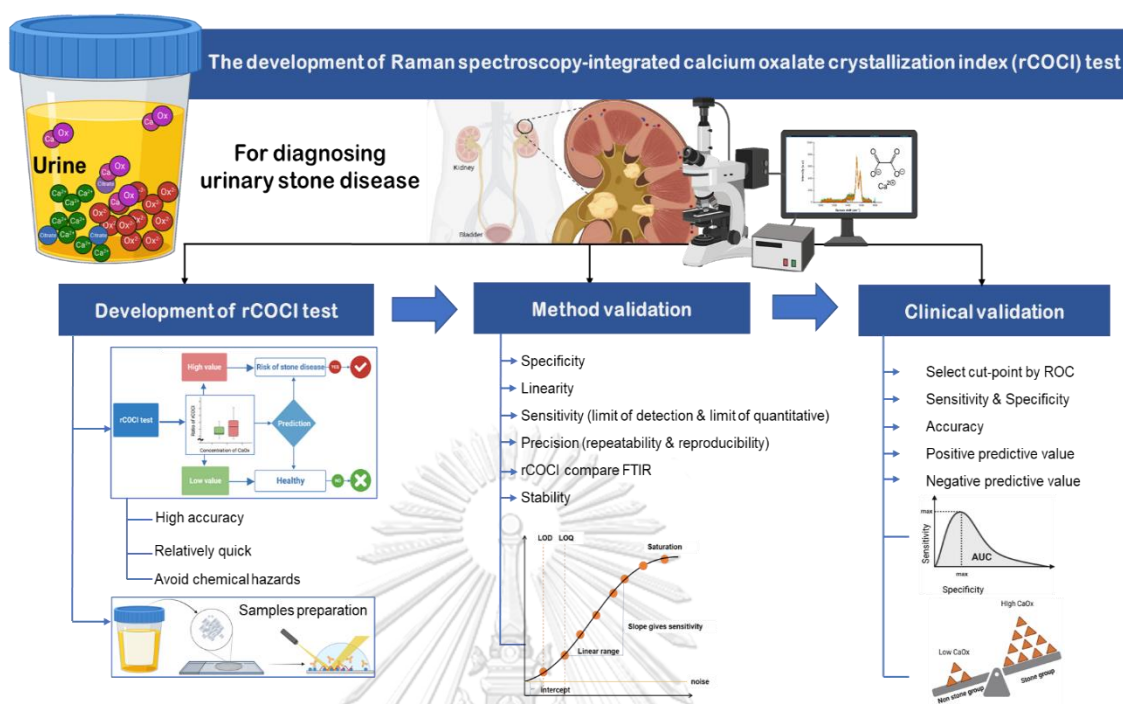


Figure 18 Workflow of the study.

3.2 Equipment and Chemicals

Table 3 List of equipment used in this study.

Equipment	Companies
Autopipette (10, 100, 200, 1000 μ L)	Biorad, California, USA
Freezer (-20 $^{\circ}$ C), (-80 $^{\circ}$ C)	Sanyo Electric, Osaka, Japan
Freezer (4 $^{\circ}$ C)	NR-BU343SN, Panasonic, Japan
Microcentrifuge tubes	Axygen, California, USA
Microplate reader	Thermo Scientific, Ohio, USA
Microplate spectrophotometer	Multiskan™ GO, USA
Syringe filter nylon 13 mm. 0.22 μ m.	Ageia Technologies, USA
Vortex mixer	VORTEX-2 GENIE, USA
Water bath	GFL, Burgwedel, Germany
Autoclave	Hirayama, Saitama, Japan
Distilled water maker	Thermo Scientific, Ohio, USA
Four decimal balances	OHAUS, Mettler-Toledo AG, Switzerland

pH meter	Hanna Instruments, UK
Beaker 50 ml, 200 ml, 1000 ml	BOECO, Boeckel + Co (GmbH + Co), Germany
Refrigerated centrifuge	Hettich, Germany
Ultrasonic cleaner	HWASHIN, Korea
Integrated vacuum concentrator	SpeedVac™ SPD2030, Thermo Scientific, USA
Hot air oven	Memmert, Germany
Raman spectroscopy	HORIBA, USA
Fourier transform infrared spectroscopy (FTIR)	FT-IR Nicolet iS50, Thermo Scientific, USA
EVOS FL Ato2 Imaging System	Invitrogen, Thermo Scientific, USA
Slide microscope	Sail, China
Water resistance pens	Advanced PAP Pen, Japan

Table 4 List of chemicals used in this study.

Chemicals	Companies
Calcium oxalate monohydrate	Merck Millipore, Massachusetts, USA
Oxalic acid (Ox)	Merck Millipore, Massachusetts, USA
Calcium chloride (CaCl ₂)	Merck Millipore, Massachusetts, USA
Sodium oxalate	Sigma-Aldrich, Missouri, USA
Urea	Merck Millipore, Massachusetts, USA
Uric acid	Sigma-Aldrich, Missouri, USA
Creatinine	Sigma-Aldrich, Missouri, USA
Indole (>99%)	TCI, USA
Acetic Acid	Merck Millipore, Massachusetts, USA
Sulfuric acid	Merck Millipore, Massachusetts, USA
Citric acid	Merck Millipore, Massachusetts, USA
Citrate dihydrate	Merck Millipore, Massachusetts, USA
Arsenazo III	Sigma-Aldrich, USA

Imidazole	Sigma-Aldrich, USA
Hydrochloric acid (HCl)	Merck KGaA, Darmstadt, Germany
Phosphate Buffer Saline (PBS)	Merck Millipore, Massachusetts, USA
Ethanol	Merck Millipore, Massachusetts, USA
Pierce™ BCA Protein Assay Kit	Thermo Scientific, Ohio, USA

3.3 24-h urine specimen collection

In this study, we used human urine samples from our previous project entitled: “Test accuracy of urinary of calcium oxalate crystallization index (COCI) for diagnosis of urolithiasis, and development of an innovation quantum dot nanoparticle-base method for determination of urinary oxalate (IRB:286/59)”. The project protocol was approved by the Ethics committee of Faculty of Medicine, Chulalongkorn University and Mahasarakham hospital. In this study, we used the leftover 24-h urine samples from 262 participants who lived in Mahasarakham province between 2017 and 2018. Based on CT scan results, the subjects were divided into two groups, non-stone group (n=117) and stone group (n=145). Of 145 stone patients, 44 patients were confirmed as CaOx stone patients (stone analysis by FTIR). The 24-h urine specimens (kept at $-20\text{ }^{\circ}\text{C}$) of both groups were thawed and filtered through the $0.22\text{ }\mu\text{m}$ membrane for rCOCI and iCOCI testing.

3.4 Procedure of urinary rCOCI test

The procedure of urinary rCOCI test separated into two parts. The first part was a procedure to produce COCI crystals and the second part was to detect and quantify CaOx crystals using Raman spectroscopy. In the first part, COCI crystals were generated by COCI procedure. 24-h urine specimens were centrifuged at 4,000 rpm for 5 min to discard debris. The urine supernatant was collected and filtrated through $0.22\text{ }\mu\text{m}$ membrane.

For CaOx crystallization by COCI procedure, $950\text{ }\mu\text{L}$ of urine sample (test) and distilled water (control) were placed into the 2 mL centrifuge tube. Then $50\text{ }\mu\text{L}$ of

100 mM oxalic acid was added both in the test tube (called oxalate-spiked urine) and control tube (to be used for oxalate subtraction in the calculation step). The final concentration of added oxalic acid was 2.5 mM. Next, 1 mL of CaCl_2 solution (100 mM) was added to the mixture. Final volume of 2 mL was obtained. The solution was incubated at 37°C for 10 min for crystallization. After that, the solution was centrifuged at 13,000 rpm, 15°C for 15 min. The COCI crystal pellet was collected and further incubated with 2 N acetic acid for 10 min to remove CaP crystals. After centrifugation at 13,000 rpm, 15°C for 15 min, the COCI crystals were collected and washed with distilled water once and centrifuged again at 13,000 rpm, 15°C for 15 min to collect the washed COCI crystals. The washed COCI crystals were dried for 15 min using SpeedVac (Thermo Scientific, USA). The dried crystals were resuspended with 10 μl of distilled water. The resuspended crystals were dropped onto a microscope glass slide and dried in the 70°C incubator for 10 min. The crystals were ready for Raman spectroscopy testing.

The Raman spectrum of COCI crystals on glass slide was generated within 5-10 min. The reference of Raman spectra of COM and COD crystals are shown in Figure 20. The specific Raman peaks of COM are 1464 cm^{-1} and 1490 cm^{-1} , while the characteristic peak of COD is 1477 cm^{-1} [69]. The presence of CaOx in COCI crystal sample were identified by matching the sample spectrum with the standard spectrum (Figure 20).

In CaOx quantitation, we calculated based on peak intensity, area under peak (AUP), and full-width half max (FWHM) derived from the Raman spectrum of CaOx crystals. To obtain total amount of CaOx both Raman peaks of COM (1464 cm^{-1} and 1490 cm^{-1}) and COD (1477 cm^{-1}) were used for calculating these three quantitative parameters. The rCOCI value was calculated the peak intensity or AUP or FWHM of the oxalate-spiked urine (test) sample divided by the peak intensity or AUP or FWHM of the oxalate-spiked water sample (control). In other words, rCOCI value was a ratio of CaOx produced in oxalate-spiked urine to CaOx produced in water containing 2.5 mM oxalic acid (Figure 21). The total time consumed to perform rCOCI test was between 1.30 and 1.45 h.

The Raman spectroscopy used in this study was purchased from HORIBA Instruments Incorporated, Park Avenue Edison, NJ 08820 USA, equipped with product detector: Sincerity CCD Camera System (serial: SYC5967-320F), compact laser module: 785 nm, power 500 mW, MM, microscope: 10X (Olympus BX53M), grating 1200, time 10 S (Figure 19), LabSpec 6 software, and range = 300 -1800 cm^{-1} . OriginLab version 2018 was employed for spectrum analysis, For data processing baseline corrected using Asymmetric Least Squares algorithm and spectra were using smoothing using the Savitzky-Golay algorithm (Figure 20) [63].

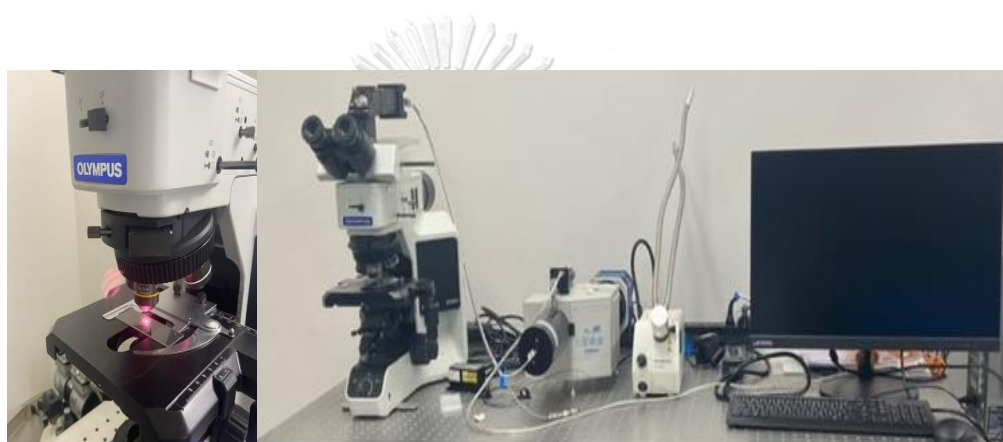


Figure 19 The Raman spectroscopy from HORIBA Instruments with laser module 785 nm.

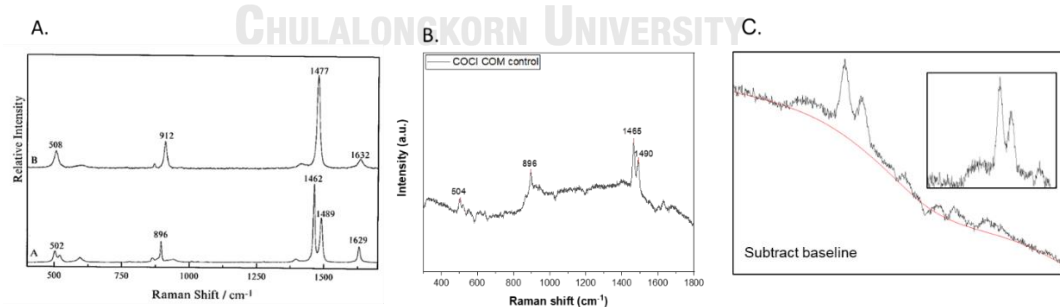


Figure 20 The characteristic Raman peaks of standard COM&COD reference (A) and characteristic of COCl crystals in the lab (B)[69]. (C.) data processing baseline corrected using Asymmetric Least Squares algorithm.

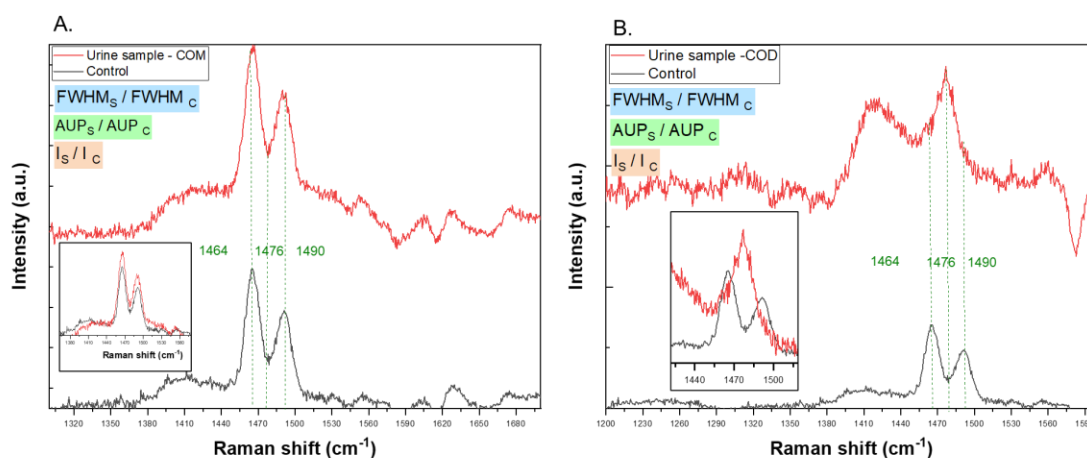


Figure 21 Calculation of urinary rCOCI value. Quantitative parameters (peak intensity (I) or AUP or FWHM) of CaOx crystals produced in urine sample were divided by quantitative parameters of CaOx crystals produced in control (urine sample: red line, water control: black line). (A.) COM. (B.) COD. Raman peaks for CaOx: 1464 and 1490 cm⁻¹ for COM and 1476 cm⁻¹ for COD.

3.5 Method validation of urinary rCOCI test

Method validation parameters including specificity, linearity, sensitivity (limit of detection and limit of quantitative), and precision (repeatability and reproducibility) were assessed and reported in this study.

Specificity is the ability of detection that can identify CaOx in the COCI crystal samples. 2 N acetic acid was used to dissolve CaP in COCI crystals to increase the ability of Raman spectroscopy to specifically detect CaOx. For testing the interfering effects of phosphate, urea, creatinine, and uric acid, we added these substances in the samples before performing COCI procedure and Raman spectroscopy.

Linearity was evaluated by performing the rCOCI test with various concentrations of spiked oxalic acid (50, 80, 100, 150, 200, 300 and 400 mM) in water and pooled urine (both non-stone and stone urine) samples.

Sensitivity (LOD and LOQ) was commonly used to estimate the actual performance of Raman spectroscopy to detect and quantify CaOx crystals at the smallest level. We performed the rCOCI test of water and pooled urine samples

using various concentrations of spiked oxalic acid (50 mM, 80 mM, 100 mM, 150 mM, 200 mM, 300 mM and 400 mM), then we defined the limit of detection and quantitation of rCOCI test.

Precision testing was performed by replicating the rCOCI test in control (water sample), individual urine samples, and pooled urine samples (spikes with 100 mM oxalic acid in the COCI procedure). For repeatability, an rCOCI test was performed on the same day (n=10). For reproducibility, the rCOCI test was performed and compared between days.

Stability testing was carried out by performing rCOCI test of the same samples (both water and pooled urine) that stored at different temperatures (4 and -20 °C) every week for 4 weeks.

3.6 Urinary iCOCI test and correlation between urinary rCOCI and iCOCI values

The iCOCI test was performed in 24-h urine samples. First, 950 μL of urine sample or distilled water (control) were mixed with 50 μL of 80 mM oxalic acid to obtain the oxalate-spiked urine and oxalate control, respectively. Then, 1 mL CaCl_2 solution (100 mM) was added to the mixture (2 mL final volume). The final concentration of spiked oxalic acid was 2 mM. The mixture was incubated at 37 °C for 10 min, and centrifuged at 13,000 rpm at 15 °C for 15 min. The pellet of COCI crystals was collected, washed once with distilled water, and centrifuged again at 13,000 rpm at 15 °C for 15 min to collect the crystals. COCI crystals were dissolved in 2 N HCl (500 mL) and transferred to the new 1 mL tubes (do not with reused tubes) for further reacting with indole reagent. The standard COM at concentrations of 0.093, 0.163, 0.375, 0.75, and 1.50 g/L in 2 N HCl were prepared for creating a standard curve. (Figure 22)

Indole reagent was freshly prepared by dissolving indole with concentrated H_2SO_4 to get the concentration of 1 mg/mL. 200 μL of COCI crystal solution or standard COM (0.093, 0.163, 0.375, 0.75, and 1.50 g/L) were slowly and carefully mixed with 200 μL of indole reagent (performed in the dark). The mixture was incubated at 80 °C for 45 min to produce the indole-oxalate complex (pink color).

Absorbance at 530 nm was measured. Time required for performing iCOCI test was around 2 - 3 h.

For iCOCI value calculation, the original absorbance of urine sample (before spiking) was calculated by subtracting the absorbance of oxalate-spiked urine from the absorbance of 2 mM oxalate control. The urinary iCOCI (COM equivalent, g/L) was calculated against the COM standard curve (Figure 22). The iCOCI values were reported in the units of COM equivalent, g/day or COM equivalent, g/L.

The urinary iCOCI values were measured in the same 24-h urine samples that were tested with the rCOCI method. Correlation between iCOCI and rCOCI values was evaluated. The specificity of iCOCI test to detect and quantify CaOx was based upon the specific chemical reaction of oxalate and indole reagent, whereas in rCOCI test the specificity of CaOx detection and quantification relied on Raman spectrum peaks of CaOx crystals.

Human urine samples were used in this study. The Institutional Ethics Committees, Faculty of Medicine, Chulalongkorn University evaluated and approved the research protocol (IRB1036/64).

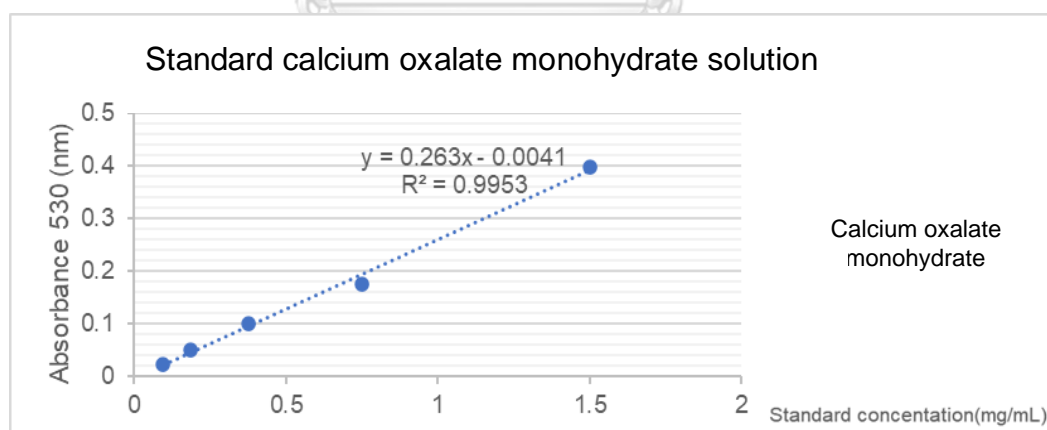


Figure 22 The standard curve of COM used in the urinary iCOCI test.

3.7 Calcium measurement in urine by Arsenazo III method

The urinary calcium was measured in the same 24-h urine samples. The Arsenazo III method has been widely used to detect free calcium[86]. Arsenazo III

reagent was prepared by mixing 100 mM Arsenazo III solution in 75 mM imidazole (50 mL) and adjusting pH to 6.5. Standard calcium chloride was prepared at concentrations of 0, 0.25, 1 and 2 mM. Calcium chloride standard curve was created (Figure 23). The urine sample was diluted 1:2 before testing. Diluted urine sample (10 μ L) or water (blank) or standard calcium solution was placed in well of 96-well plate. Arsenazo III reagent (250 μ L) was added, mixed thoroughly, and incubated at room temperature for 5 min. Absorbance at 603 nm was measured.

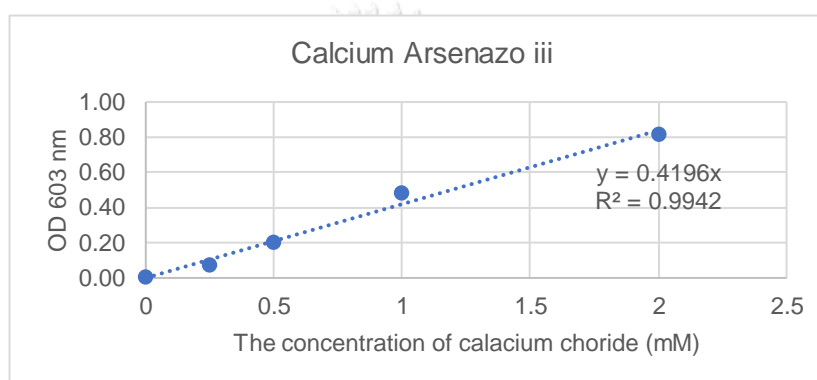


Figure 23 The standard curve of calcium chloride used in the Arsenazo III for urinary calcium determination.

3.8 The creatinine assay

Standard curve of creatinine with varied concentrations of 0, 0.5, 1, 2, 4, and 8 mg% (Figure 24) was created. Urine sample was diluted to 1:200 with distilled water. Urine samples, creatinine standard, and water (as blank) (150 μ L) were placed into wells of the 96-well plate. Then, 50 μ L of 0.04 N picric acid was added and mixed thoroughly. After that, 25 μ L of 1.4 N NaOH was added, mixed, and incubated for 15 min in the dark. Absorbance at 520 nm was measured.

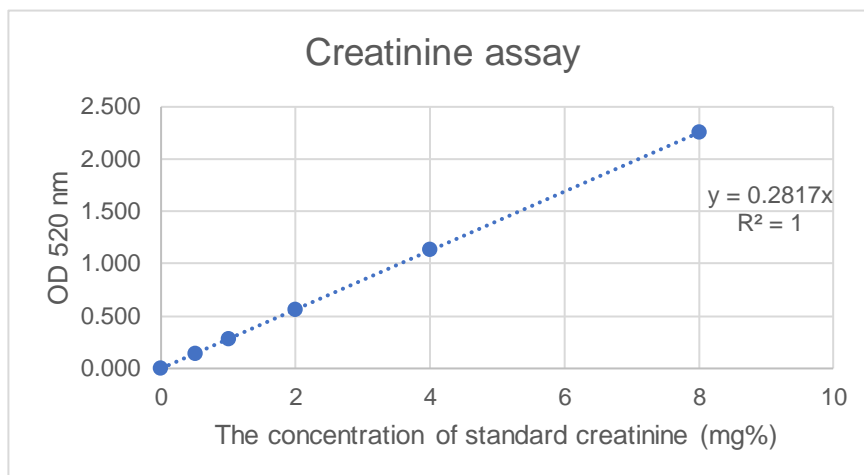


Figure 24 The standard curve of creatinine.

3.9 Protein concentration measurement in urine

Urinary protein was measured by bicinchoninic acid (BCA) assay. Standard protein was bovine serum albumin (BSA 2 mg/mL) prepared at concentrations of 0, 0.25, 0.5 and 1 mg/mL for generating the standard curve (Figure 25).

The BCA reagents (196 μ L of reagent A mixed with 4 μ L of reagent B) was freshly prepared and placed into wells of 96-well plate. Samples/standard/blank (25 μ L) was added. Plate was covered with foil and incubated at 37 $^{\circ}$ C for 30 min (changed color from green to purple). Absorbance was measured at 562 nm.

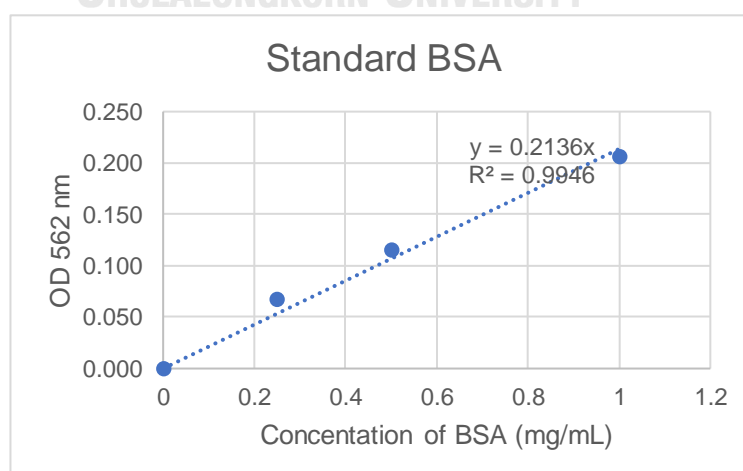


Figure 25. The standard curve of BSA.

3.10 2 x 2 Table for calculation of diagnostic values of rCOCI test

The diagnostic performance of the urinary rCOCI test was assessed by ROC analysis. After ROC analysis, an appropriate cutoff of the urinary rCOCI value was selected and 2 x 2 Table was created. The diagnostic values including sensitivity, specificity, positive predictive value (PPV), negative predictive value (NPV), positive likelihood ratio (LH+), negative likelihood ratio (LH-) and accuracy were calculated as shown in Figure 25. Positive and negative likelihood ratios were calculated.

		Ground truth / label Gold standard / Reference test			
		Condition Positive	Condition Negative		
ML model Index test	Predicted Positive	True Positive TP	False Positive FP	Precision Positive predictive value $\frac{TP}{(TP + FP)}$	
	Predicted Negative	False Negative FN	True Negative TN	Negative predictive value $\frac{FN}{(FN + TN)}$	
		Recall Sensitivity $\frac{TP}{(TP + FN)}$	Specificity $\frac{TN}{(TN + FP)}$		
				Accuracy $\frac{TP + TN}{(TP + FP + TN + FN)}$	F1 Score $\frac{2TP}{(2TP + FP + FN)}$

Figure 25 2 x 2 Table for calculation of diagnostic values [84].

3.11 Statistical analysis

As appropriate, data was presented as mean \pm standard deviation (SD) or median (interquartile range; IQR). Whether rCOCI levels were different between stone and non-stone groups were tested by two-sample t-test and Mann-Whitney test. Difference among three or more groups was tested by one-way ANOVA or Kruskal-Wallis test. ROC analysis was performed to evaluate how well the rCOCI test could diagnose CaOx urolithiasis. Diagnostic values were calculated, including sensitivity, specificity, PPV, NPV, positive and negative likelihood ratios, false-positive rate (FPR), false-negative rate (FNR), and accuracy. Statistical analysis was calculated by GraphPad Prism Software version 9.0 (GraphPad Software, Inc, California). P-value < 0.05 is considered statistically significant.

Chapter 4 Results

Part I: Development and optimization of the urinary rCOCl test

4.1 Establishment of rCOCl method for detecting and quantitating CaOx crystallization in 24-h urine

4.1.1 CaOx in liquid form could not be measured properly by Raman spectroscopy.

We compared the Raman spectra of CaOx samples between liquid and solid forms to see which form was the most appropriate form for measuring by the Raman spectroscopy. Calcium oxalate monohydrate (COM) standard was used for the testing. For preparing the liquid CaOx sample, COM powder was dissolved in 2 N HCl at various concentrations (0.093, 0.186, 0.375, 0.75, and 1.5g/L). For solid CaOx sample, the COM powder was analyzed directly by Raman spectroscopy. The seed COM produced in our lab, as the other solid CaOx sample, was also measured by Raman spectroscopy. The Raman characteristic of CaOx of each sample was generated and compared. The result showed that the standard COM powder generated 5 major Raman shifts (cm^{-1}), consisted of 505 (for O-C=O), 895 (for C-C), 1462 and 1488 (for C=O) and below 300 (for Ca-O) cm^{-1} (Figure 26A). Our synthetic seed COM (prepared in the lab) produced Raman shift peaks of 502, 895, 1465 and 1490 cm^{-1} that were perfectly matched with the standard COM (Figure 26B).

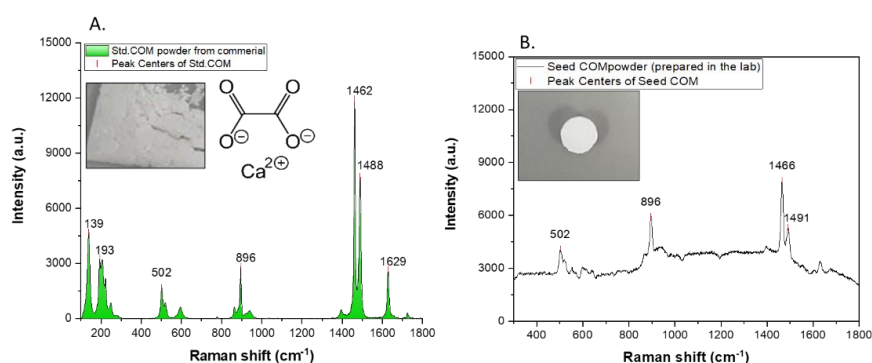


Figure 26 Raman spectra of solid CaOx samples. (A) The commercial COM powder sample. (B) The synthetic seed COM prepared in our lab. Spectra of both solid

samples were relatively similar, showing the same typical characteristic of CaOx (1490, 1465, 895 cm^{-1}).

Raman spectrum of liquid form of CaOx sample was measured. Only the characteristics of COM samples at concentrations of 1.5, 0.75 and 0.375 mg/mL could identify (in the areas that crystals were seen under the microscope) (Figure 27A). The Raman characteristic of liquid COM sample was observed at 1462 ± 2 and $1490 \pm 2 \text{ cm}^{-1}$. In contrast, the COM solution at concentrations of 0.186 and 0.093 mg/ml showed no signal, and no crystals were observed under the microscope (all crystals completely dissolved). Furthermore, HCl itself produced very high noise signals at 1352, 1424 cm^{-1} (Figure 27B).

From these results, we concluded that CaOx sample to be measured by Raman spectroscopy must be in a solid form.

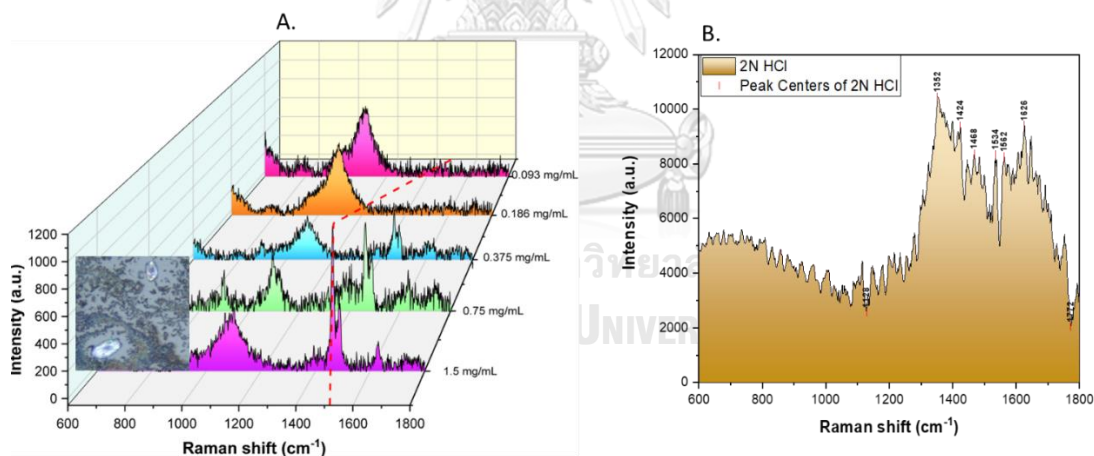


Figure 27 Raman spectra of liquid CaOx samples. (A) Standard COM solution in 2 N HCl at concentrations of 1.5, 0.75, 0.375, 0.186 and 0.093 mg/mL. (B) Background noise of HCl.

4.1.2 Light and coverslip were interfered with the Raman signal.

According to the COCl procedure, CaOx crystals were produced in water (control) and urine (test) samples after adding oxalic acid and CaCl_2 . We tested

whether light and coverslip interfered with the Raman signal of CaOx. CaOx crystals prepared in water by COCl procedure were put on the microscopic slide (as sample holder) and subjected to the Raman spectroscopy measurement (measurement setting condition: wavelength 785 nm, time 10 S, grating 1600 l/mm, lens 10x). The result showed that noise signal of CaOx crystal spectrum generated under the dark condition was lower (along with higher specific CaOx signal) than that generated under the condition with light on (Figure 28A). Likewise, CaOx sample with coverslip on produced a higher noise signal than that without coverslip (Figure 28B)

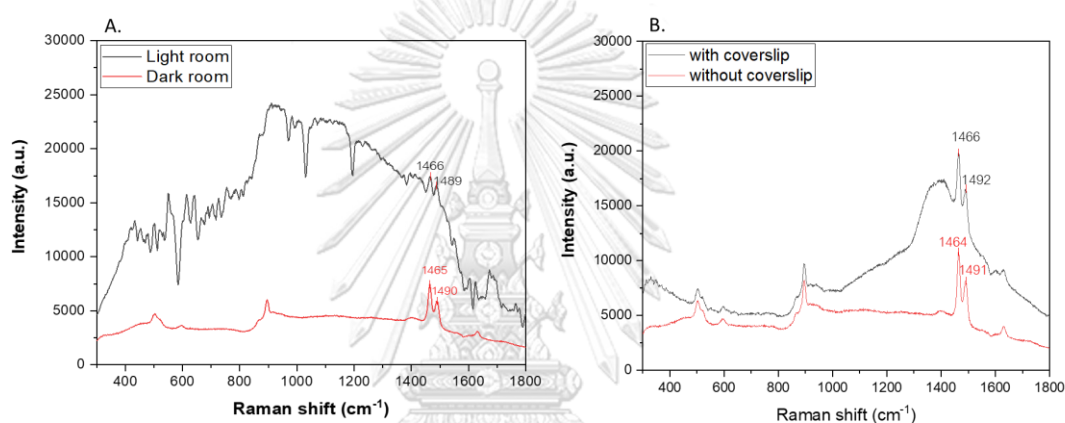


Figure 28 Effect of light and coverslip on Raman signal. (A) light vs dark (B) with coverslip vs without coverslip.

4.1.3 To increase the Raman signal, CaOx crystal sample must be placed on slide as a small disc (0.3 cm diameter).

Based on the signal optimization data, we chose to analyze the Raman spectrum of CaOx sample in a solid form, placed the CaOx crystal sample on a microscopic slide without coverslip, and measured the Raman spectrum under the dark. Basically, thickness of the sample affects the Raman signal. We increased the thickness of CaOx crystal sample by placing the crystal suspension (10 μ L) inside a small circle (1.0 or 0.3 cm diameter). After dried, a small disc of sample appeared (Figure 29). The Raman signals of both control (CaOx formed in water) and test (CaOx formed in urine) were compared between CaOx samples of 1.0 cm (Figure 29A) and

0.3 cm (Figure 29B) diameter discs. The result clearly showed that CaOx sample of 0.3 cm diameter disc generated a higher specific signal of CaOx than that of 1.0 cm diameter disc both in control and test samples. The background signal of microscopic slide is shown in Figure 29C. Additionally, CaOx sample of 1.0 cm diameter showed the high microscopic slide background signal. Therefore, we opted to prepare the CaOx crystal sample as a 0.3 cm diameter disc for Raman spectroscopy analysis.

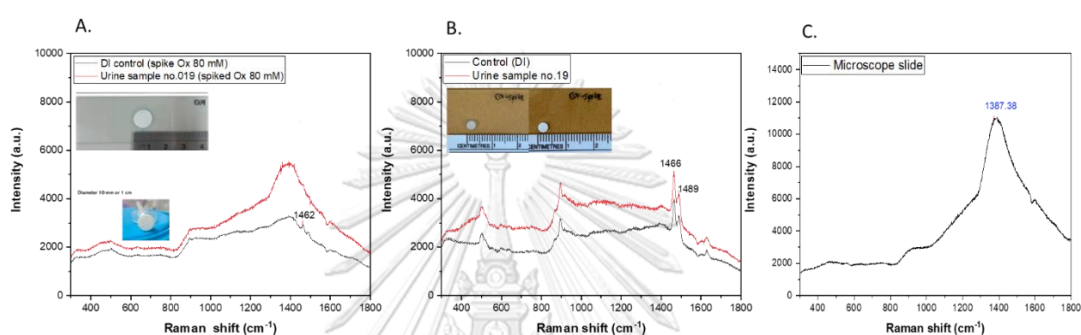


Figure 29 The optimized diameter of CaOx crystal samples for Raman spectroscopy analysis. (A) Disc diameter 1 cm. (B) Disc diameter 0.3 cm. (C) Microscopic slide background.

4.1.4 The precision of CaOx Raman spectra measurement in one sample with different microscopic areas.

We aimed to develop an rCOCI test for measuring the amount of CaOx. We observed CaOx Raman signals in different microscopic areas to confirm that the signal of CaOx was consistent within the sample disc (0.3 cm). The precision of the quantitative measurement was evaluated from %CV. The results showed that %CV of peak intensity, area under peak (AUP), full wide half max (FWHM) in control (CaOx produced in water) were 3.03%, 2.21%, and 1.30%, respectively. For the CaOx signal in the test (CaOx produced in healthy urine), the %CV of peak intensity, AUP, and FWHM were 2.57%, 3.49% and 2.73%, respectively (Figure 30).

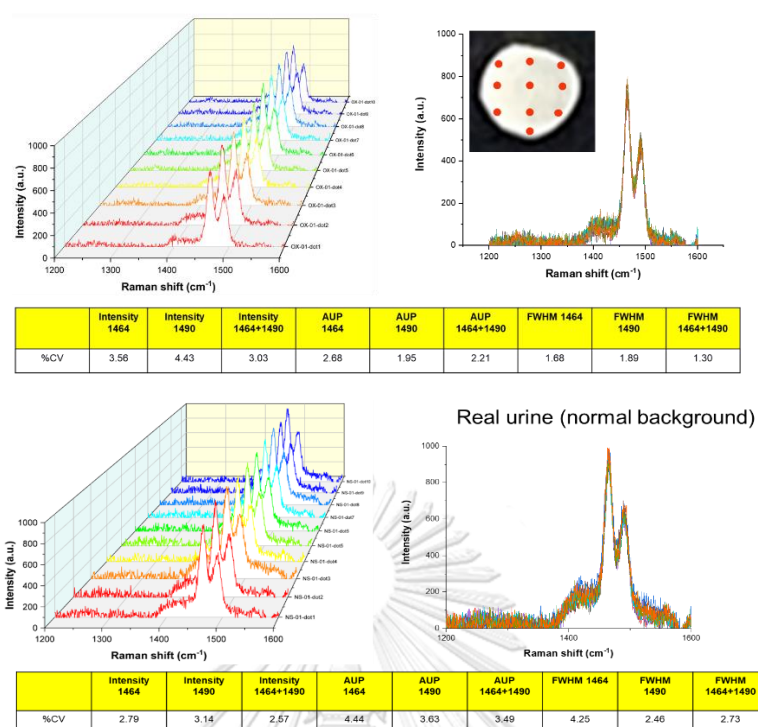


Figure 30 Precision of the quantitative measurement of the CaOx Raman signal in control (water) and test (real urine). The %CV of peak intensity, area under peak (AUP), full wide half max (FWHM) in control and test were less than 5%.

4.1.5 Optimization of spiked oxalic acid concentration to be able to clearly detect the Raman signal.

According to the iCOCI test, CaOx crystals in sample are induced by adding 80 mM of oxalic acid (called spiked oxalic acid, final concentration of 2 mM). To find the appropriate concentration of spiked oxalic acid that could give the CaOx Raman signal stand out from the background, we varied concentrations of spiked oxalic acid from 50 to 300 mM (50 mM, 80 mM, 100 mM, 150 mM, 200 mM, and 300 mM) to precipitate CaOx both in control (in water) and test (in urine). The results showed that the concentrations of spiked CaOx in control (Figure 31A) and test (Figure 31B) were proportionated to peak intensity 1464 cm^{-1} and 1490 cm^{-1} . The concentrations of 50-80 mM spiked oxalic acid showed relatively low signal with high background noise. Moreover, the test (real urine) had higher noise background signal than control.

We opted to choose the concentration of spiked oxalic acid at 100 mM (final concentration of 2.5 mM) for further testing.

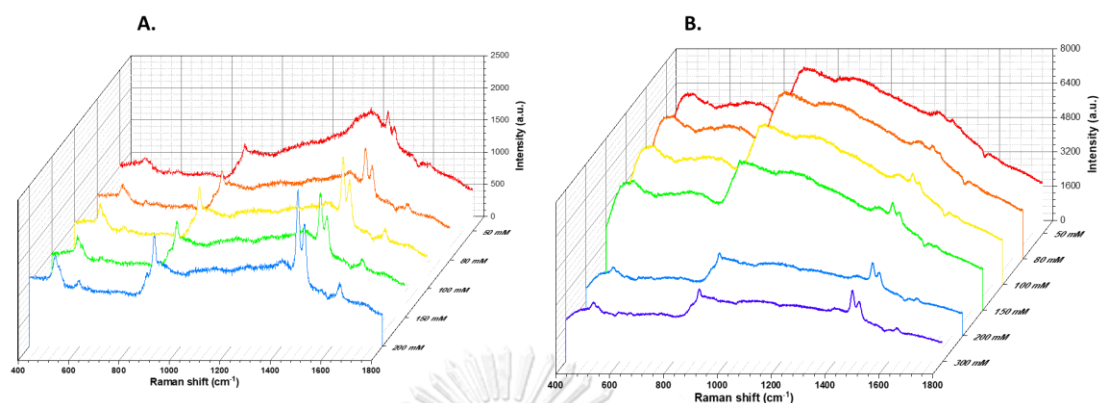


Figure 31 The CaOx crystals are produced from different concentrations of spiked oxalic acid in control (A) and test (B) conditions.

4.1.6 Removal of calcium phosphate interference by acetic acid.

In urine samples, calcium phosphate is frequently precipitated together with CaOx after adding oxalic acid and CaCl_2 , and it interferes with the CaOx Raman signal. Calcium phosphate can be dissolved in acetic acid, but CaOx cannot. We tested whether acetic acid could improve the CaOx Raman signal in urine sample. Before analyzing with Raman spectroscopy, the crystal sample produced from the COCl procedure was incubated with 2 N acetic acid at room temperature (RT) for 15 min, washed once with DI water, and dried using the SpeedVac vacuum concentrator. The result showed that crystal sample treated with acetic acid had an increased Raman signal compared with crystal sample without acetic acid treatment (Figure 32A). However, in some urine samples, treatment with acetic acid could not clearly reduce the background signal (Figure 32B).

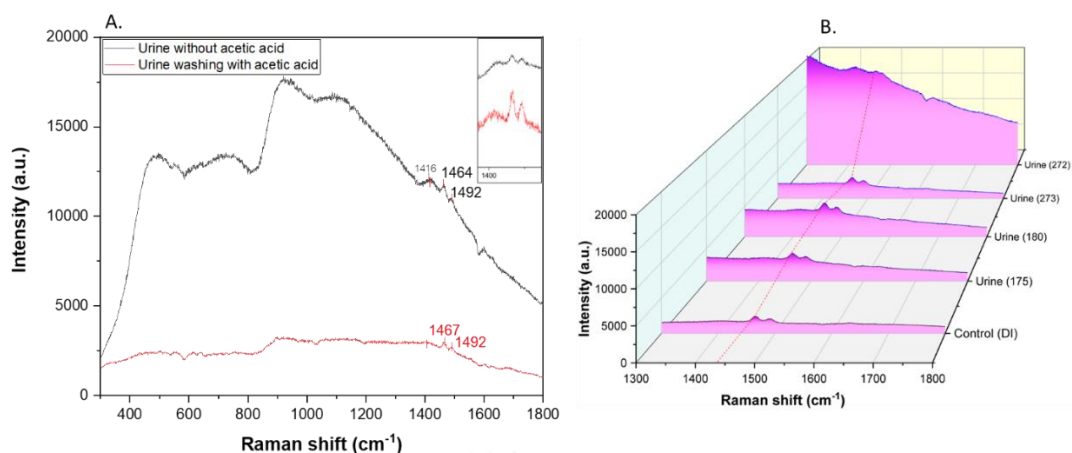


Figure 32 Removing calcium phosphate interference by acetic acid. (A) The CaOx Raman signal of COCI crystal sample treated with acetic acid (red line) was higher signal than in sample without acetic acid treatment (black line). (B) The CaOx Raman signal of crystals produced in urine samples and treated with acetic acid showed low background signal comparable to control. However, some urine samples (urine sample no.272) still exhibited a high background.

4.1.7 Not only COM, COD could also co-precipitated in urine sample after adding oxalic acid and CaCl_2 .

In urine samples, Raman characteristics of COM (1464 cm^{-1} and 1490 cm^{-1}) and COD (1476 cm^{-1}) were observed. Most urine samples contained only COM Raman peaks (156 cases, 60%). Some urine samples contained solely COD Raman peaks (106 cases, 40%). To confirm the COD Raman characteristics, we prepared COD crystals combining 100 mM of CaCl_2 , 100 mM of oxalic acid, and 4.5 mM of sodium citrate, and analyzed them with Raman spectroscopy. The result showed that Raman shifts of COD were located at 911 cm^{-1} (C-C) and 1479 cm^{-1} (C=O) (highest intensity). For morphology, COD had an envelope-like shape, while COM was showed needle-like shape. (Figure 33)

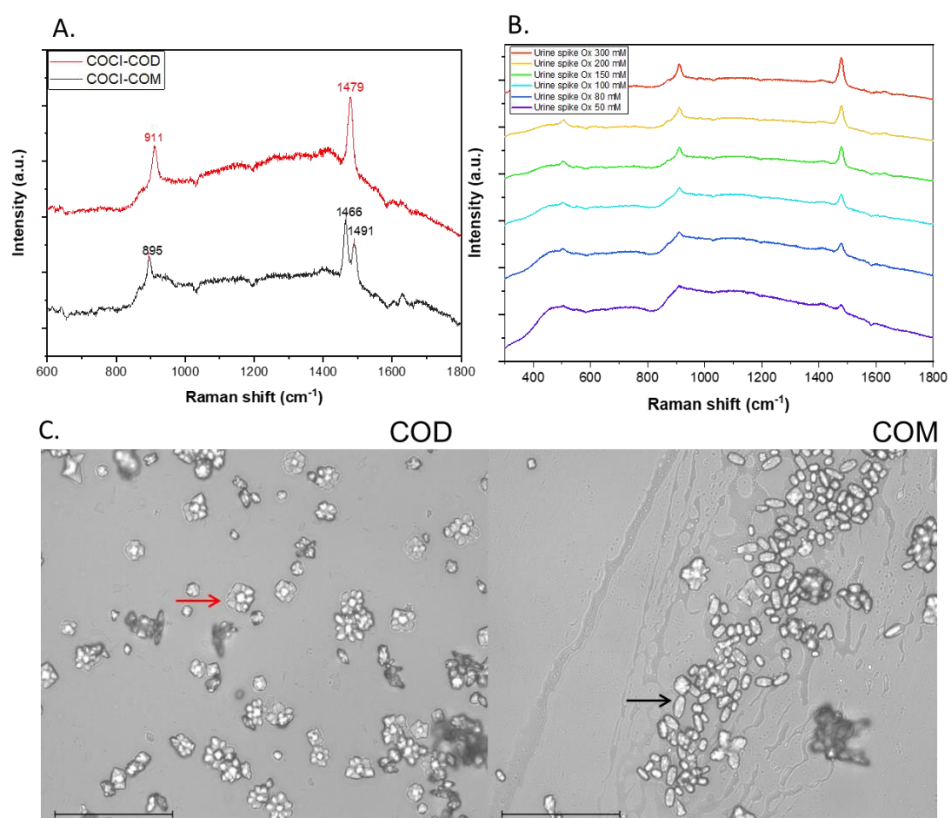


Figure 33 Raman spectroscopy of COM and COD. (A) The Raman spectrum of synthetic COM compared with synthetic COD. (B) Raman spectra of urine sample with COD Raman peak compared among different concentrations of spiked oxalic acid (50 mM, 80 mM, 100 mM, 150 mM, 200 mM, and 300 mM). (C) Micrographs of COM and COD crystals showing COM as needle-shaped (black arrow) and COD as envelope-shaped (red arrow) (Magnification 400x).

4.1.8 COD crystals were confirmed by FTIR analysis.

We found the presence of COD at characteristic peak of 1476 cm^{-1} in Raman spectroscopy in urine samples. The COD crystals were further analyzed by FTIR. The FTIR result showed that the specific spectrum of COD was at wavenumbers of 1321, and 1615 cm^{-1} , while COM was at 776, 1312, and 1604 cm^{-1} (Figure 34).

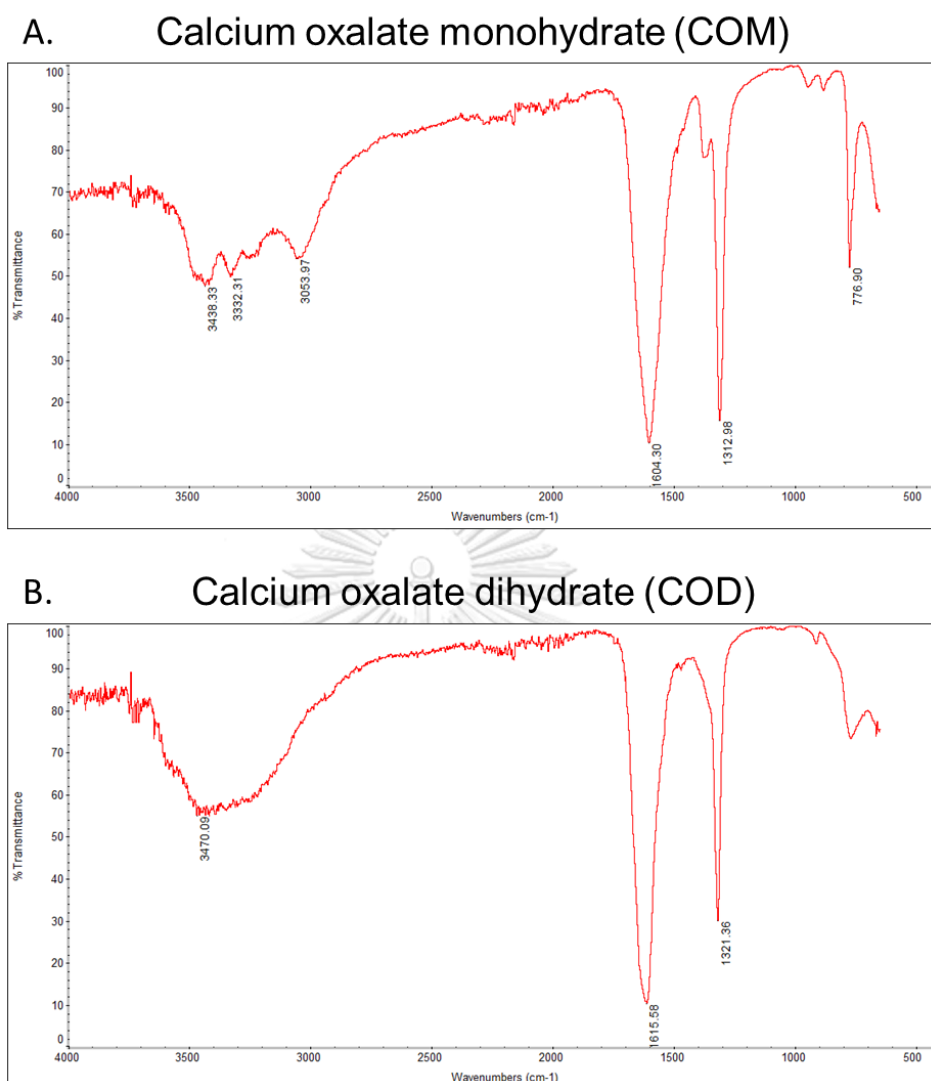


Figure 34 Comparison of FTIR spectrum of COM and COD. (A) COM showed a specific FTIR spectrum at 781, 1312, and 1604 cm^{-1} . (B) COD exhibited FTIR spectrum at 1321, and 1615 cm^{-1} .

4.1.9 The quantification of calcium oxalate crystals in the rCOCl test.

We used three quantitative parameters derived from Raman spectrum, i.e., (1) the peak intensity (peak height), (2) area under peak (AUP) and (3) full wide half max (FWHM) of the peaks for quantifying amount of CaOx in sample. All these three parameters are well proportionated to the amount of CaOx. We plotted the standard curve of these three quantitative parameters against the concentration of spiked

oxalic acid. The result showed that the peak intensity gave the highest correlation ($R^2 = 0.98$) to spiked oxalic acid concentrations (range: 50 - 200 mM) (Figure 35). When considered at the narrower concentration range of spiked oxalic acid (50 - 100 mM), the correlation coefficient was even higher ($R^2 = 0.999$). Based on these data, we selected the concentration of spiked oxalic acid of 100 mM for rCOCl procedure in order to maximize the CaOx Raman signal. The urinary rCOCl value was calculated from the ratio of CaOx Raman signal (intensity or AUP or FWHM) of urine sample to the CaOx Raman signal (intensity or AUP or FWHM) of control (100 mM spiked oxalic acid in water).

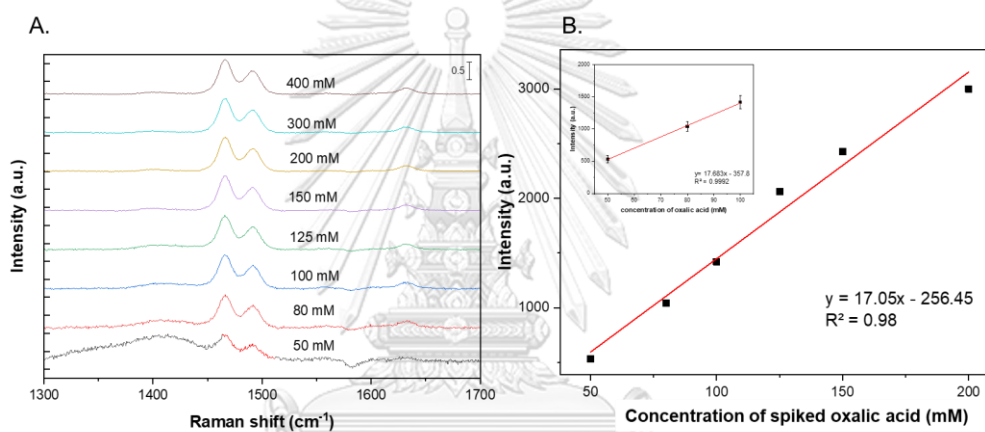


Figure 35 The standard curve of the Raman intensity against spiked oxalic acid concentrations. (A) Intensity signal of each concentration of spiked oxalic acid (50 – 400 mM). (B) The standard curve shows correlation of peak intensity and spiked oxalic acid concentrations ($R^2 = 0.98$).

4.1.10 The size of CaOx crystals produced by COCl procedure.

We measured the size of crystals produced after adding oxalic acid and CaCl₂ (COCl crystals). The crystals were observed under the light microscope (Magnification 400x). The result showed that the COCl crystals consisted of both small and large sizes. The average size of single crystal was found between 0.4 and 0.6 μm, while the size of aggregated crystals ranged from 1-10 μm, with an average aggregate size of 5

μm . (Figure 36). The electron micrographs confirmed the size of aggregated crystals around $5 \mu\text{m}$ (Figure 37).

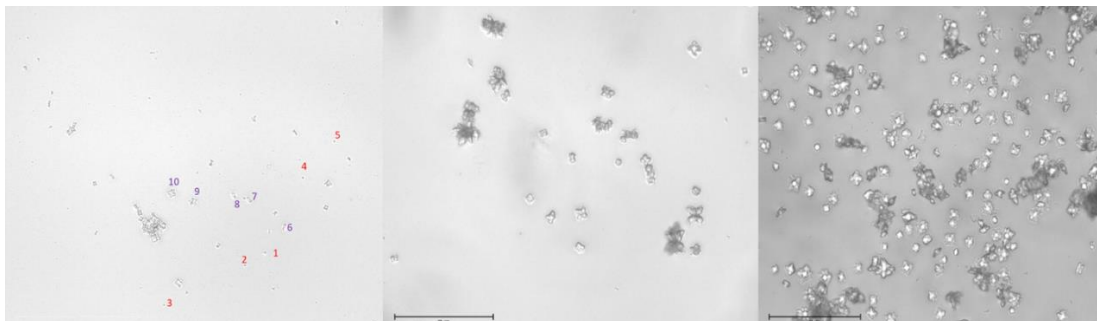


Figure 36 The COCI crystals imaged by EVOS FL Ato2 Imaging System.

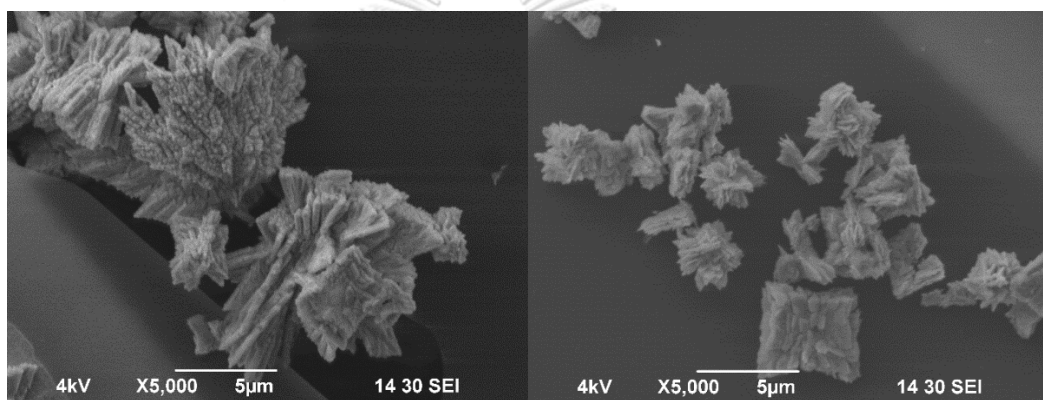


Figure 37 Electron micrographs of COCI crystals. The aggregated crystal size was approximately $5\text{-}10 \mu\text{m}$ measured by SEM.

Part II. Method validation

4.2 Method validation of the rCOCI procedure

After establishing the rCOCI procedure, we conducted a method validation to demonstrate that the new rCOCI method was suitable for the intended application (estimating risk of CaOx stone formation). For the quantitative method, selectivity (specificity), linearity (calibration model), accuracy (bias), precision (repeatability and reproducibility), and limit of detection (LOQ), lower limit of quantification (LOQ) were validation parameters that needed to be characterized and reported.

4.2.1 The specificity

As mentioned above, we found that calcium phosphate (confirmed by FTIR) was frequently precipitated along with CaOx, and it falsely caused increased CaOx Raman signals. We used acetic acid to remove calcium phosphate contaminant. The results showed that the urinary crystals treated with acetic acid had an increased signal of CaOx and generated a low background (range 900-100 cm^{-1}) (Figure 38A). Additionally, FTIR showed that the phosphate peak (1000 cm^{-1}) disappeared after treatment with acetic acid (Figure 38B).

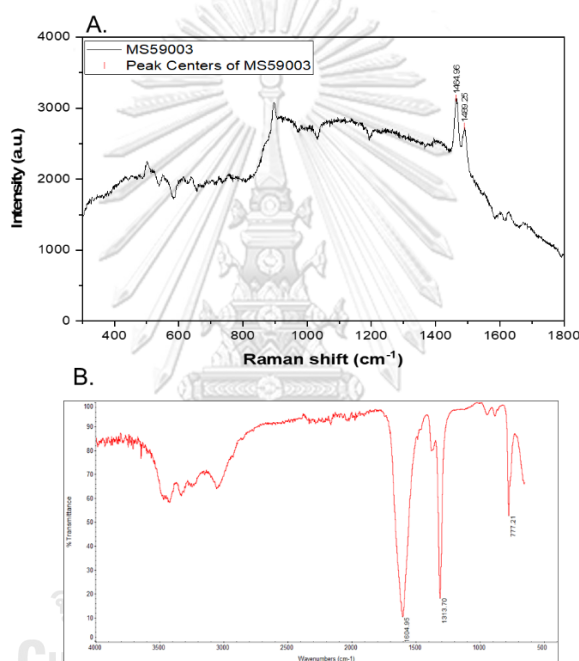


Figure 38 Removal of calcium phosphate by acetic acid treatment. (A) Raman spectrum of COCI crystals treated with 2 N acetic acid. (B) FTIR spectrum of COCI crystals after the acetic acid treatment showing an absence of phosphate (peak at 1000 cm^{-1}).

We further tested the interfering effect of other main urinary substances including urea, creatinine, phosphate, and uric acid on quantifying amount of CaOx by Raman spectroscopy. The normal ranges of these urinary substances are shown in Figure 39. To assess the interfering effect of these compounds, three concentrations (low, medium, and high) of each compound (urea, creatinine, phosphate, and uric

acid) were spiked in the water before performing rCOCl test using the non-spiked sample as control. Additionally, Raman spectrum of each compound (commercially available powder: urea, creatinine, calcium phosphate, and uric acid) was investigated.

The Raman spectroscopy result showed that the main Raman peaks of creatinine were located at 604 cm^{-1} , 674 cm^{-1} and 903 cm^{-1} , urea at 1011 cm^{-1} , CaP at 961 cm^{-1} , uric acid at 1038 cm^{-1} and 1407 cm^{-1} (Figure 40).

For testing the effect of interferences, we performed the rCOCl measurement in water spiked with various concentrations of the potential interfering compounds.

We also asked if CaOx crystals produced in artificial urine were the same as those produced in artificial urine. We confirmed that Raman spectra of CaOx crystals produced in artificial urine and in water (control) was comparable (Figure 41).

Property and Composition	Molar Mass (g/mol)	Normal Range in humans (reference age in years)	Molarity (mmol/1.5L)
Volume		0.8–2L	
pH		4.5–8.0	
Specific gravity (SG)		1.002–1.030 g/ml (all)	
Osmolality		150–1150 mOsm/kg (>1)	
→ Urea ($\text{CH}_4\text{N}_2\text{O}$)	60.06	10–35 g/d (all)	249.750
→ Uric Acid ($\text{C}_5\text{H}_4\text{N}_4\text{O}_3$)	168.11	<750 mg/d (>16)	1.487
→ Creatinine ($\text{C}_4\text{H}_7\text{N}_3\text{O}$)	113.12	Males: 955–2936 mg/d Females: 601–1689 mg/d (18–83)	7.791
Citrate ($\text{C}_6\text{H}_5\text{O}_7^{3-}$)	192.12	221–1191 mg/d (20–40)	2.450
Sodium (Na^+)	22.99	41–227 mmol/d (all)	92.625
Potassium (K^+)	39.10	17–77 mmol/d (all)	31.333
Ammonium (NH_4^+)	18.05	15–56 mmol/d (18–77)	23.667
Calcium (Ca^{2+})	40.08	Males: <250 mg/d Females: <200 mg/d (18–77)	1.663
Magnesium (Mg^{2+})	24.31	51–269 mg/d (18–83)	4.389
Chloride (Cl^-)	35.45	40–224 mmol/d (all)	88.000
Oxalate ($\text{C}_2\text{O}_4^{2-}$)	88.02	0.11–0.46 mmol/d (all)	0.277
Sulphate (SO_4^{2-})	96.06	7–47 mmol/d (all)	18.000
→ Phosphate (PO_4^{2-})	94.97	20–50 mmol/d (>18)	23.33

Figure 39 The normal ranges of urine components in healthy urine.

(Sarigul, N., Korkmaz, F. and Kurultak, I, 2019)

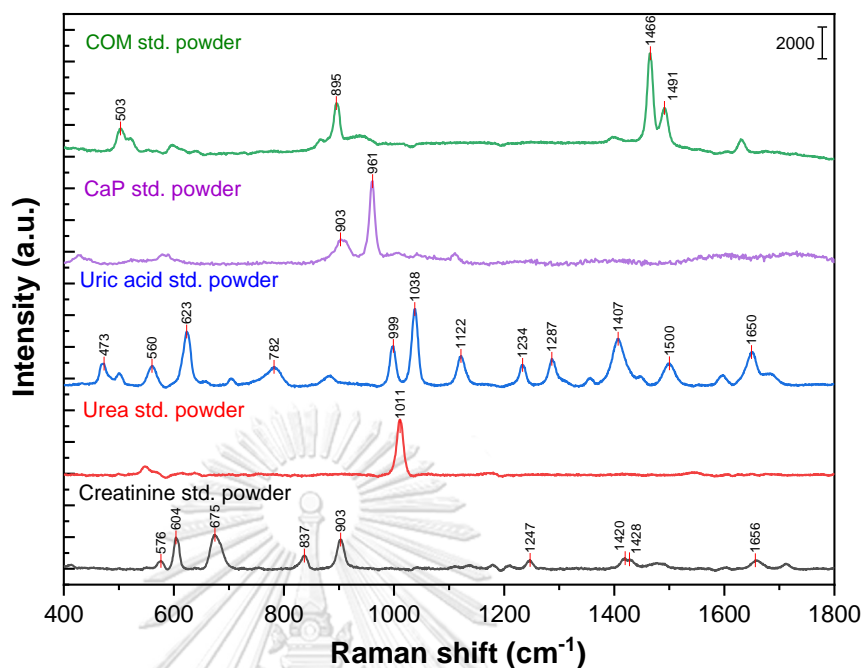


Figure 40 The Raman characteristics of creatinine, urea, CaP, and uric acid.

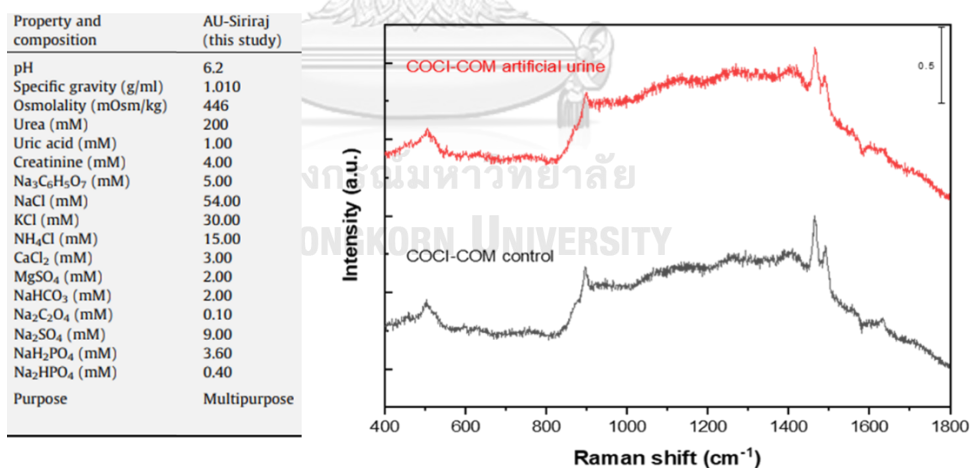


Figure 41 Comparison of Raman spectrum of CaOx crystals produced in artificial urine and water (control). The formula of artificial urine was obtained from AU-Siriraj (S. Chutipongtanate and V. Thongboonkerd, 2010).

For testing selectivity of CaOx measurement by Raman spectroscopy, water samples (control) were spiked with creatinine, urea, phosphate, and uric acid before adding oxalic acid and CaCl₂ and analyzing Raman spectrum. The result found that water control spiked with creatinine at low (2.6 mM), medium (5.2 mM), and high (10.4 mM) concentrations exhibited the similar Raman spectrum with the non-spiked control (Figure 42). The FWHM of spiked samples with low creatinine (39), medium creatinine (38) and high creatine (38) were slightly higher than the non-spiked control (37) (Figure 42).

For phosphate interference testing, water samples were spiked with NaH₂PO₄ at low (7.78 mM), medium (15.5 mM), and high (31 mM) concentrations. The result showed that FWHM of spiked sample with low phosphate was comparable to the non-spiked control (38 vs. 37). In contrast, FWHM of spiked samples with medium and high phosphate levels were relatively higher than the non-spiked control (Figure 43).

For testing the interfering effect of urea, samples were spiked with urea at low (83 mM), medium (167 mM), high (322 mM) concentrations. The result showed that low and high urea spiked samples had no difference of FWHM compared with non-spiked control. However, the high urea-spiked sample had a lower FWHM than the non-spiked control (Figure 44).

In testing the interfering effect of uric acid, samples were spiked with uric acid at low (0.5 mM), medium (1 mM), high (2 mM) levels. The result found that FWHM of spiked sample with low uric acid was relatively higher than non-spiked control (40 vs. 37). Likewise, FWHM of spiked samples with medium uric acid was higher than the non-spiked control (43 vs. 37). Moreover, FWHM of spiked sample with high concentration of uric acid was clearly higher than the non-spiked control (61 vs. 37) (Figure 45).

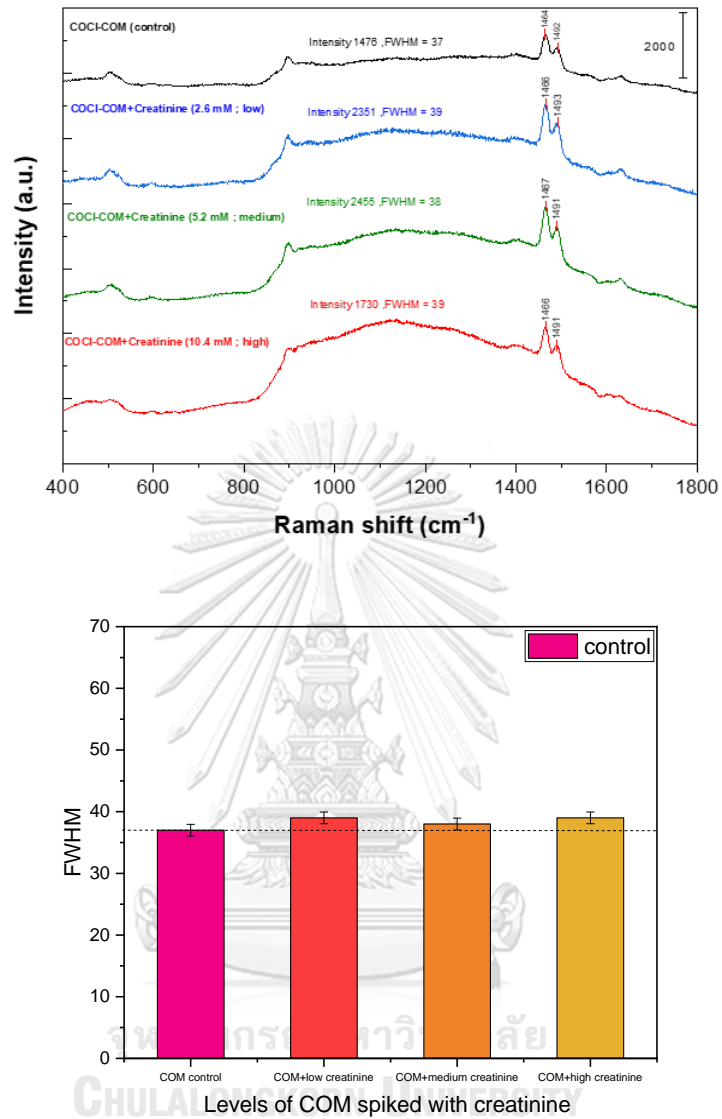


Figure 42 Interfering effect of creatinine in quantifying CaOx.

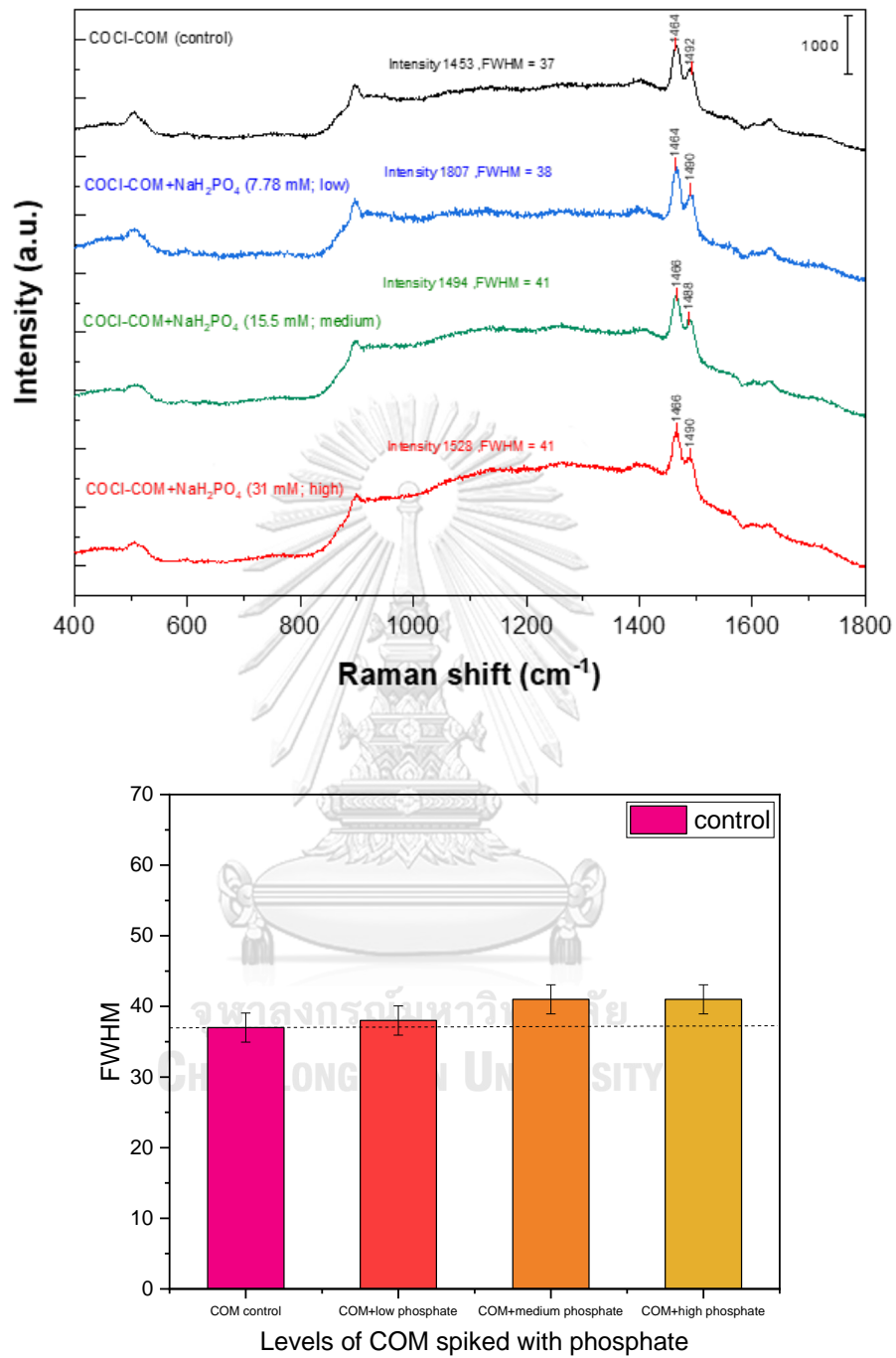


Figure 43 Interfering effect of phosphate in quantifying CaOx.

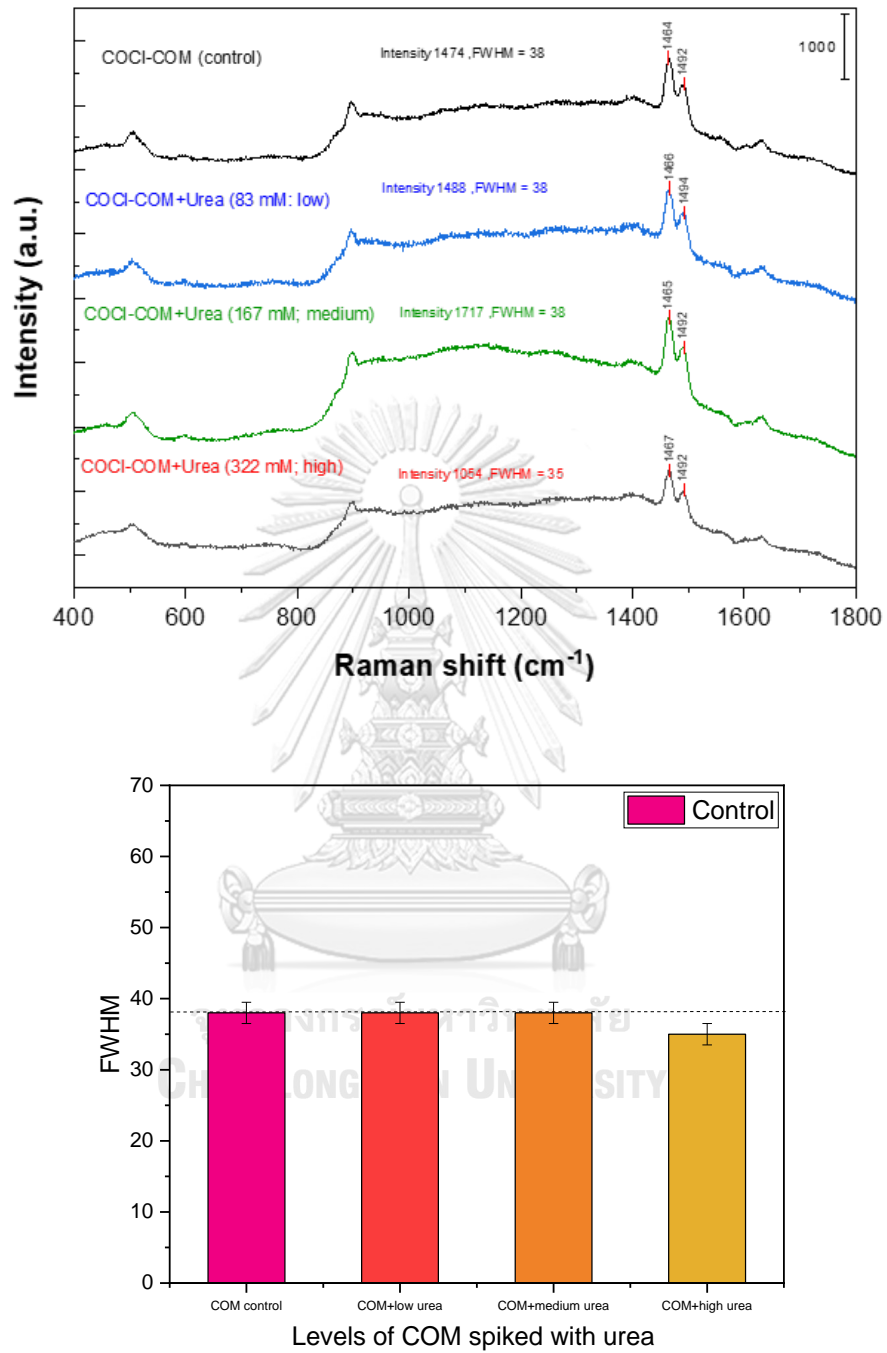


Figure 44 Interfering effect of urea in quantifying CaOx.

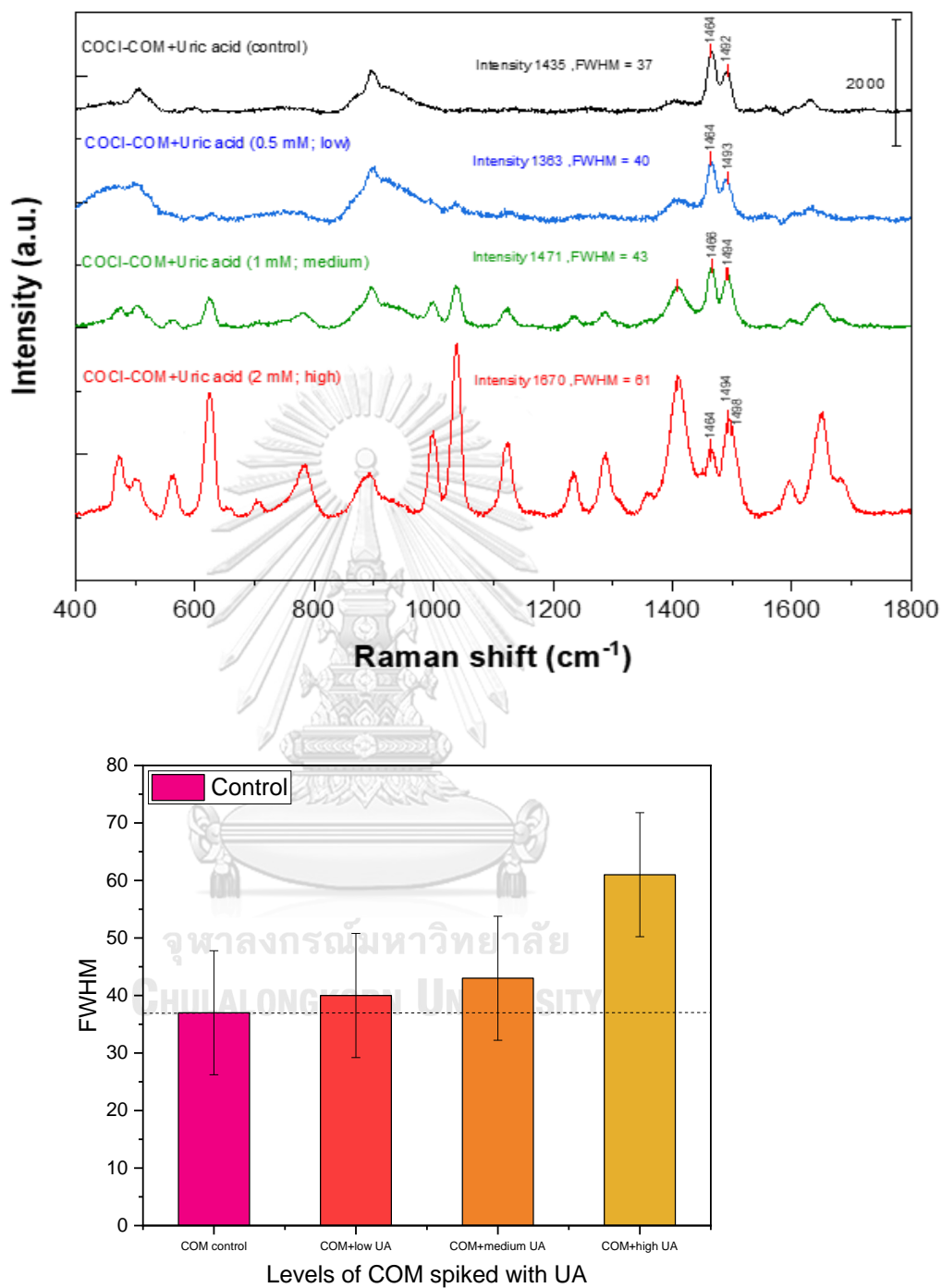


Figure 45 Interfering effect of uric acid (UA) in quantifying CaOx.

4.2.2 The linearity

We tested linearity of rCOCl measurement in control (CaOx formed in water) and test samples (CaOx formed in pooled urine from non-stone subjects and stone patients). CaOx crystals were produced from the COCl procedure with different concentrations of spiked oxalic acid (50, 80, 100, 125, 150, 200, 300, and 400 mM). We quantified amount of CaOx from Raman spectrum using three quantitative parameters including peak intensity, AUP, and FWHM. Raman spectra of CaOx formed in the water condition (control) are shown in Figure 46A. The intensity, AUP, and FWHM of CaOx signals (1464 and 1490 cm^{-1}) were increased when the concentrations of spiked oxalic acid increased (Figure 46B). Moreover, concentrations of spiked oxalic acid above 100 mM were not well linearly proportional to intensity, AUP, and FWHM of CaOx. The best linearity range was between 50 and 100 mM of spiked oxalic acid for all three quantitative parameters. Based on the linear curve of 50 - 100 mM spiked oxalic acid, R^2 for intensity, FWHM, and AUP were 0.9995, 0.9899, and 0.9992, respectively (Figure 46D).

In pooled non-stone urine, the CaOx Raman signals consisted of both COM (1464+1490 cm^{-1}) and COD (1477 cm^{-1}) depending on the oxalic acid concentrations (Figure 47A). The intensity, AUP, and FWHM of CaOx signals were increased when the concentrations of spiked oxalic acid increased (Figure 47B). The best linearity range was between 50 and 100 mM of spiked oxalic acid concentrations (R^2 for intensity = 0.9309, R^2 for AUP = 0.9999, R^2 for FWHM = 1.00), (Figure 47D).

For pooled stone urine, the Raman spectrum result showed that CaOx signal increased when spiked oxalic acid concentrations increased (COD as the main CaOx type, 1477 cm^{-1}) (Figure 48A). The best linearity range was between 50 and 100 mM of spiked oxalic acid concentrations for (R^2 for intensity = 0.7499, R^2 for AUP = 0.7958), R^2 for FWHM = 0.9829) (Figure 48D).

From these data, we concluded that the linearity range for measuring CaOx by rCOCl method was 50–100 mM. Among three quantitative parameters of the CaOx

signal (intensity, AUP, and FWHM), the peak intensity showed the best result to reflect total amount of CaOx in the sample.

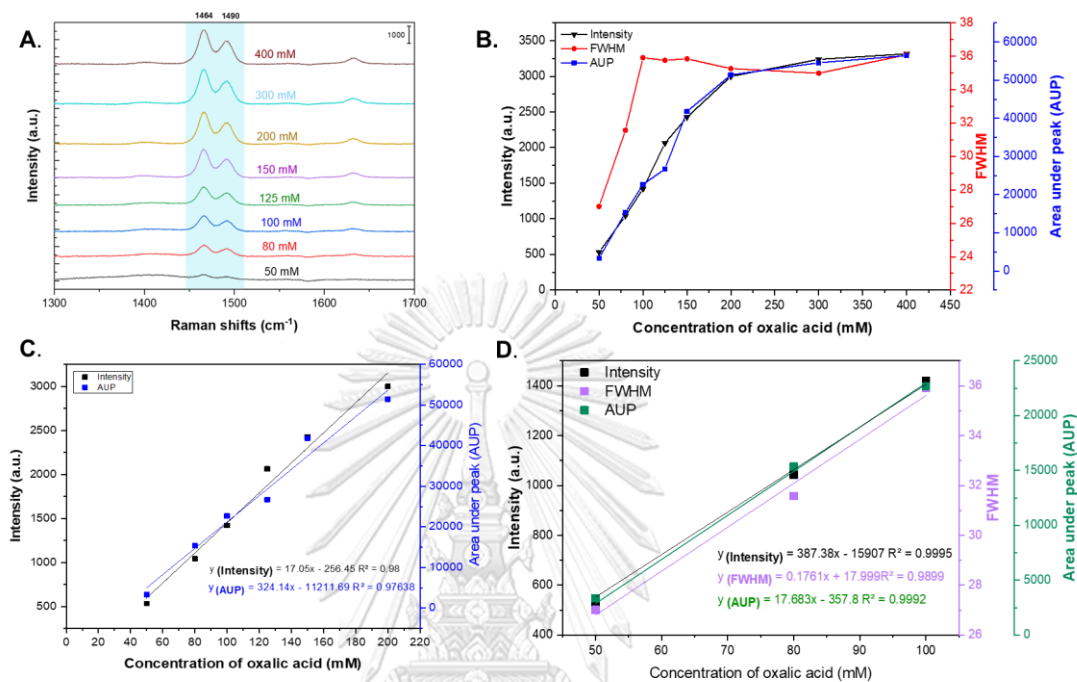


Figure 46 Characteristics of CaOx generated in water (control).

- (A) CaOx Raman spectrum of each concentration of spiked oxalic acid.
- (B) Correlation between CaOx quantitative parameters (intensity, AUP and FWHM) and concentrations of spiked oxalic acid (50-400 mM).
- (C) The linearity of spiked oxalic acid concentrations between 50 and 200 mM.
- (D) The best linearity of spiked oxalic acid concentrations was observed between 50 mM and 100 mM.

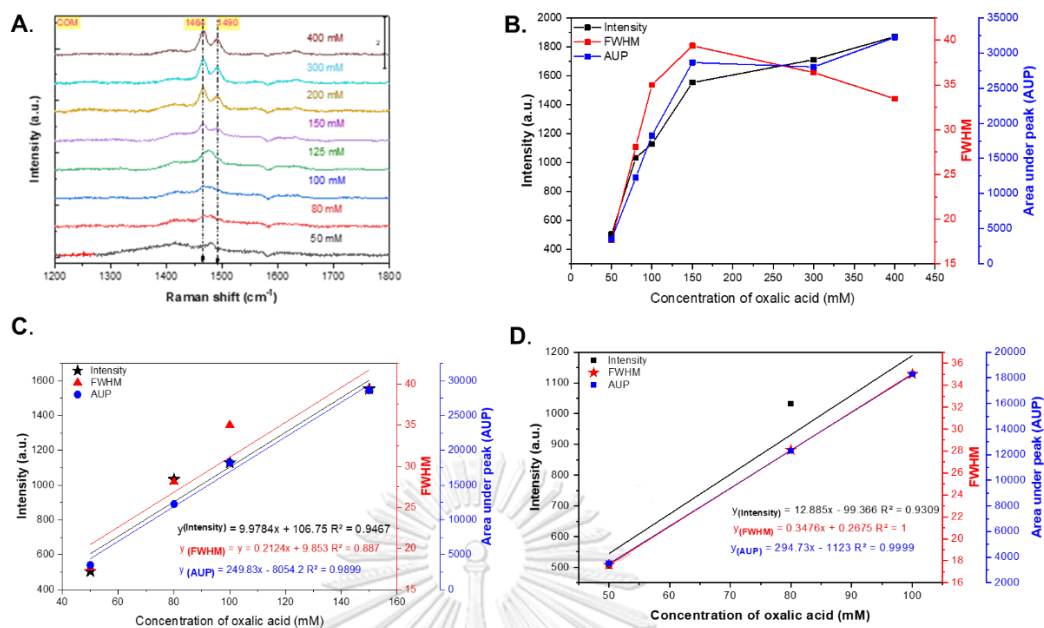


Figure 47 Characteristics of CaOx generated by COCl procedure in pooled non-stone urine.

- (A) CaOx Raman spectrum of each concentration of spiked oxalic acid.
- (B) Correlation between CaOx quantitative signals and spiked oxalic acid concentrations (50-400 mM).
- (C) The linearity for spiked oxalic acid concentrations between 50 and 150 mM.
- (D) The best linearity of spiked oxalic acid concentrations was observed between 50 and 100 mM.

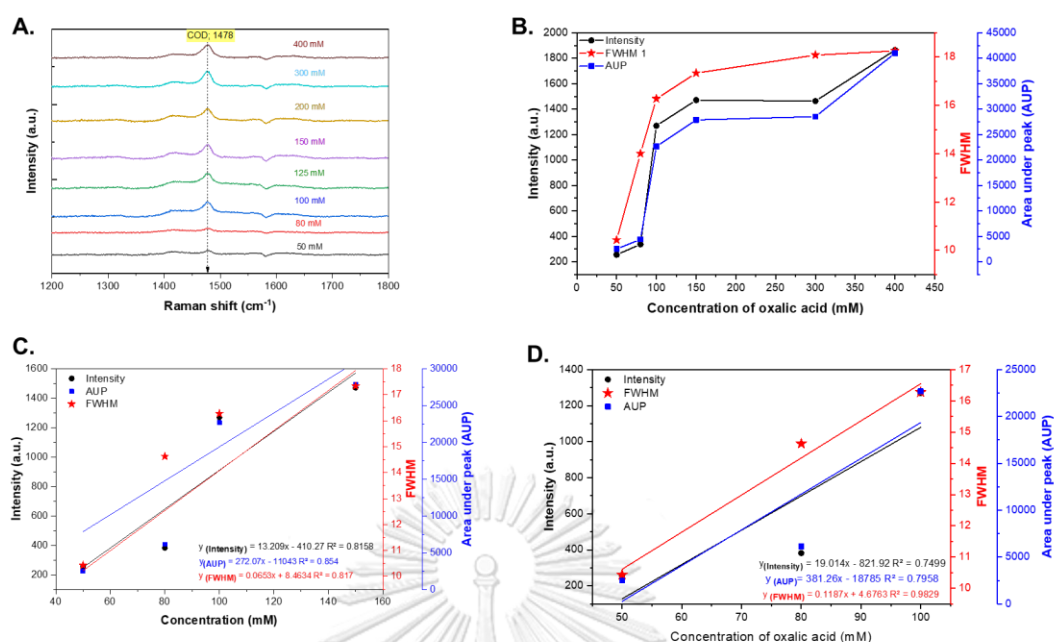


Figure 48 Characteristics of CaOx generated by COCl procedure in pooled stone urine.

- (A) Raman spectrum of CaOx generated in each spiked oxalic acid concentration.
- (B) Correlation between CaOx quantitative signals and spiked oxalic acid concentrations (50-400 mM).
- (C) The linearity for spiked oxalic acid concentrations between 50 and 150 mM.
- (D) The best linearity of spiked oxalic acid concentrations was observed between 50 and 100 mM.

4.2.3 Sensitivity

Limit of detection (LOD) and limit of quantitation (LOQ)

To determine the LOD, we varied concentrations of spiked oxalic acid from 10 mM to 400 mM to define the lowest concentration of spiked oxalate that was able to produce enough CaOx to be able to detect and quantify by Raman spectroscopy. We performed in both water and pooled urine samples (both non-stone and stone urine). We found that spiked oxalic acid at concentration of 10-30 mM could not

produce CaOx crystals (Figure 49). At concentration of 50 mM, it showed a low CaOx precipitation and gave a low CaOx Raman signal. Also, a high background of microscopic slide microscope appeared both in water and pooled urine samples. Fundamentally, LOD is calculated from $3.3 \times \text{SD}$ of intercept/slop, and LOQ is $10 \times \text{SD}$ of intercept/slop. Based on our data, the urinary rCOCl test had LOD of 31 mM, and LOQ of 95 mM for water sample. In pooled non-stone urine, the LOD was 24 mM and LOQ was 72 mM. In pooled stone urine, LOD was 35 mM and LOQ was 105 mM (Figures 50).

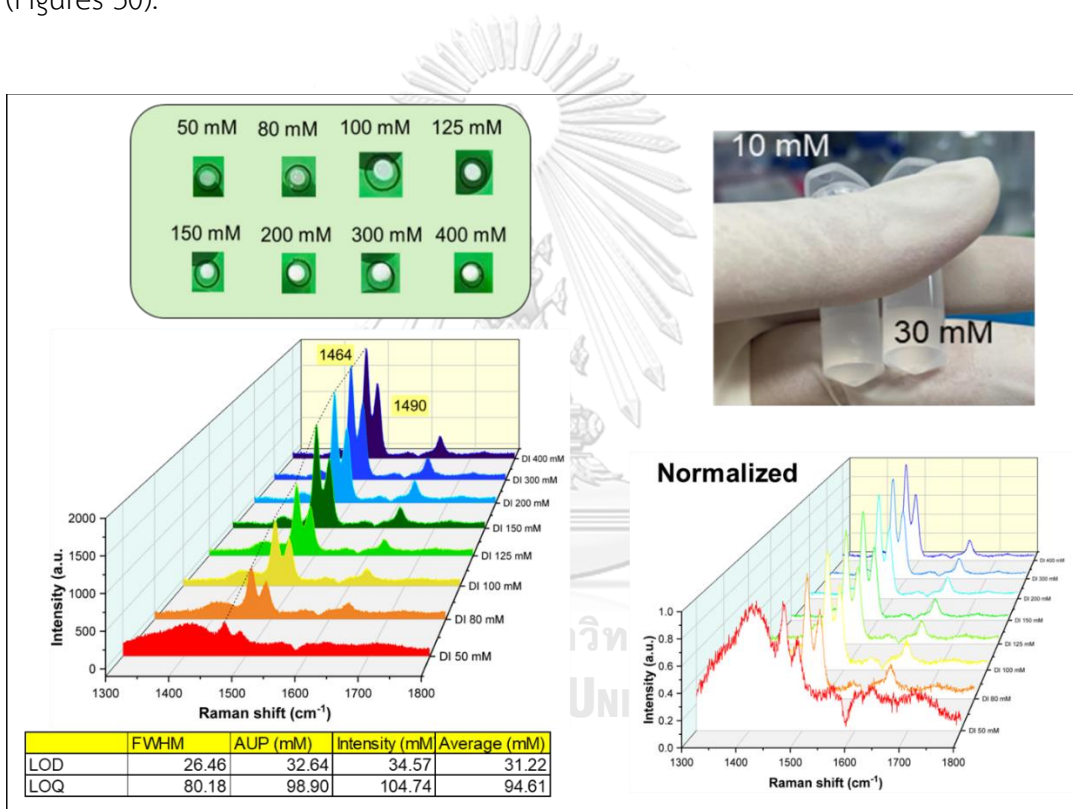


Figure 49 LOD and LOQ of rCOCl measurement performed in water sample. No CaOx precipitation was observed at the spiked oxalic acid concentrations between 10 and 30 mM.

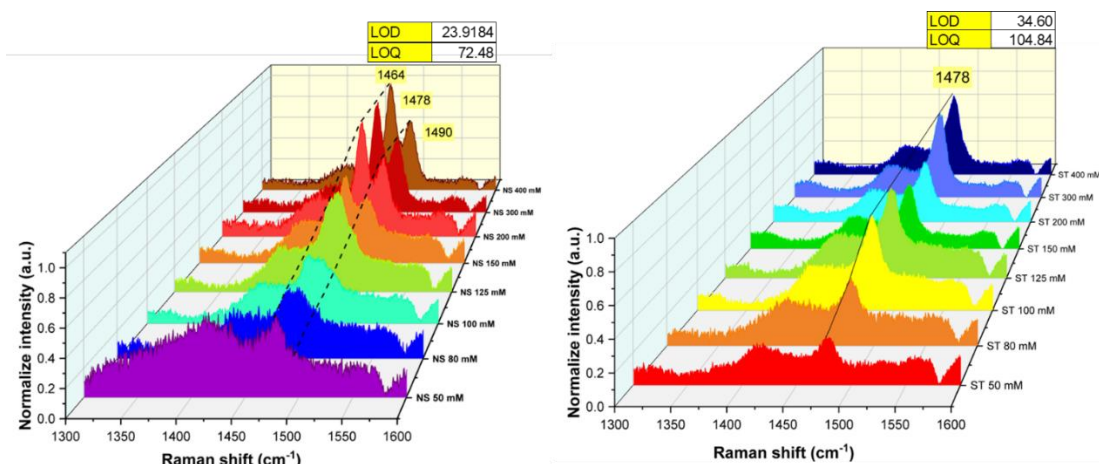


Figure 50 LOD and LOQ of rCOCl measurement performed in pooled non-stone (NS) and pooled stone (ST) urine samples.

4.2.4 Precision (repeatability and reproducibility)

Precision is a characteristic that indicates the ability to obtain similar results when testing the same sample multiple times (e.g., $n=10$).

Repeatability

We measured repeatability, indicated by the relative standard deviation (RSD), in control (CaOx formed in water), individual urine, and pooled urine (non-stone and stone) samples spiked with 100 mM oxalic acid (as described in the COCl procedure). The rCOCl test was performed at the same time and on the same day.

The result showed that the RSD of control sample ($n=10$) was of 4.08% for AUP, 6.94% for peak intensity (peaks: $1464+1478+1490$) and 1.35% for FWHM (Figure 51). When separating the peaks, the RSD of intensity at 1464 cm^{-1} = 6.53% (for COM), RSD of intensity at 1490 cm^{-1} = 7.72% (for COM), and RSD of intensity at 1478 cm^{-1} = 8.38% (for COD).

In individual non-stone urine sample ($n=10$), RSD for AUP was 11.27%, RSD for intensity 1478 cm^{-1} (COD) was 9.32% and RSD for FWHM was 13.78. Individual stone

urine sample (repeated for 10 times) showed RSD of AUP = 10.62%, RSD intensity of $1464+1490\text{ cm}^{-1}$ (COM) = 16.5% and RSD of FWHM = 4.37% (Figure 52).

For pooled non-stone urine sample, the result showed that RSD of AUP = 7.15 % and RSD of normalized intensity (reduced background) of $1464+1490\text{ cm}^{-1}$ (COM) = 13.26%, and RSD of FWHM = 18.63%. Pooled stone urine sample exhibited RSD of AUP (COD) = 10.32%, and RSD intensity of 1478 cm^{-1} = 20.53% and RSD of FWHM = 12.81 (Figure 53).

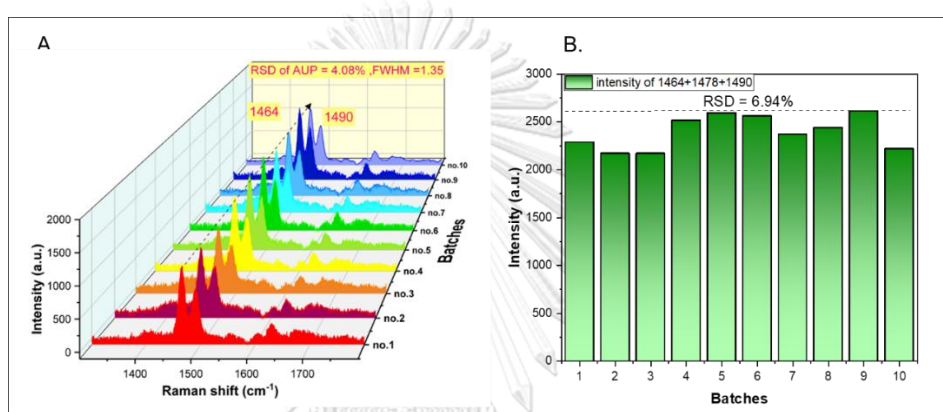


Figure 51 10 different batches of rCOCl measurement in control (water).

- (A) Repeatability measurements of AUP and FWHM signal for detection of CaOx from the same batch.
- (B) Repeatability measurements of intensity signal for detection of CaOx from the same batch.

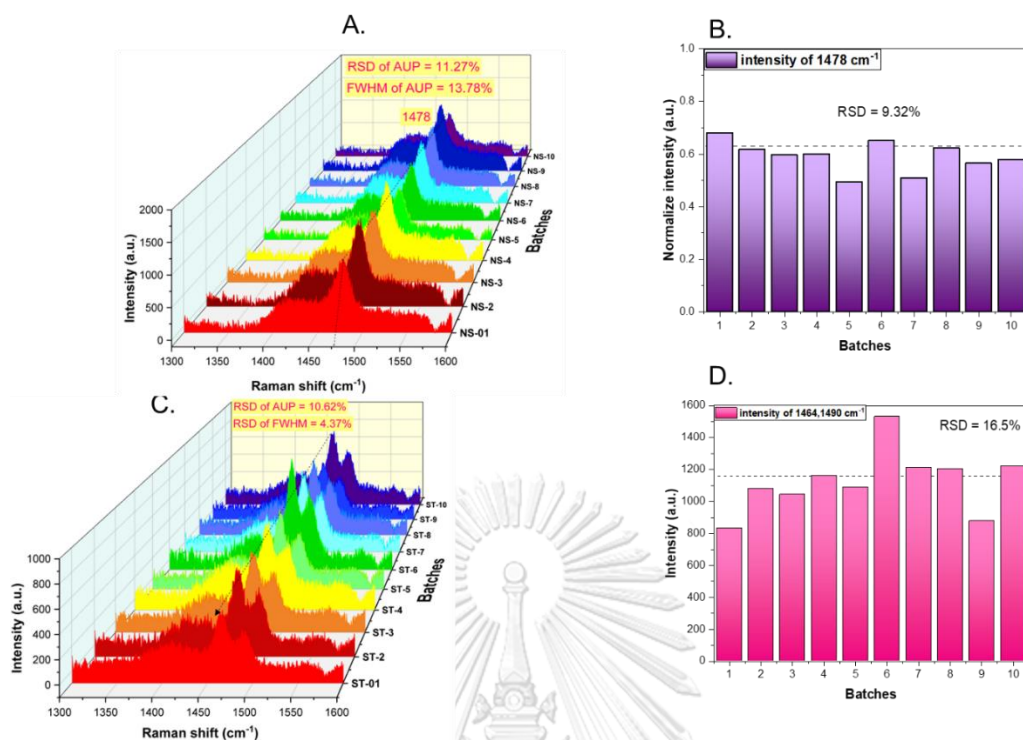


Figure 52 10 different batches of rCOCI measurement in urine samples.

(A) Raman spectrum for detecting CaOx (COD) in individual non-stone urine sample from the same batch (B) RSD (repeatability) of rCOCI measurement (intensity 1478 cm⁻¹ signal) for detection of COD in individual non-stone urine sample from the same batch (C) Raman spectrum for detecting CaOx (COM) in individual stone urine from the same batch (D) RSD (repeatability) of rCOCI measurements (intensity 1464 and 1490 cm⁻¹ signals) for detection of COM in individual stone urine from the same batch.

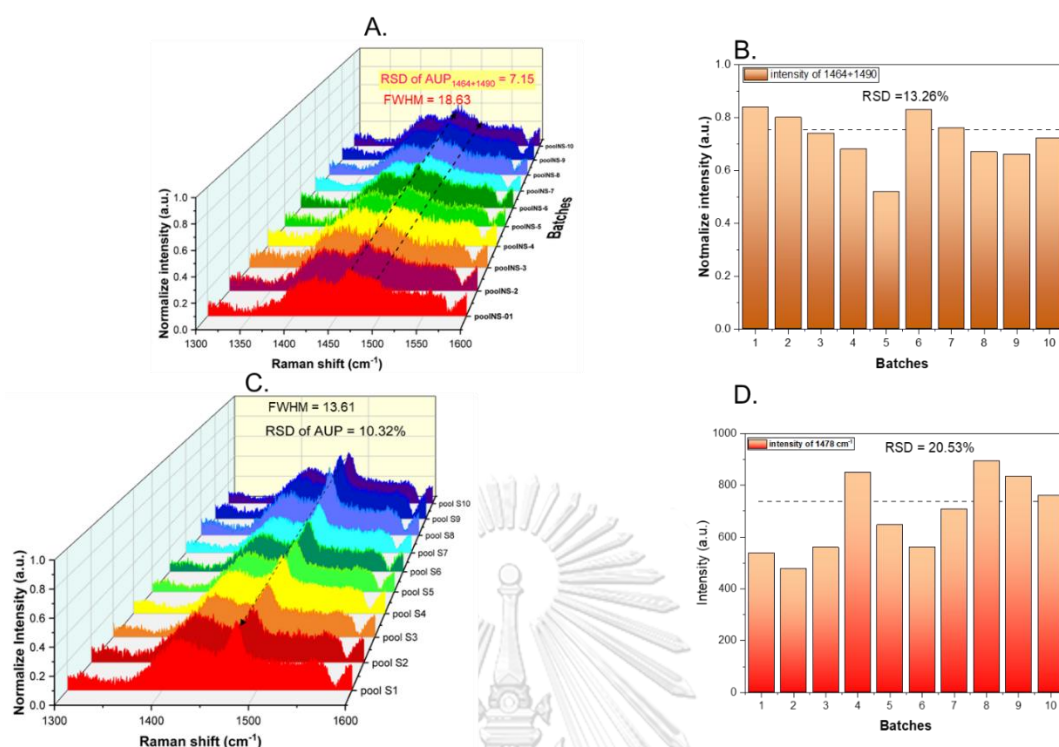


Figure 53 10 different batches of rCOCI measurement in pooled urine samples. (A) Raman spectrum for detecting COM in pooled non-stone urine sample from the same batch (B) RSD (repeatability) of rCOCI measurements (intensity 1464+1490 cm⁻¹ signals) for detection of COM in pooled non-stone urine sample from the same batch (C) Raman spectrum for detecting COD in pooled stone urine sample from the same batch (D) RSD (repeatability) of rCOCI measurements (intensity 1478 cm⁻¹ signal) for detection of COD in pooled stone urine sample from the same batch.

Reproducibility

For assessing reproducibility, we performed rCOCI measurement 4-5 replicate in control (water), pooled non-stone urine, and pooled stone urine samples (spiked with 100 mM oxalic acid). The measurement was performed on different days. The result showed that RSD of AUP = 1.81%, RSD of FWHM = 1.17% and RSD of intensity (COM) = 3.59%. In addition, the single peak of COM showed RSD of intensity at 1464 cm⁻¹ and 1490 cm⁻¹ were 4.67% and 1.94%, respectively. In pooled non-stone urine,

the RSD of AUP and intensity were of 10.24% and 18.08%, respectively. Pooled stone sample showed RSD of AUP = 9.95% and RSD of intensity = 9.30% (Figure 54).

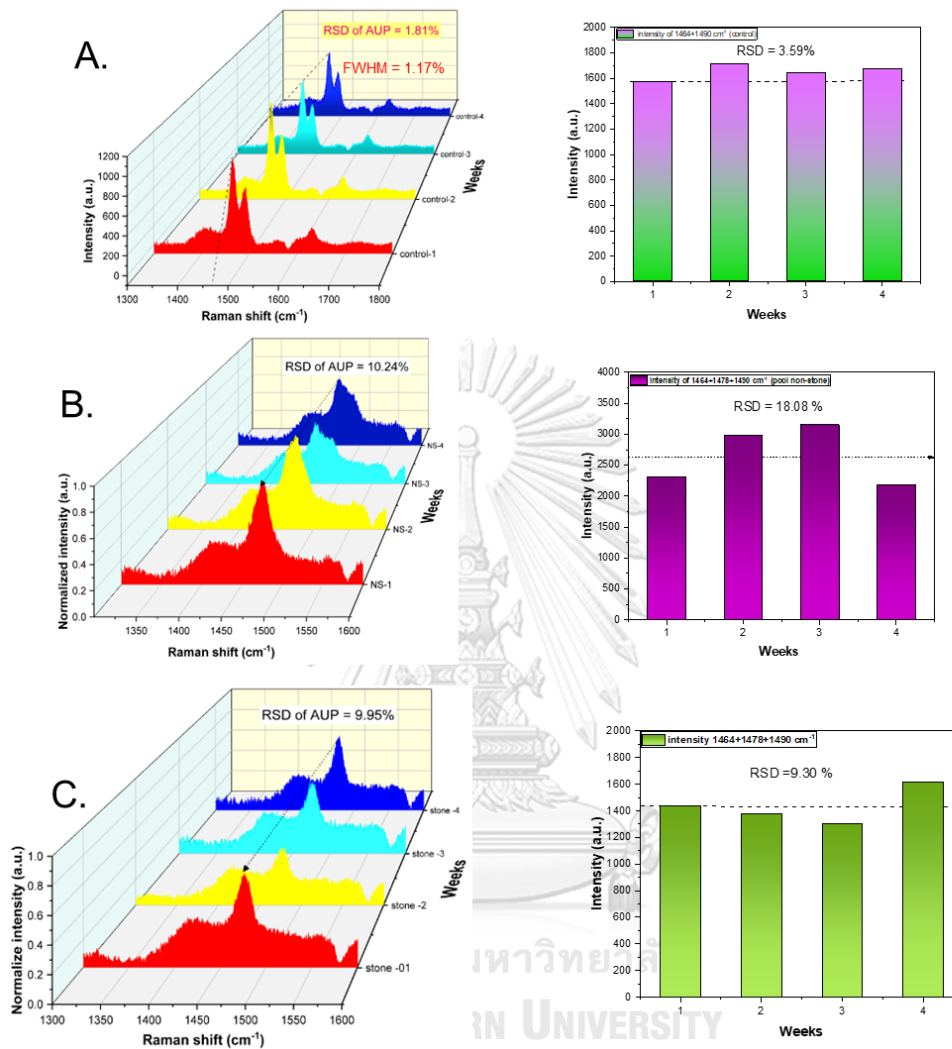


Figure 54 Reproducibility of rCOCI measurement (between day measurement). (A) control (water). (B) Pooled non-stone urine sample. (C) Pooled stone urine sample.

Stability of CaOx crystals produced by COCl procedure.

The long-term stability of CaOx crystals produced by COCl procedure (after adding spiked oxalic acid and CaCl_2) was evaluated. In this study, we tested the stability of CaOx produced in control (water) and pooled non-stone urine and pooled stone urine samples. The stability period tested was one month compared between storage at RT and at 4°C . The result showed that the Raman characteristics of CaOx crystals were stable. Storage either at RT or 4°C did not alter the Raman characteristics of CaOx crystals (Figure 55).

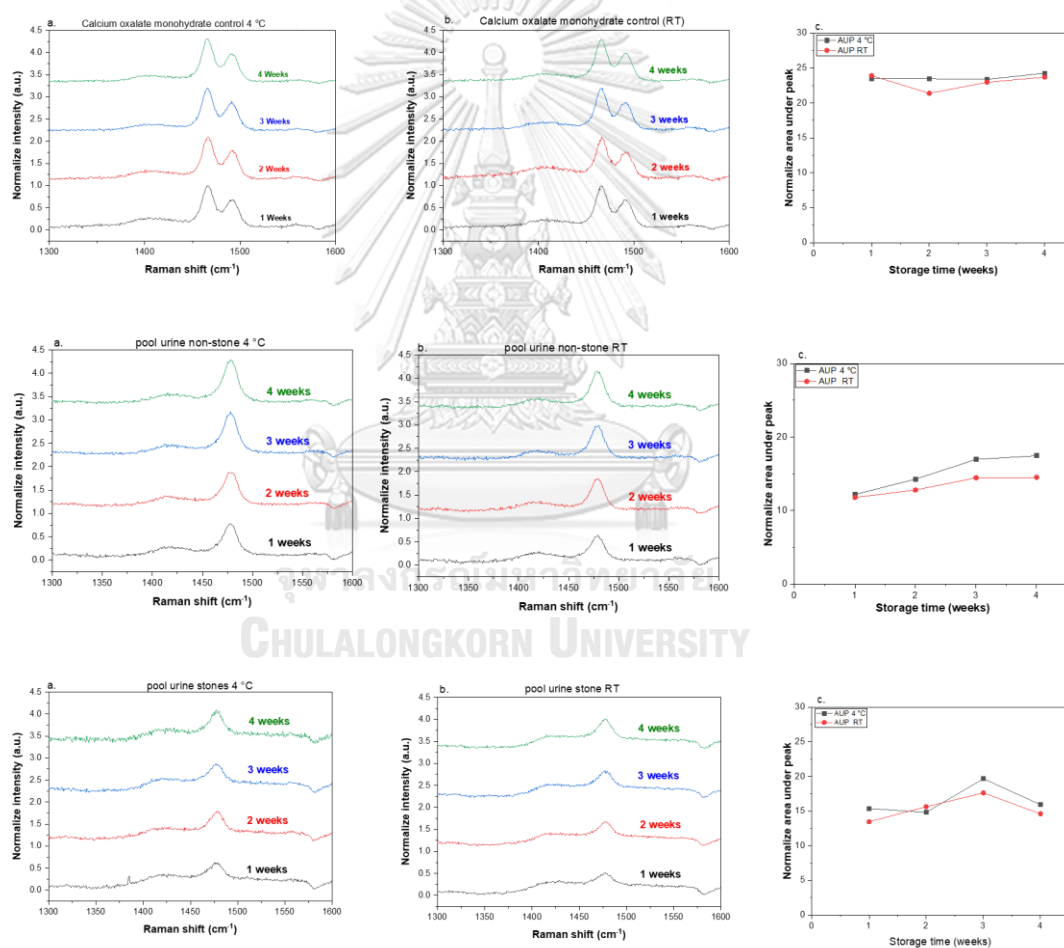


Figure 55 Stability of CaOx crystals produced from COCl procedure in a month.

Correlation of urinary rCOCl values calculated from spectrum of FTIR and Raman spectroscopy.

We compared the result of CaOx quantitative measurement between Raman spectroscopy and FTIR in 10 urine samples. The results showed that quantitative measurement of CaOx by Raman spectroscopy and FTIR were positively correlated with R^2 of 0.78 ($r = 0.89$) (Figure 56).

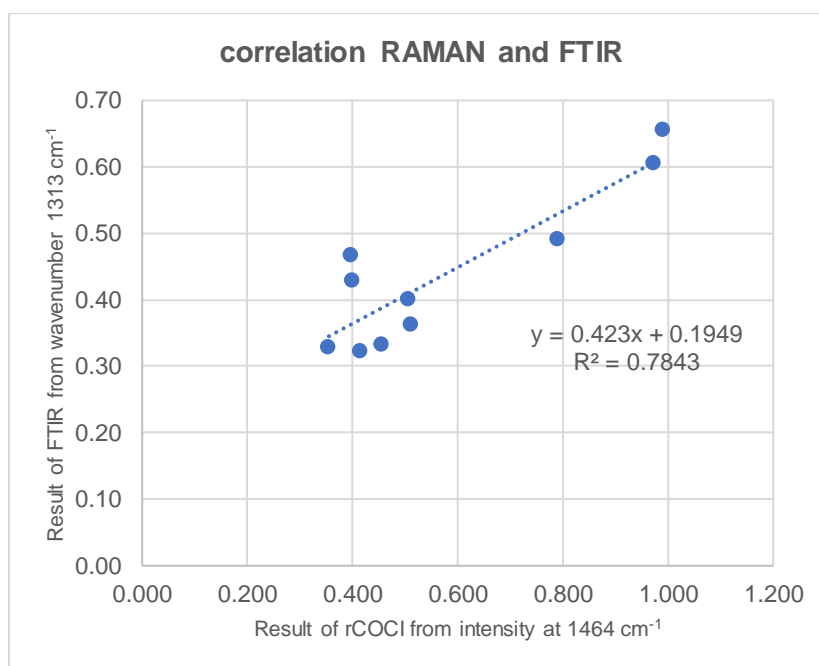


Figure 56 Correlation of CaOx quantitative measurement by Raman spectroscopy and FTIR technique.

Part III: Clinical validation

4.3 Clinical validation of rCOCI test

4.3.1. 24-h urine samples

In this study, a total of 225 24-h urine samples were obtained from 98 non-stone subjects (NS) and 127 stone (ST) patients. These urine samples were leftover samples from the research project “Test accuracy of urinary of calcium oxalate crystallization index (COCI) for diagnosis of urolithiasis, and development of an innovation quantum dot nanoparticle-base method for determination of urinary oxalate (IRB:286/59)”. The urinary stone condition was diagnosed by CT scan. Fourier transform infrared spectroscopy (FTIR) was used to identify types of 60 urinary stone samples. Based on FTIR results, stone types were divided into three main types, including calcium oxalate (CaOx, n=44, 75.86%), calcium phosphate (CaP, n=4, 6.90%), and uric acid (UA, n=10, 17.24%). The average age (51 ± 8 vs 56 ± 11 years), creatinine (555 ± 385 vs 714 ± 555 mg/day), and urinary iCOCI (0.59 ± 0.56 vs 1.51 ± 2.37 COM equivalent g/day) of ST group were significantly higher than the NS group. Urinary calcium (40 ± 42 vs 24 ± 40 mg/day) in NS group was significantly higher than in ST group (Table 5).

Table 5 Characteristics of the studied subjects (n=225).

Characteristic	CT scan negative	CT scan positive	P value
Number of samples	98	127	-
Age (years)			<0.0001***
Mean \pm SD	51 \pm 8	56 \pm 11	
Median (IQR)	50	55	
Sex			-
Male (%)	28 (28.57%)	83 (65.35%)	
Female (%)	70 (71.43%)	44 (34.66%)	
BMI (Kg/m ²)			0.0553
Mean \pm SD	25.03 \pm 4.44	23.61 \pm 4.83	

Median (IQR)	24.04	23.43	
Urine volume (mL)			0.7004
Mean \pm SD	1402 \pm 667	1457 \pm 559	
Median (IQR)	1260	1355	
Urine creatinine (mg/day)			0.0152*
Mean \pm SD	555 \pm 385	714 \pm 555	
Urine iCOCI (g/day)			<0.0001***
Mean \pm SD	0.59 \pm 0.56	1.51 \pm 2.37	
Urine calcium (mg/day)			0.0012**
Mean \pm SD	40 \pm 42	24 \pm 40	
Stone type by FTIR (n=58)		44 (75.86%)	
Calcium Oxalate (CaOx,CaOx+CaP)		4 (6.90%)	
Calcium phosphate (CaP)		10 (17.24%)	
Uric acid (UA)			

4.3.2. Determination of rCOCI levels in 24-h urine samples.

At the beginning, a total of 277 24-h urine samples were included in the study (122 from non-stone subjects (NS) and 155 from urolithiasis patients). The rCOCI was measured in all 277 urine samples. The Raman spectra of 15 samples were excluded because of high background noise. The specific CaOx Raman signal could not be derived from those 15 cases (Figure 57). We further excluded 37 cases because of high background noise. Therefore, the urinary rCOCI values used for further calculation of diagnostic accuracy were from 225 urine samples (98 NS subjects and 127 stone patients).

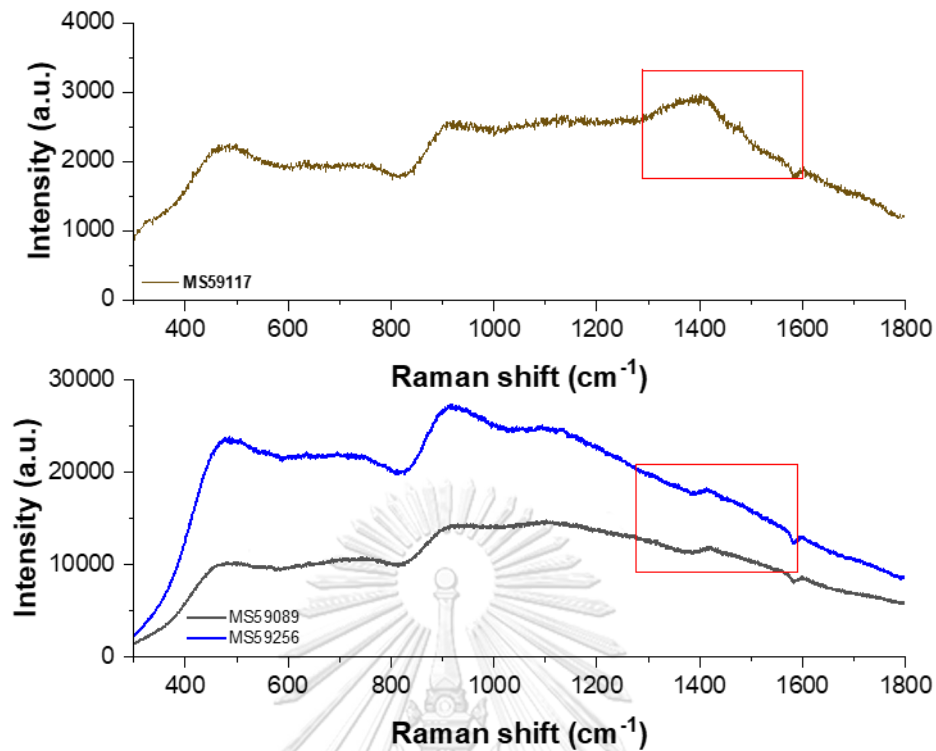


Figure 57 Raman spectra of urine samples with high background noise and no signal of CaOx.

4.3.3. rCOCI measurement in 24-hour urine samples

1. rCOCI measurement in 98 NS subjects and 127 stone patients (n= 225)

After excluding the sample with high background, the urinary rCOCI levels were compared between 98 NS subjects and 127 stone (ST) patients (Table 5). The urinary rCOCI values calculated from peak intensity, AUP, and FWHM. The result revealed that urinary rCOCI of ST group was significantly higher than the NS group (Figure 58).

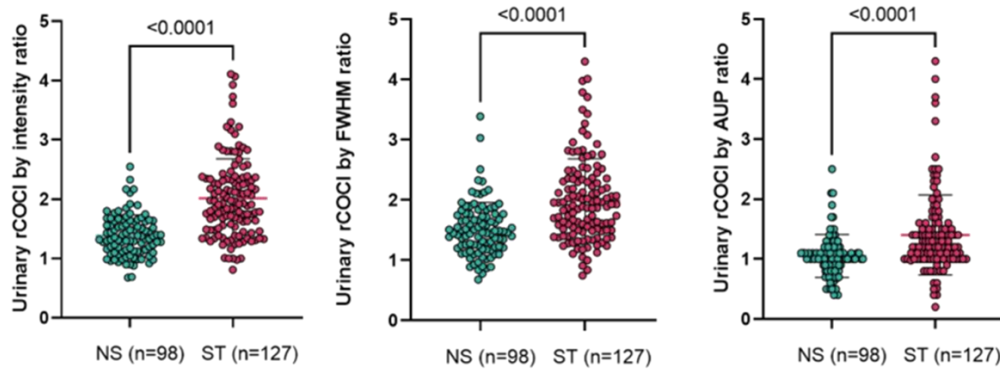


Figure 58 The level of urinary rCOCI calculated from peak intensity (left), FWHM (middle), and AUP (right). For all three quantitative parameters, urinary rCOCI level in the stone group was significantly higher than that in the NS group.

2. Urinary rCOCI levels compared between the NS (n=98) subjects and stone patients with known stone type (n=58).

The obtained result was still the same as the previous result. The urinary rCOCI levels in the NS group (n=98) were significantly greater than and the stone group (n=58) ($p < 0.0001$ for all calculations) (Figure 59).

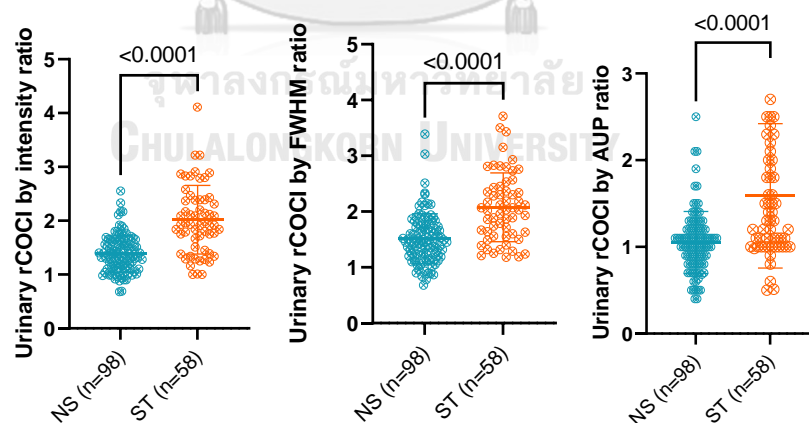
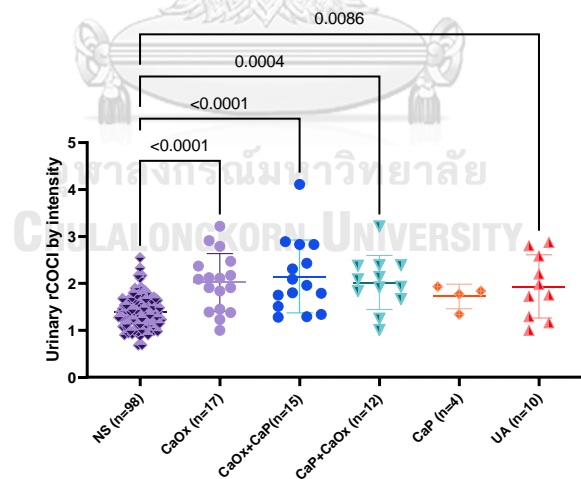


Figure 59 The levels of urinary rCOCI compared between 58 stone patients and 98 NS subjects.

3. The urinary rCOCI levels compared among the NS subjects (n=98) and stone patients (n=58) with different stone types.

After excluding the high background sample, 225 samples with reliable rCOCI data were remained (98 NS and 58 ST). We used these data for further diagnostic accuracy analysis. According to the type of stones, ST group was subdivided into five groups, including CaOx (n=17), CaOx+CaP (n=15), (CaP+CaOx) (n=12), CaP (4), and uric acid (n=10). Comparison of urinary rCOCI level calculated from peak intensity among groups revealed that the urinary rCOCI levels in CaOx, CaOx+CaP, CaP+CaOx, and uric acid groups were significantly higher than the NS group ($p < 0.0001$, $p < 0.0001$, $p = 0.0004$, $p = 0.0086$, respectively). For urinary rCOCI level calculated from the FWHM, the rCOCI levels in CaOx, CaOx+CaP, and CaP+CaOx groups were significantly higher than the NS group ($p = 0.0002$, $p < 0.0001$, $p = 0.0068$, respectively). Comparison of urinary rCOCI levels calculated from AUP showed that only CaP+CaOx group was significantly higher than the NS group ($p < 0.0001$) (Figure 60).



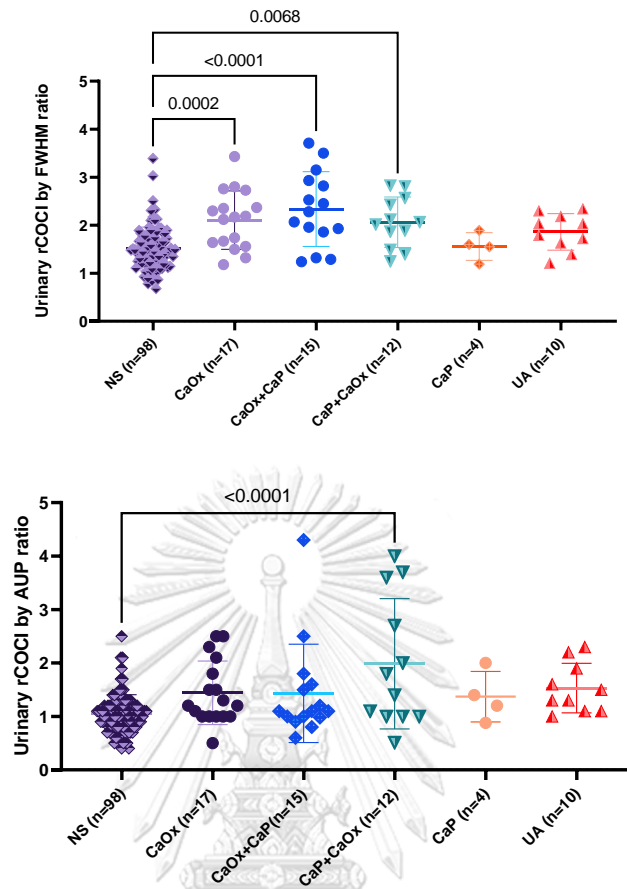


Figure 60 Comparison of urinary rCOCI levels calculated from intensity of peak, FWHM, and AUP between NS subjects and ST patients with different type of stones.

4. The urinary rCOCI levels compared between the NS subjects (n=98) and CaOx stone patients (n=44).

Because rCOCI test measured capacity of CaOx formation in supersaturated urine, and we aimed to use this test to estimate the risk of CaOx stone development. Therefore, we re-grouped the ST group to CaOx group by combing all stone cases who had CaOx stone (including CaOx (n=17), CaOx+CaP (n=15), and CaP+CaOx (n=12), 44 cases in total). Levels of urinary rCOCI in the CaOx group (n=44) were significantly higher than the NS group (n = 98) ($p < 0.0001$ for all calculations) (Figure 61).

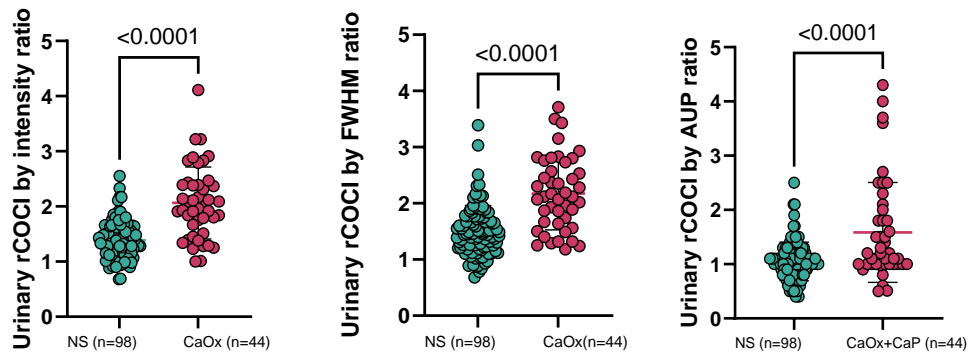


Figure 61 The comparison of urinary rCOCI levels between 98 NS subjects and 44 CaOx stone patients.

5. ROC analysis of the urinary rCOCI test

5.1 The result of ROC analysis to classify NS (n=98) and ST (n=127) subjects

ROC analysis of all rCOCI data to assess how good the test could separate NS subjects (n=98) from ST patients (n=127). The area under ROC curve (AUC) of urinary rCOCI calculated from peak intensity, FWHM and AUP were 0.8069 (95%CI: 0.7511-0.8627), 0.7248 (95%CI: 0.6694-0.7903), and 0.6954 (95%CI: 0.6270-0.7638), respectively (Figure 62).

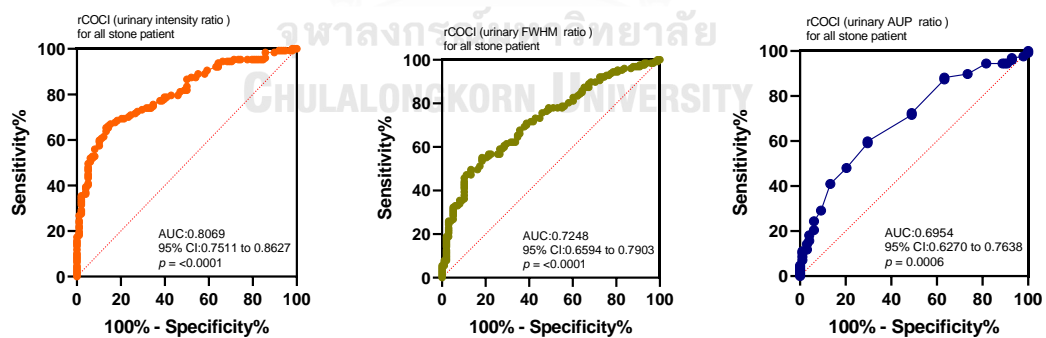


Figure 62 ROC analysis of urinary rCOCI calculated from peak intensity, FWHM, and AUP for distinguishing NS subjects (n=98) from ST patients (n=127).

5.2 The result of the ROC analysis of the urinary rCOCI test for classifying NS subjects (n=98) and ST patients with known type of stones (n=58).

ROC analysis of reliable rCOCI data to assess how good the test could separate NS subjects (n=98) from stone patients with known stone type (n = 58). The area under ROC curve of urinary rCOCI calculated from the intensity of peak, FWHM, AUP were 0.8112 (95%CI: 0.7365-0.8859), 0.7763 (95%CI: 0.7001-0.8525), and 0.7195 (95%CI: 0.6351-0.8039), respectively (Figure 63).

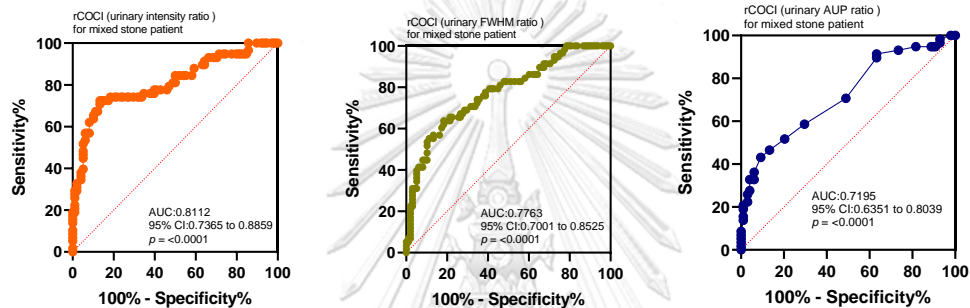


Figure 63 ROC analysis of urinary rCOCI calculated from the intensity of peak, and FWHM for separating NS subjects from stone patients with known stone type (n=58)

5.3 The result of the ROC analysis of the urinary rCOCI test for classifying NS subjects (n = 98) and CaOx stone patients (n=44).

From ROC analysis, the AUC of urinary rCOCI calculated from the intensity of peak, FWHM, AUP for separating the NS subjects from CaOx stone patients (n=44) were 0.8244 (95%CI: 0.7438-0.9051), 0.8011 (95%CI: 0.7198-0.8824), and 0.6821 (95%CI: 0.5833-0.7808), respectively (Figure 64).

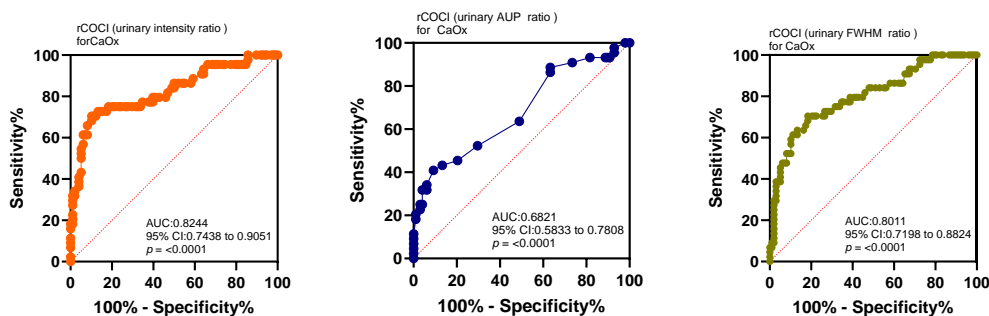


Figure 64 ROC analysis of urinary rCOCI calculated from the intensity of peak, FWHM and AUP to distinguish NS subjects (N=98) from CaOx stone patients (n=44).

6. Selection of urinary rCOCI cutoff values

We aimed to use urinary rCOCI test as a screening test for CaOx urolithiasis, therefore, we chose cutoff value that gave the highest accuracy with the sensitivity of the test at least 80%. According to these criteria, the cutoff values of urinary rCOCI test calculated from peak intensity, FWHM, and AUP were 1.40, 1.50 and 1.05, respectively.

7. Diagnostic values of urinary rCOCI test for CaOx urolithiasis

The diagnostic values including sensitivity, specificity, positive predictive value (PPV), negative predictive value (NPV), positive likelihood ratio (LH^+), negative likelihood ratio (LH^-), and accuracy were calculated based on the cutoff value of urinary rCOCI test calculated from peak intensity of 1.40. Sensitivity, specificity, PPV, NPV, LH^+ , LH^- , and accuracy were 80.00%, 57.00%, 70.63%, 68.29%, 1.86, 0.36, and 70.00%, respectively (Table 6).

The diagnostic values of urinary rCOCI test (FWHM ratio cutoff = 1.50) for separating all stone patients from the NS subjects were calculated. Sensitivity, specificity, PPV, NPV, LH^+ , LH^- , and accuracy were 75.59%, 55.10%, 68.57%, 63.53%, 1.68, 0.44, and 66.67%, respectively (Table 6).

The diagnostic values of urinary rCOCI test (AUP ratio cutoff = 1.05) for separating all stone patients from the NS subjects were also calculated. Sensitivity, specificity, PPV, NPV, LH⁺, LH⁻, and accuracy were 71.65%, 41.84%, 61.49%, 53.25%, 1.23, 0.68, and 58.67%, respectively (Table 6).

For diagnosis of CaOx stone, sensitivity, specificity, PPV, NPV, LH⁺, LH⁻, and accuracy were of urinary rCOCI calculated from peak intensity were 80.00%, 57.00%, 45.45%, 86.15%, 1.86, 0.36, and 64.00%, respectively. For urinary rCOCI calculated from FWHM ratio, sensitivity, specificity, PPV, NPV, LH⁺, LH⁻, and accuracy were 80.00%, 55.00%, 44.30%, 85.71%, 1.82%, 0.33, and 63.00%, respectively (Table 6).

Table 6 Diagnostic values of urinary rCOCI test.

	Urinary rCOCI (Intensity ratio)	Urinary rCOCI (FWHM ratio)	Urinary rCOCI (AUP ratio)
Cut off values	1.40	1.50	1.05
For all stone cases			
Sensitivity	80.00	75.59	71.65
Specificity	57.00	55.10	41.84
PPV	70.63	68.57	61.49
NPV	68.29	63.53	53.25
LH ⁺	1.86	1.68	1.23
LH ⁻	0.36	0.44	0.68
Accuracy	70.00	66.67	58.67
For CaOx stone cases (NS = 98, CaOx = 44)			
Sensitivity	80.00	80.00	n.d.
Specificity	57.00	55.00	n.d.
PPV	45.45	44.30	n.d.
NPV	86.15	85.71	n.d.
LH ⁺	1.86	1.82	n.d.
LH ⁻	0.36	0.33	n.d.

Accuracy	64.00	63.00	n.d.
----------	-------	-------	------

PPV: positive predictive values, NPV: negative predictive value

LH⁺: positive likelihood ratio, LH⁻: negative likelihood ratio

n.d.: not determined.

8. The correlation among urinary rCOCl values calculated from peak intensity, AUP and FWHM

We quantified the total amount of CaOx produced in urine after adding spiked oxalic acid and CaCl₂ using three quantitative parameters (peak intensity, AUP and FWHM). We assessed which parameter was the best for diagnosing CaOx urolithiasis. According to our present data, urinary rCOCl calculated from peak intensity had the highest diagnostic performance and provided the best diagnostic values. We further investigated whether urinary rCOCl calculated from peak intensity was correlated well to the urinary rCOCl calculated from AUP and FWHM. We found that urinary rCOCl levels calculated from peak intensity were well correlated to urinary rCOCl calculated from FWHM ($r = 0.402$, $p < 0.0001$) and AUP ($r = 0.424$, $p < 0.0001$). (Figure 65).

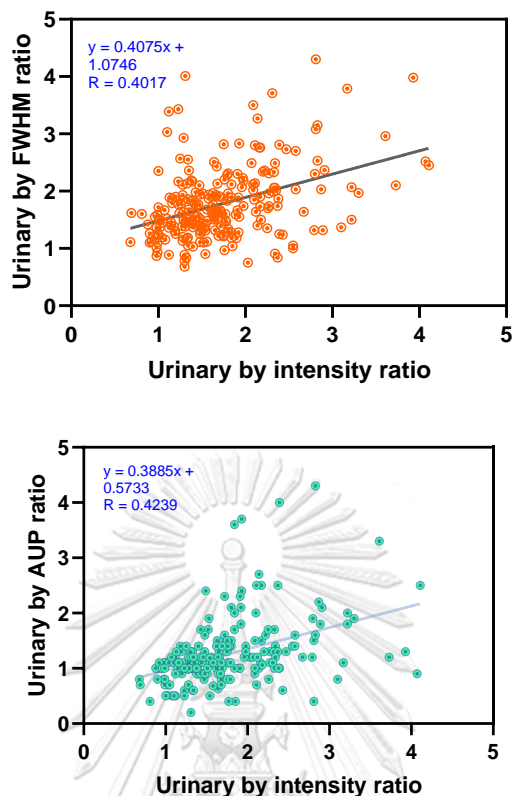
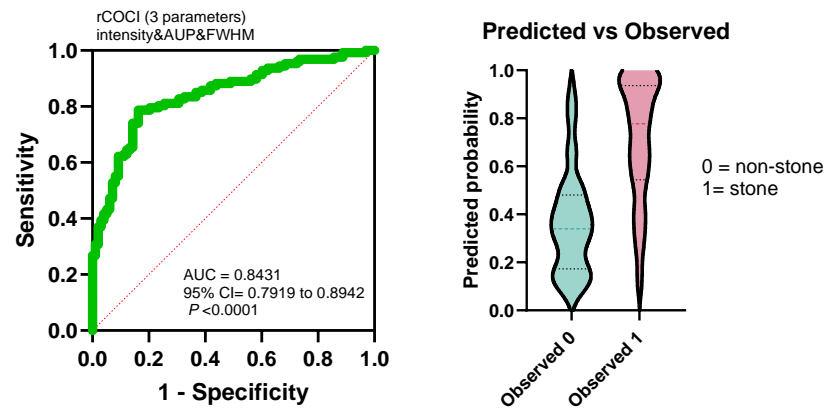


Figure 65 The correlation of urinary rCOCI levels calculated from intensity, FWHM, and AUP.

9. The diagnostic performance of all three calculations of urinary rCOCI test assessed by multiple logistic regression.

Urinary rCOCI values calculated from all three parameters (peak intensity, AUP and FWHM) were evaluated for prediction of urolithiasis using a multiple logistic regression model. The result showed that the AUC of ROC curve of the use of these three parameters in the same model was 0.8431 that was higher than the use of single parameter (either peak intensity or AUP or FWHM). In the predicted vs observed graph, it showed that the stone group had higher predicted probabilities than non-stone group. It provided specificity, sensitivity, and accuracy of 79.53%, 77.55%, and 78.67%, respectively (Figure 66).



Classification table	Predicted 0	Predicted 1	Total	% Correctly classified
Observed 0	76	22	98	77.55 Specificity
Observed 1	26	101	127	79.53 Sensitivity
Total	102	123	225	78.67 Accuracy
Negative predictive power (%)	74.51			
Positive predictive power (%)	82.11			

Figure 66 The combination of rCOCI values (Intensity, FWHM, AUP) for predicting urolithiasis.

Chapter 5 Discussion and Conclusion

In this study, we aimed to develop a new method for detecting and quantifying CaOx crystals produced in the supersaturated urine (challenged with oxalic acid and CaCl₂) by Raman spectroscopy. The method was designated “Raman spectroscopy-integrated calcium oxalate crystallization index or rCOCI” test. The proposed rCOCI test measured the total capacity of urine sample to crystallize CaOx after the urine was induced to be supersaturated by adding oxalic acid and CaCl₂. The clinically intended use of this test is to estimate the risk of CaOx stone formation or to be used as a screening test to identify people at of CaOx urolithiasis. We performed the method validation and reported analytical method validation parameters of urinary rCOCI test including specificity (selectivity), linearity, limit of detection (LOD), limit of quantitative, repeatability, and reproducibility. For clinical validation, we determined rCOCI levels in 24-h urine samples obtained from CaOx stone patients and non-stone forming subjects. ROC analysis was performed and diagnostic values specificity, sensitivity, positive predictive value (PPV), negative predictive value (NPV), positive likelihood ratio (LH⁺), negative likelihood ratio (LH⁻), and accuracy were calculated to evaluate whether the rCOCI test had a good performance for diagnosing CaOx urolithiasis.

To date, diagnosis of urinary stones relies on imaging techniques such as kidney-ureter-bladder (KUB) x-ray, ultrasonography, and computed tomography (CT). These diagnostic imaging tools are not available in all hospitals, and they have relatively high cost. The simple, inexpensive, reliable, and accurate urinary test for estimating the risk of CaOx stone development has been lacking and not routinely using in the hospitals. There are some urinary methods that have been developed to detect urinary supersaturation and CaOx crystallization and proposed to be used for diagnosing CaOx urolithiasis. For CaOx stone, the most widely used stone risk index are the appropriate risk factor of CaOx index (reported in 1997), Bonn risk index (Ca²⁺/Ox²⁻ ratio) (reported in 2000)[87][13]. In 2020, the urinary iCOCI test was

developed for quantifying CaOx crystallization in the supersaturated urine samples using an indole-oxalate chemical reaction, and it had high sensitivity (95%) and accuracy (88%)[17]. However, performing iCOCl test is relatively time-consuming for the whole procedure (approximately 2-3 h.) and involves using hazardous chemicals, including indole reagent and sulfuric acid. We proposed that the rCOCl test would work better than iCOCl test, in terms of ease of use, less time consuming, and relatively low cost.

The rCOCl procedure was developed based on the COCl protocol¹⁶. Urine sample was induced to be at the supersaturated stage by adding oxalic acid and CaCl₂ leading to formation and precipitation of CaOx crystals. The CaOx crystals produced by this COCl procedure were further quantified by Raman spectroscopy. Basically, there are three forms of CaOx depending on incorporation of water molecule including calcium oxalate monohydrate (COM), calcium oxalate dihydrate (COD), and calcium oxalate trihydrate (COT). COM (54%) and COD (13%) are the most commonly observed forms in urine[88], and they are usually found in kidney stones[89]. The obvious differences in the Raman spectrum of different forms of CaOx were in the region ranging from 1300 to 1800 cm⁻¹ [90]. Phosphate is a normal electrolyte in the human body, and it frequently presents in urine. In our COCl procedure, calcium phosphate is usually co-precipitated with CaOx depending on concentration of phosphate in urine sample, and it interferes quantitation of CaOx by Raman spectroscopy. Therefore, to reduce this interference the obtained CaOx precipitate must be treated with acetic acid to dissolve and remove calcium phosphate before performing Raman spectroscopy analysis[14]. In real urine samples, the precipitates were confirmed that they contained CaOx crystals by FTIR and XRD.

We studied the characteristics Raman spectrum of standard COM in solid form and found the main Raman peaks at 505, 895, 1462, and 1488 cm⁻¹. The Raman shifts of seed COM produced in our lab were found at 1465 and 1490 cm⁻¹.

According to the literature, Raman shifts of COM at 1462 and 1489 cm^{-1} are attributed to the C-O symmetric stretching. Additionally, Raman peaks at 502, 896, and 1629 cm^{-1} could be assigned to the O-C-O in-plane bending, C-C stretching, and C-O asymmetric stretching, respectively[67]. Raman peaks of COD were observed at 508 (O-C-O), 912 (C-C), and 1632 cm^{-1} (C-O). The previous study demonstrated that the characteristics at 1462, 1490 and 1477 cm^{-1} were suitable for quantitative analysis[69]. In the monohydrate form, the double band was present at 1464 and 1490 cm^{-1} , while the dihydrate form appeared as a single band at 1477 cm^{-1} (an average of symmetric COO- stretching in COM) [67, 70, 90].

We investigated whether light and coverslip interfered with the Raman spectrum measurement. We found that both light and coverslip interfered with the signal detected by Raman spectroscopy compared with conditions in the dark and without coverslip. To increase the CaOx Raman signal, we increased the thickness of CaOx samples by confining the sample to a disc shape diameter of 0.3 cm.

As mentioned above, we found that calcium phosphate interfered with the Raman signal measurement of CaOx. After treating the CaOx precipitate with acetic acid, we confirmed by FTIR that calcium phosphate was clearly removed, as described in the previous study[14]. The Raman spectrum for phosphate-containing kidney stones showed peaks at 940 cm^{-1} for struvite and 960 cm^{-1} for carbonate apatite[66, 68, 91]. In FTIR analysis, the presence of calcium phosphate is typically identified by a peak at 1000 cm^{-1} [91][60]. Previous study indicated that small calcium phosphate is often found in calcium oxalate stone[92]. The concentration of phosphate in urine is found to be nearly equivalent in stone patients and healthy individuals[93].

The rCOI measurement in many of 24-h urine samples exhibited COD characteristic peak at 1478 cm^{-1} in the Raman spectra. The presence of COD in the CaOx precipitates was confirmed by FTIR (wavenumber at 1321 and 1615 cm^{-1} with low signal of 776 cm^{-1}) and light microscope (envelope-shaped or octahedral shape).

We concluded that rCOCl test could identify and gave more information of forms of CaOx crystals (either COM or COD) produced after adding oxalic acid and CaCl₂, but the iCOCl test could not. In iCOCl method, all forms of CaOx in the precipitate were measured using the indole-oxalate chemical reaction.

The mechanism of COD formation and transformation to COM (a more stable form) has been delineated[89, 94, 95]. Citrate is a potent inhibitor of CaOx nucleation, aggregation, and stone formation, and it promotes the formation of COD [69, 89, 94]. Stanković et al. performed an experiment of CaOx formation in vitro and demonstrated that approximately 75% COD were mixed with COM[89]. Ster, A. et al. demonstrated the COD formation by varying the concentrations of citrate (0.001-0.012 mol dm⁻³), and they found an average size of the crystals between 20 and 30 μm at 37 °C. They concluded that an increased concentration of citrate does not lead to an increase in crystal size. The normal range of urine citrate is >320 mg/day (1.67 mmol/L)[96]. We tested CaOx precipitation in our COCl procedure in water (by adding oxalic acid and excessive calcium chloride) without addition of citrate, and we found only COM in the CaOx precipitate. However, when we added citrate (varied citrate concentration), the formation of COD was gradually increased regarding the citrate concentration. Other studies also reported that no COD precipitation was seen in the examined systems without addition of citrate, and the absence of citrate produced only COM and COT forms[89, 97]. In addition to the presence of citrate ions, other factors such as a high calcium/oxalate ratio, an excess of calcium ions, high ionic strength, and elevated temperature were also found to promote the precipitation of COD[94, 95, 98].

To understand COD formation, previous studies demonstrated that precipitated COD and COT in the presence of sodium citrate (0.12% citrate ion) or sodium malate had a strong affinity to water on their crystal surface[99]. Citric acid has the ability to regulate the water content of amorphous nucleated precipitates[100]. The citrate absorption is influenced by the presence of citrate ions

atop a water layer that is either adsorbed or penetrating the surface, in which the citrate ions are bound to calcium ion (Ca^{2+}) and hydrogen ion (H^+)[101]. The thermodynamic metastable of COD and COT can easily be eliminated through urinary excretion. Basically, COD is a precursor of COM[98]. Regulated parameters of COM and COD formation include pH, aging time, temperature, and volume of water[102].

For CaOx quantitation based on Raman spectrum, peak intensity was the best parameter (compared with AUP and FWHM) to be used for a quantitative calculation. Oxalic acid concentration used for precipitating CaOx (ranging from 50-200 mM) was linearly correlated with peak intensity with R^2 of 0.98. However, the best linearity was obtained at the range of oxalic acid concentrations of 50-100 mM (R^2 of 0.999). For inducing supersaturation and CaOx crystallization in urine samples, we used a spike oxalic acid concentration of 100 mM (to get the final concentration of 2.5 mM). Water spiked with oxalic acid (100 mM) was used as control (reference that showed the total amount of CaOx crystals produced in water containing 2.5 mM oxalic acid under the condition of excessive calcium ions).

The rCOCI value was the ratio of amount of CaOx produced urine sample-to-amount of CaOx produced in water control (peak intensity of CaOx in urine divided by peak intensity of CaOx in control). In this study, in addition to peak intensity, we also calculated the amount of CaOx from FWHM and AUP. As mentioned above, peak intensity was the best quantitative parameter to reflect the amount of CaOx. In 1997, Kontoyannis. et al. quantified the amount of CaOx from synthesized COM and COD by using peak intensity from Raman spectrum[69]. In 2012, Chiu, Yichun, et al. reported that the quantitative multicomponent from 18 urine samples calculated by ratio of intensity[103]. In 2020, Zhu W. et al. quantified creatinine by peak area[65]. In 2020, Zhang, Jing, et al. studied the role of hyperoxaluria/hypercalciuria based on the concentrations calculated from FWHM[98].

In the second part, we conducted a method validation of urinary rCOCI test. The validation parameters for quantitative method were calculated and reported including specificity, linearity, accuracy, repeatability, reproducibility, stability, limit of detection (LOD), and limit of quantitation (LOQ)[18]. Several studies employed Raman spectroscopy for detection and quantitation of urinary organic components, for instances, urea, uric acid, creatinine, and albumin and their method validation parameters were reported[104]. The key urine components including phosphate, urea, uric acid, and creatinine were tested if they interfered with the CaOx quantitation in urinary rCOCI test. These components were spiked in the sample together with oxalic acid, the crystals were collected and analyzed by Raman spectroscopy. We found that only the high concentrations of uric acid showed a high interfering effect. Therefore, our urinary rCOCI test has a limitation for measuring urine sample with very high concentration of uric acid (more than 2 mM).

We tested linearity in control (water) and pooled urine (both pooled non-stone and pooled stone urine). The best linearity of rCOCI standard curve was found in the range oxalic acid concentration of 50-150 mM with R^2 was 0.98 in water, 0.95 in pooled NS urine and 0.82 in pooled ST urine. The calculated LOD and LOQ of the urinary rCOCI method was 31 mM and 95 mM in control (water), 24 mM and 35 mM in pooled NS urine, and 73 mM and 105 mM in pooled ST urine, respectively. It could indicate that the LOQ range of the rCOCI test was between 90 and 100 mM of spiked oxalic acid.

To validate the feasibility of using the developed method, precision of rCOCI measurement, indicated by repeatability and reportability, were evaluated. In general, validation of a new method, precision is accepted at RSD of <15% (%RSD. = $(SD/mean) \times 100$) [18, 20, 105]. For rCOCI measurement, the repeatability (RSD within day) in control was less than 10%. In pooled urine sample, RSD of rCOCI method was also less than 15%. However, RSD measured in individual urine samples was 16.5% and in pooled ST urine was RSD 20.53%. For reproducibility (RSD between day), it

showed RSD less than 5% in control, less than 10% in pooled non-stone urine and less than 20% in pooled stone urine. For stability of rCOCI, we showed that COCI crystals stored at either 4 °C or RT were relatively stable. Comparison of CaOx quantitation between Raman spectroscopy and FTIR showed that both quantitation techniques were well correlated ($R = 0.89$).

In clinical validation, we aimed to develop rCOCI test for screening CaOx urolithiasis. The level of urinary rCOCI in the stone group was significantly higher than in the non-stone group. Among the three quantitative parameters, urinary rCOCI level by intensity provided the best diagnostic power with ROC AUC of 0.8069 (95%CI: 0.7511-0.8627). Based on multiple logistic regression using all three quantitative parameters (calculated from intensity, AUC and FWHM), it provided a better diagnostic performance (AUC of 0.84) than a use of one quantitative parameter. For separating stone patients and non-stone subjects, AUC of 0.84 (95% CI =0.7919-0.8942) was obtained for the urinary rCOCI test. Basically, ROC AUC between 0.7-0.9 was accepted as moderate accuracy whereas AUC between 0.9-1.0 is highly accurate [106]. In CaOx stone cases, ROC AUC of rCOCI values calculated from intensity, FWHM, and AUP were 0.8244 (95%CI: 0.7438-0.9051), 0.8011 (95%CI: 0.7198-0.8824), and 0.6821 (95%CI: 0.5833-0.7808), respectively. This indicated that rCOCI values calculated from peak intensity provided a good performance for distinguishing CaOx stone patients from non-stone subjects. In contrast, rCOCI values calculated from AUP had a relatively low diagnostic performance (AUC less than 0.7). We selected cutoff rCOCI test based on ROC analysis result, and we aimed to have the sensitivity at least 80% (as for screening purpose). The cutoff values of urinary rCOCI test calculated from intensity and FWHM were 1.40 and 1.50, respectively.

In diagnosis of CaOx urolithiasis, the diagnostic values of urinary rCOCI test, i.e., sensitivity, specificity, PPV, NPV, positive likelihood ratio (LH^+), negative likelihood ratio (LH^-) and accuracy were 80.00%, 57.00%, 45.45%, 86.15%, 1.86, 0.36, and 64.00%, respectively. Furthermore, we performed a multiple logistic regression using

all three calculated rCOCI values (from intensity, AUC and FWHM) to see if it could increase accuracy of rCOCI test. The results showed that the sensitivity, specificity, and accuracy were increased to 80%, 78%, and 79%, respectively.

The limitations of the present study should be mentioned. Urine samples used for rCOCI testing were only from Mahasarakham Province, not from all provinces of Thailand. The urine samples were kept -20°C since 2016, some urinary compounds might be degraded. In the Raman spectroscopy analysis, the crystals produced in some urine samples had high background noise that might interfere with the CaOx quantitation. However, samples with very high background noise (could not be removed by acetic acid treatment) were excluded, and it might be a selection bias. High concentration of uric acid interfered with the CaOx Raman signal, and this interference was hard to eliminate. Accuracy of rCOCI measurement in urine samples with high uric acid was compromised. Urine samples from the stone group usually had higher background noise than those from NS group. It might be explained by the fact that stone urine had more agglomerated compounds with higher autofluorescence than the NS urine. We have planned determined rCOCI values in the freshly collected urine samples to compare with the stored frozen urine samples, and to investigate the normal range of urinary rCOCI in healthy individuals.

In conclusion, we have successfully developed a urinary rCOCI test for determining CaOx crystals formed in the supersaturated urine samples using Raman spectroscopy. The hazardous chemicals were not required for the urinary rCOCI test, and measurement time was about 1.30-1.45 hours for 262 urine samples. The unit cost of urinary rCOCI test was reduced because many chemicals were not required. Moreover, the urinary rCOCI test could identify types of CaOx including COM and COD, while the urinary iCOCI test could not. The sensitivity, specificity, and accuracy of urinary rCOCI test for diagnosing CaOx urolithiasis were 80%, 57%, and 64%, respectively. The present data suggested our newly developed rCOCI test could be used as a screening test for estimating the risk of CaOx stone formation.

APPENDIX

Appendix 1

Observation interference from calcium phosphate (CaP)

In this study, we tested interference by observing the CaOx signal from the original urine, adding only calcium chloride compared with spiked oxalic acid and calcium chloride by FTIR. The result showed that Raman characteristics of urine sample without spiked oxalic acid (upper) showed CaP wavenumber at 1000 cm^{-1} , whereas urine spiked oxalic acid (lower) additionally exhibited Raman peaks of CaOx at 1312 cm^{-1} and 1604 cm^{-1} . We also confirmed the presence of CaOx in urine sample spiked oxalic acid and calcium chloride by XRD.

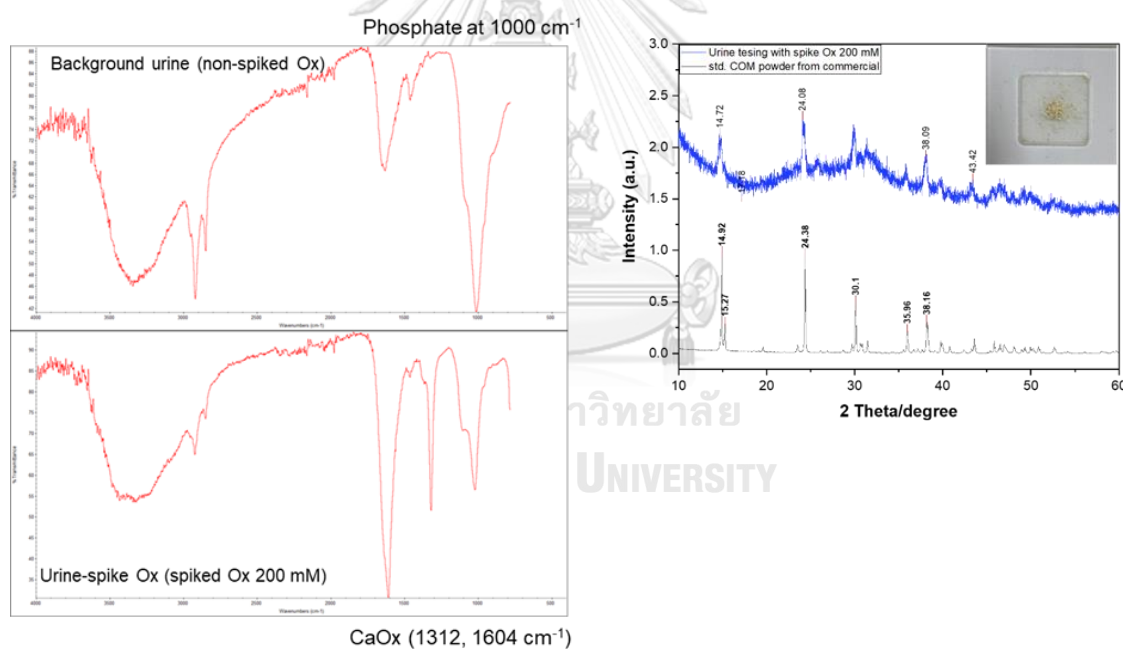


Figure 67 The characteristics of CaOx were confirmed by FTIR and XRD in the urine sample spiked with oxalic acid and CaCl_2 .

Observation of Raman characteristics of COM and COD

We studied the Raman characteristic of COD by varying the concentrations of sodium citrate and CaCl_2 . The results showed that the COCI crystals generated by varying the concentration of CaCl_2 had only the Raman characteristic of COM. In contrast, COCI crystals generated by varying the concentration of sodium citrate showed both COM and COD. The COD characteristic was exclusively observed in high concentration of sodium citrate (5.6 and 11.25 mM), while low sodium citrate concentration showed both COM and COD. Therefore, the formation of COD depended on citrate concentration.

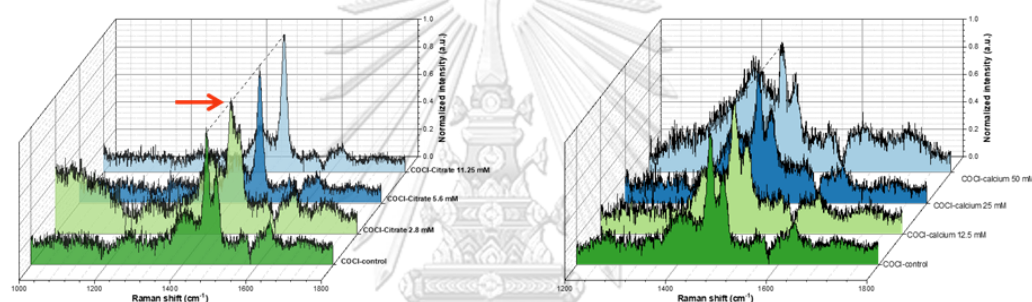


Figure 68 The Raman characteristic of COCI crystals that were produced by varying sodium citrate and calcium chloride concentrations.

The urinary rCOCI values of COM and COD

We calculated the urinary rCOCI values (based on intensity, FWHM, and AUP) of COM (62.22%) and COD (37.78%) separately. For COM, the result showed that urinary rCOCI level of the ST group (n=78) was significantly higher than in the NS group (n=62) ($p < 0.0001$) (Figure 69). For COD, the urinary rCOCI level of ST group (n=49) was also significantly higher than NS group (n=36) (Figure 70).

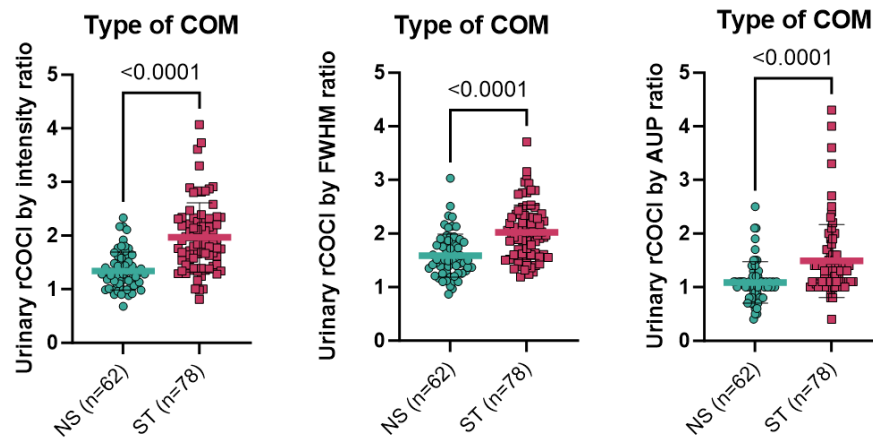


Figure 69 The level of urinary rCOCI calculated for COM compared between stone and non-stone groups.

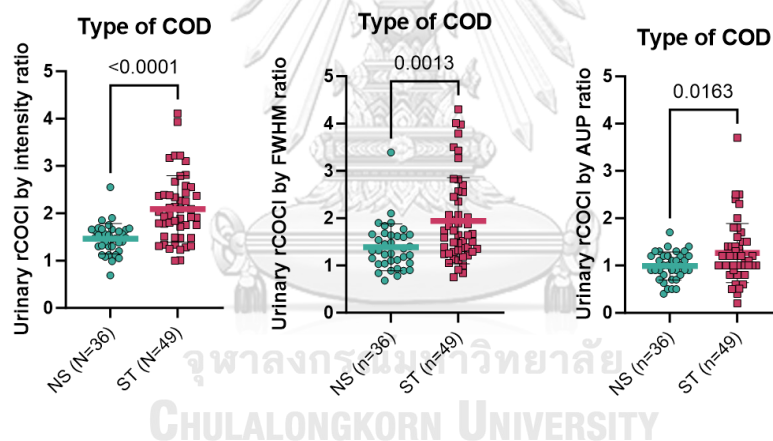


Figure 70 The level of urinary rCOCI calculated for COD compared between stone and non-stone groups.

ROC analysis of urinary rCOCI for COM and COD

ROC analysis of urinary rCOCI value for COM and COD were performed separately. For COM, the results showed areas under the ROC curve (AUC) of urinary rCOCI calculated from peak intensity, FWHM, and AUP were 0.8177 (95%CI: 0.7484-0.8870), 0.7582 (95%CI: 0.6787-0.8376), 0.7360 (95%CI: 0.6526-0.8195), respectively.

For COD, the results showed AUC of urinary rCOCI calculated from peak intensity, FWHM, and AUP were 0.8177 (95%CI: 0.7484-0.8870), 0.7582 (95%CI: 0.6787-0.8376), 0.7360 (95%CI: 0.6526-0.8195), respectively.

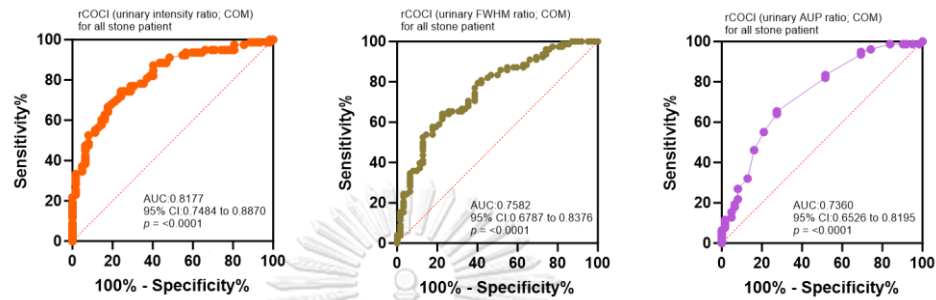


Figure 71 ROC analysis of urinary rCOCI value of COM for distinguishing NS subjects (n=62) from ST patients (n=78).

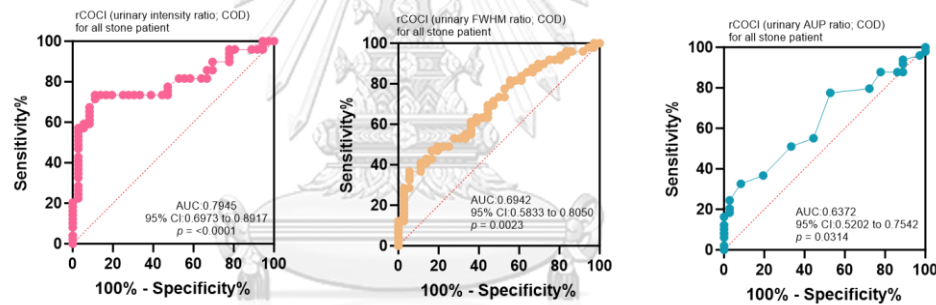


Figure 72 ROC analysis of urinary rCOCI of COD for distinguishing NS subjects (n=36) from ST patients (n=49).

Appendix 2

Reagents used in this study.

1. Reagent for rCOCI test

- 1.1. 100 mM of oxalic acid
 - Oxalic acid (MW=126.07) 12.6 g
 - Dissolve in water 1000 mL
- 1.2. 100 mM of calcium chloride (CaCl₂)
 - Calcium chloride (CaCl₂) 7.3505 g
 - dissolved in water 500 mL
- 1.3. 2N Acetic acid
 - Acetic Acid bottle 57.417 mL
 - dissolved in distilled water until the volume reaches 1000 mL

2. Reagent for iCOCI test

- 2.1. 100 mM of Oxalic acid concentration
 - Oxalic acid (MW=126.07) 12.6 g
 - Dissolve in water 1000 mL
- 2.2. 100 mM of Calcium chloride (CaCl₂) concentration
 - Calcium chloride (CaCl₂) 7.3505 g
 - dissolved in water 500 mL
- 2.3. 2N of Hydrochloric acid (HCl)
 - HCl (37% w/w) in volume 82.117 mL
 - Adjust volume with distilled water to 500 mL
- 2.4. Indole reagent concentration 1 mg/ml (TCI)
 - indole 10 mg dissolved in H₂SO₄ (97% w/w) in volume 10 mL
- 2.5. Standard calcium oxalate monohydrate (0.093, 0.187, 0.375, 0.75, 1.5 mg/mL)
 - COM 150 mg dissolved in 2N HCL 100 ml (stock solution 1.5 mg/ml)

3. Reagent for calcium Arsenazo III assay

3.1 0.075 M Imidazole

- imidazole 450 mg (MW= 68.08 g/mol)
- Dissolve in water 100 mL

3.2 0.1 M Arsenazo III

- Arsenazo III 510.6 mg
- Dissolve in imidazole (0.075 M) 100 mL
- Adjust pH 6.5

3.3 Standard calcium chloride concentration 0, 0.25, 0.5, 1, 2 mM

- CaCl_2 (MW=147.01) 7.3505 g (stock solution 100 mM)
- Dissolve in water 500 mL

4. Reagent for creatinine assay

4.1 0.04 N Picric acid

4.2 1.4 N NaOH

- NaOH in volume 7.39 mL (50% w/w)
- Adjust the final volume solution to 100 mL

4.3 Standard Creatinine Stock 200 mg% (0, 0.5, 1, 2, 4, 8 mg%)

5. Reagent for BSA assay

5.1 BCA reagent (A and B) from Thermo Fisher Scientific

- Mixed 196 μL of reagent A with 4 μL of reagent B (Final volume 200 μL)

5.2 Bovine serum albumin (BSA) from Thermo Fisher Scientific (standard BSA)

- Prepare standard concentration 0, 0.25, 0.5, 1 mg/mL

REFERENCES

1. Corrales, M., et al., *Classification of Stones According to Michel Daudon: A Narrative Review*. Eur Urol Focus, 2021. **7**(1): p. 13-21.
2. Liu, Y., et al., *Epidemiology of urolithiasis in Asia*. Asian J Urol, 2018. **5**(4): p. 205-214.
3. Kamphuis, G.M., et al., *Method of alkalization and monitoring of urinary pH for prevention of recurrent uric acid urolithiasis: a systematic review*. Translational andrology and urology, 2019. **8**(Suppl 4): p. S448.
4. Boarin, M., et al., *Dietary and lifestyle recommendations for urolithiasis prevention: A systematic literature review*. International Journal of Urological Nursing, 2018. **12**(2-3): p. 53-70.
5. Uribarri, J., *Chronic kidney disease and kidney stones*. Curr Opin Nephrol Hypertens, 2020. **29**(2): p. 237-242.
6. Sigurjonsdottir, V.K., et al., *Impact of nephrolithiasis on kidney function*. BMC Nephrol, 2015. **16**: p. 149.
7. Alelign, T. and B. Petros, *Kidney Stone Disease: An Update on Current Concepts*. Adv Urol, 2018. **2018**: p. 3068365.
8. Grases, F., A. Costa-Bauza, and R.M. Prieto, *Renal lithiasis and nutrition*. Nutr J, 2006. **5**: p. 23.
9. Jabbar, F., et al., *Assessment of the role of general, biochemical and family history characteristics in kidney stone formation*. Saudi J Biol Sci, 2015. **22**(1): p. 65-8.
10. Zeng, G., et al., *Prevalence of kidney stones in China: an ultrasonography based cross-sectional study*. BJU Int, 2017. **120**(1): p. 109-116.
11. Knoll, T. and O. Traxer, *Urolithiasis: Medical and surgical treatment*. Eur Urol Focus, 2021. **7**(1): p. 1-2.
12. Rule, A.D., J.C. Lieske, and V.M. Pais, Jr., *Management of Kidney Stones in 2020*. JAMA, 2020. **323**(19): p. 1961-1962.

13. Laube, N., A. Schneider, and A. Hesse, *A new approach to calculate the risk of calcium oxalate crystallization from unprepared native urine*. Urological research, 2000. **28**(4): p. 274-280.
14. Sriboonlue, P., S. Suwantrai, and V. Prasongwatana, *An indirect method for urinary oxalate estimation*. Clinica chimica acta, 1998. **273**(1): p. 59-68.
15. Laube, N. and S. Hergarten, *Can the Bonn Risk Index be replaced by a simple measurement of the urinary concentration of free calcium ions?* J Urol, 2005. **173**(6): p. 2175-7.
16. Yang, B., et al., *Calcium oxalate crystallization index (COCI): an alternative method for distinguishing nephrolithiasis patients from healthy individuals*. Annals of Clinical & Laboratory Science, 2014. **44**(3): p. 262-271.
17. More-Krong, P., et al., *Clinical validation of urinary indole-reacted calcium oxalate crystallization index (iCOCI) test for diagnosing calcium oxalate urolithiasis*. Sci Rep, 2020. **10**(1): p. 8334.
18. Peters, F.T., O.H. Drummer, and F. Musshoff, *Validation of new methods*. Forensic Sci Int, 2007. **165**(2-3): p. 216-24.
19. Kumar, A., et al., *Method development and validation: Skills and tricks*. Chronicles of Young Scientists, 2012. **3**(1).
20. Taleuzzaman, M., *Bio-Analytical Method Validation-A Review*. 2016.
21. Trinchieri, A., *Epidemiology of urolithiasis: an update*. Clinical cases in mineral and bone metabolism, 2008. **5**(2): p. 101.
22. Lopez, M. and B. Hoppe, *History, epidemiology and regional diversities of urolithiasis*. Pediatr Nephrol, 2010. **25**(1): p. 49-59.
23. Shah, J. and H. Whitfield, *Urolithiasis through the ages*. BJU international, 2002. **89**(8): p. 801-810.
24. Khan, S.R., et al., *Kidney stones*. Nat Rev Dis Primers, 2016. **2**: p. 16008.
25. Haley, W.E., et al., *Kidney Function After the First Kidney Stone Event*. Mayo Clin Proc, 2016. **91**(12): p. 1744-1752.
26. Sorokin, I., et al., *Epidemiology of stone disease across the world*. World J Urol, 2017. **35**(9): p. 1301-1320.

27. Cassell, A., 3rd, et al., *Surgical Management of Urolithiasis of the Upper Tract - Current Trend of Endourology in Africa*. Res Rep Urol, 2020. **12**: p. 225-238.
28. Faridi, M.S. and K.S. Singh, *Preliminary study of prevalence of urolithiasis in North-Eastern city of India*. J Family Med Prim Care, 2020. **9**(12): p. 5939-5943.
29. Yanagawa, M., et al., *Incidence of urolithiasis in northeast Thailand*. International journal of urology, 1997. **4**(6): p. 537-540.
30. Raheem, O.A., et al., *Burden of Urolithiasis: Trends in Prevalence, Treatments, and Costs*. Eur Urol Focus, 2017. **3**(1): p. 18-26.
31. Shin, S, et al., *Confounding risk factors and preventative measures driving nephrolithiasis global makeup*. World J Nephrol, 2018. **7**(7): p. 129-142.
32. Sayer, J.A., S.H. Moochhala, and D.J. Thomas, *The medical management of urolithiasis*. British Journal of Medical and Surgical Urology, 2010. **3**(3): p. 87-95.
33. Jayaraman, U.C. and A. Gurusamy, *Review on Uro-Lithiasis Pathophysiology and Aesculapian*, 2018.
34. Pfau, A. and F. Knauf, *Update on Nephrolithiasis: Core Curriculum 2016*. Am J Kidney Dis, 2016. **68**(6): p. 973-985.
35. Butterweck, V. and S.R. Khan, *Herbal medicines in the management of urolithiasis: alternative or complementary?* Planta Med, 2009. **75**(10): p. 1095-103.
36. Tosukhowong, P., et al., *Crystalline composition and etiologic factors of kidney stone in Thailand: update 2007*. Asian Biomedicine 2007;1:87-95.
37. Chaiyarit, S., S. Mungdee, and V. Thongboonkerd, *Non-radioactive labelling of calcium oxalate crystals for investigations of crystal-cell interactions and internalization*. Analytical Methods, 2010. **2**(10): p. 1536-1541.
38. Boonla, C., T. Thummaborworn, and P. Tosukhowong, *Urolithiasis in Udon Thani Hospital: A rising prevalence of uric acid stone*. 2006.
39. Beara-Lasic, L. and D.S. Goldfarb, *Nephrolithiasis in women: how different from men?* Curr Opin Nephrol Hypertens, 2020. **29**(2): p. 201-206.
40. Mayans, L., *Nephrolithiasis*. Prim Care, 2019. **46**(2): p. 203-212.

41. Daudon, M., et al., *Recurrence rates of urinary calculi according to stone composition and morphology*. *Urolithiasis*, 2018. **46**(5): p. 459-470.
42. Sritippayawan, S., et al., *Evidence suggesting a genetic contribution to kidney stone in northeastern Thai population*. *Urol Res*, 2009. **37**(3): p. 141-6.
43. Moe, O.W., *Kidney stones: pathophysiology and medical management*. *The Lancet*, 2006. **367**(9507): p. 333-344.
44. Wang, Z., et al., *Recent advances on the mechanisms of kidney stone formation (Review)*. *Int J Mol Med*, 2021. **48**(2).
45. Boonla, C., *Oxidative Stress in Urolithiasis*. *Reactive Oxygen Species (ROS) in Living Cells*: IntechOpen, 2018: p. 129-159.
46. McCarthy, C.J., et al., *Radiology of renal stone disease*. *Int J Surg*, 2016. **36**(Pt D): p. 638-646.
47. Masselli, G., M. Weston, and J. Spencer, *The role of imaging in the diagnosis and management of renal stone disease in pregnancy*. *Clin Radiol*, 2015. **70**(12): p. 1462-71.
48. Brisbane, W., M.R. Bailey, and M.D. Sorensen, *An overview of kidney stone imaging techniques*. *Nat Rev Urol*, 2016. **13**(11): p. 654-662.
49. Kavanagh, J.P. and N. Laube, *Why Does the Bonn Risk Index Discriminate Between Calcium Oxalate Stone Formers and Healthy Controls?* *Journal of Urology*, 2006. **175**(2): p. 766-770.
50. Porowski, T., et al., *Normative data on the Bonn Risk Index for calcium oxalate crystallization in healthy children*. *Pediatric Nephrology*, 2007. **22**(4): p. 514-520.
51. Cohen, J.F., et al., *STARD 2015 guidelines for reporting diagnostic accuracy studies: explanation and elaboration*. *BMJ Open*, 2016. **6**(11): p. e012799.
52. Bossuyt, P.M.M., et al., *STARD 2015: An Updated List of Essential Items for Reporting Diagnostic Accuracy Studies*. *Clinical chemistry*, 2015. **61** **12**: p. 1446-52.
53. Bergerman, J. and J.S. Elliot, *Method for direct colorimetric determination of oxalic acid*. *Analytical Chemistry*, 1955. **27**(6): p. 1014-1015.

54. Kong, K., et al., *Raman spectroscopy for medical diagnostics--From in-vitro biofluid assays to in-vivo cancer detection*. *Adv Drug Deliv Rev*, 2015. **89**: p. 121-34.
55. Tu, Q. and C. Chang, *Diagnostic applications of Raman spectroscopy*. *Nanomedicine*, 2012. **8**(5): p. 545-58.
56. Xu, Z., et al., *Topic Review: Application of Raman Spectroscopy Characterization in Micro/Nano-Machining*. *Micromachines (Basel)*, 2018. **9**(7).
57. Hong, J.K., et al., *Microbial phenomics linking the phenotype to function: The potential of Raman spectroscopy*. *J Microbiol*, 2021. **59**(3): p. 249-258.
58. Kanter, E.M., et al., *Application of Raman spectroscopy for cervical dysplasia diagnosis*. *J Biophotonics*, 2009. **2**(1-2): p. 81-90.
59. Nijssen, A., et al., *Towards oncological application of Raman spectroscopy*. *J Biophotonics*, 2009. **2**(1-2): p. 29-36.
60. Guerra-Lopez, J.R., J.A. Guida, and C.O. Della Vedova, *Infrared and Raman studies on renal stones: the use of second derivative infrared spectra*. *Urol Res*, 2010. **38**(5): p. 383-90.
61. Eberhardt, K., et al., *Advantages and limitations of Raman spectroscopy for molecular diagnostics: an update*. *Expert Rev Mol Diagn*, 2015. **15**(6): p. 773-87.
62. Cui, S., S. Zhang, and S. Yue, *Raman Spectroscopy and Imaging for Cancer Diagnosis*. *J Healthc Eng*, 2018. **2018**: p. 8619342.
63. Castiglione, V., et al., *Raman chemical imaging, a new tool in kidney stone structure analysis: Case-study and comparison to Fourier Transform Infrared spectroscopy*. *PLoS One*, 2018. **13**(8): p. e0201460.
64. Tonannavar, J., et al., *Identification of mineral compositions in some renal calculi by FT Raman and IR spectral analysis*. *Spectrochim Acta A Mol Biomol Spectrosc*, 2016. **154**: p. 20-26.
65. Zhu, W., et al., *Rapid and low-cost quantitative detection of creatinine in human urine with a portable Raman spectrometer*. *Biosens Bioelectron*, 2020. **154**: p. 112067.

66. Lo, P.-A., et al., *Automatic Raman spectroscopic urine crystal identification system using fluorescent image-guided 2D scanning platform with Fe₃O₄ crystal violet nanoclusters*. *Journal of Raman Spectroscopy*, 2019. **50**(1): p. 34-40.
67. Kontoyannis, C.G., N.C. Bouropoulos, and P.G. Koutsoukos, *Raman spectroscopy: A tool for the quantitative analysis of mineral components of solid mixtures. The case of calcium oxalate monohydrate and hydroxyapatite*. *Vibrational Spectroscopy*, 1997. **15**(1): p. 53-60.
68. Daudon, M., et al., *Infrared spectrometry and Raman microprobe in the analysis of urinary calculi*. *Kidney Int*, 1983. **23**(6): p. 842-50.
69. Kontoyannis, C.G., N.C. Bouropoulos, and P.G. Koutsoukos, *Use of Raman spectroscopy for the quantitative analysis of calcium oxalate hydrates: application for the analysis of urinary stones*. *Applied spectroscopy*, 1997. **51**(1): p. 64-67.
70. Chiu, Y.-C., et al., *Micro-Raman spectroscopy identification of urinary stone composition from ureteroscopic lithotripsy urine powder*. *Journal of Raman Spectroscopy*, 2009.
71. Kodati, V.R., et al., *Raman spectroscopic identification of calcium-oxalate-type kidney stone*. *Applied spectroscopy*, 1990. **44**(8): p. 1408-1411.
72. Subscription, C., *A Review Article on Analytical Method Validation*. 2020. **1**: p. 48-58.
73. Mudavath, S., *Analytical Method Validation Report for Essay of Glycopyrrocate and Formoterol Fumerate by RP-HPLC*. 2018: p. 1-08.
74. Kotte, S., P.K. Dubey, and M. Panchapagesa, *CORE COMPONENTS OF ANALYTICAL METHOD VALIDATION FOR SMALL MOLECULES-AN OVERVIEW*. *International Research Journal of Pharmacy*, 2012. **3**: p. 1-11.
75. Sule, S., et al., *A PRACTICAL APPROACH TO RP HPLC ANALYTICAL METHOD DEVELOPMENT*. 2014. **3**.
76. Bretnall, A.E. and G.S. Clarke, *Validation of Analytical Test Methods*, in *Handbook of Modern Pharmaceutical Analysis*. 2011. p. 429-457.

77. Sankar, R. and P. Babu, *Analytical Method Validation Parameters An Updated Review*. 2020.
78. Saxena, N., et al., *Validation of Optimized Method for Quantitative Estimation of Extracellular Ethanol from Micro-algae*. *Acta Scientific Microbiology*, 2021. **4**: p. 28-37.
79. Tien, N., et al., *Diagnosis of Bacterial Pathogens in the Urine of Urinary-Tract-Infection Patients Using Surface-Enhanced Raman Spectroscopy*. *Molecules*, 2018. **23**(12).
80. Inoue, M., et al., *Transmission Low-Frequency Raman Spectroscopy for Quantification of Crystalline Polymorphs in Pharmaceutical Tablets*. *Anal Chem*, 2019. **91**(3): p. 1997-2003.
81. Lu, Y., L. Lin, and J. Ye, *Human metabolite detection by surface-enhanced Raman spectroscopy*. *Mater Today Bio*, 2022. **13**: p. 100205.
82. Cheng, J., et al., *Highly Sensitive Detection of Clenbuterol in Animal Urine Using Immunomagnetic Bead Treatment and Surface-Enhanced Raman Spectroscopy*. *Sci Rep*, 2016. **6**: p. 32637.
83. Liu, J., et al., *Rapid Quantitative Detection of Voriconazole in Human Plasma Using Surface-Enhanced Raman Scattering*. *ACS Omega*, 2022. **7**(51): p. 47634-47641.
84. Faes, L., et al., *A Clinician's Guide to Artificial Intelligence: How to Critically Appraise Machine Learning Studies*. *Transl Vis Sci Technol*, 2020. **9**(2): p. 7.
85. Davis, J.W., *Biomarker classification, validation, and what to look for in 2017 and beyond*. *BJU Int*, 2017. **119**(5): p. 812-814.
86. Chutipongtanate, S. and V. Thongboonkerd, *Ceftriaxone crystallization and its potential role in kidney stone formation*. *Biochem Biophys Res Commun*, 2011. **406**(3): p. 396-402.
87. Tiselius, H.-G., *Risk formulas in calcium oxalate urolithiasis*. *World Journal of Urology*, 1997. **15**(3): p. 176-185.
88. Singh, V.K. and P.K. Rai, *Kidney stone analysis techniques and the role of major and trace elements on their pathogenesis: a review*. *Biophys Rev*, 2014. **6**(3-4): p. 291-310.

89. Stanković, A., et al., *Preparation and characterization of calcium oxalate dihydrate seeds suitable for crystal growth kinetic analyses*. Journal of Crystal Growth, 2018. **500**: p. 91-97.
90. Edwards, H., et al., *Vibrational Raman spectroscopic studies of calcium oxalate monohydrate and dihydrate in lichen encrustations on Renaissance frescoes*. Journal of Raman Spectroscopy, 1992. **23**(3): p. 185-189.
91. Cui, X., et al., *Analysis and classification of kidney stones based on Raman spectroscopy*. Biomedical optics express, 2018. **9**(9): p. 4175-4183.
92. Daudon, M., P. Jungers, and D. Bazin, *Stone Morphology: Implication for Pathogenesis*. AIP Conference Proceedings, 2008. **1049**: p. 199-215.
93. Raina, A., et al., *24-hour urinary constituents in stone formers: a study from Kashmir*. International Journal of Advances in Medicine, 2017. **4**: p. 1477.
94. Werner, H., et al., *Calcium Oxalate Crystallization: Influence of pH, Energy Input, and Supersaturation Ratio on the Synthesis of Artificial Kidney Stones*. ACS Omega, 2021. **6**(40): p. 26566-26574.
95. Laffite, G., et al., *Calcium oxalate precipitation by diffusion using laminar microfluidics: toward a biomimetic model of pathological microcalcifications*. Lab Chip, 2016. **16**(7): p. 1157-60.
96. Zuckerman, J. and D. Assimos, *Hypocitraturia: Pathophysiology and Medical Management*. Reviews in urology, 2009. **11**: p. 134-44.
97. Ster, A., et al., *The effect of hydrodynamic and thermodynamic factors and the addition of citric acid on the precipitation of calcium oxalate dihydrate*. Urolithiasis, 2018. **46**(3): p. 243-256.
98. Zhang, J., et al., *Role of Hyperoxaluria/Hypercalciuria in Controlling the Hydrate Phase Selection of Pathological Calcium Oxalate Mineralization*. Crystal Growth & Design, 2020. **21**(1): p. 683-691.
99. Ishii, Y. and K. Takiyama, *FORMATION OF CALCIUM OXALATE PRECIPITATE IN AQUEOUS SOLUTION*. Analytical Sciences, 1991. **7**(Supple): p. 391-394.
100. Li, S., et al., *Understanding the Role of Citric Acid on the Crystallization Pathways of Calcium Oxalate Hydrates*. Crystal Growth & Design, 2019. **19**(6): p. 3139-3147.

101. Su, Y., et al., *A molecular understanding of citrate adsorption on calcium oxalate polyhydrates*. *Phys Chem Chem Phys*, 2023. **25**(17): p. 12148-12156.
102. Valido, I.H., et al., *Characterization of Calcium Oxalate Hydrates and the Transformation Process*. *Chemphyschem*, 2020. **21**(22): p. 2583-2593.
103. Chiu, Y., et al., *Quantitative and multicomponent analysis of prevalent urinary calculi using Raman spectroscopy*. *Journal of Raman Spectroscopy*, 2012. **43**(8): p. 992-997.
104. Premasiri, W.R., R.H. Clarke, and M.E. Womble, *Urine analysis by laser Raman spectroscopy*. *Lasers Surg Med*, 2001. **28**(4): p. 330-4.
105. Tiwari, G. and R. Tiwari, *Bioanalytical method validation: An updated review*. *Pharm Methods*, 2010. **1**(1): p. 25-38.
106. Greiner M, Pfeiffer D, Smith RD. Principles and practical application of the receiver-operating characteristic analysis for diagnostic tests. *Prev Vet Med*. 2000;45(1-2):23-41.

REFERENCES



จุฬาลงกรณ์มหาวิทยาลัย
CHULALONGKORN UNIVERSITY



จุฬาลงกรณ์มหาวิทยาลัย
CHULALONGKORN UNIVERSITY

VITA

NAME	Kamonchat Boonkam
DATE OF BIRTH	5 February 1995
PLACE OF BIRTH	Tak
INSTITUTIONS ATTENDED	Chulalongkorn University
HOME ADDRESS	52 Moo.4 Mae Tho, Muang Tak, Tak, 63000

